VAPOR-LIQUID EQUILIBRIA FOR THE ETHANOL-METHYL METHACRYLATE SYSTEM

by

Jin-Min Yu

A THESIS SUBMITTED IN PARTIAL FULFILLMENT OF

THE REQUIREMENT FOR THE DEGREE OF

MASTER OF APPLIED SCIENCE

IN THE

DEPARTMENT OF CHEMICAL ENGINEERING

UNIVERSITY OF OTTAWA

1979.

ABSTRACT

A modified Dvorak and Boublik (1) recirculation still was used in the determination of isothermal vapor-liquid equilibrium data for the binary system ethanol - methyl methacrylate at 313.15, 323.15 and 333.15K. Liquid activity coefficients, γ_i^L, and excess Gibbs free energies G^E were evaluated and correlated by a three-constant Redlich-Kister equation (2); a binary azeotrope exists at all three temperatures studied and the mole fraction of ethanol in the azeotrope increases with increasing temperature.

In order to evaluate liquid activity coefficients, a new empirical correlation of second virial coefficients for pure polar compounds has been developed by extending a modified Pitzer-Curl correlation of non-polar gases proposed by Tsonopoulos (3).

In this development, the effect of hydrogen-bonding on the second virial coefficients was correlated separately from the effect of polarity. For each compound, only one more parameter is required to describe the effect of polarity. Using this parameter, expressed as a function of reduced dipole moment (μ_R), the second virial coefficients of non-hydrogen-bonding polar substances can be predicted in good agreement with the experimental data. As for the explanation of the hydrogen-bonding effect, two additional parameters are needed. Together with the parameter for polar effect, the second virial coefficients of hydorgen-bonding polar substances (alcohols) can be fitted satisfactorily.

ACKNOWLEDGEMENTS

The author is indebted to Dr. Benjamin C.-Y. Lu for directing this research work. He would like to express his sincere gratitude to Dr. T. Ishikawa whose continued help and advice during these one and half years, has made this possible. Special thanks to Dr. W.K. Chung for his help with the computation and Mr. J. Gasperetti for his technical assistance.

TABLE OF CONTENTS

LIST OF FIGURES

LIST OF TABLES

APPENDIX II

NOMENCLATURE

a, c	= parameters of polar contribution term, $f^{(2)}$; see Equation (4.8)
a_T, b_T	= parameters in Equations (2.20) and (2.22)
B, C	= Virial Coefficients of the Virial Equation
B_{12}, C_{12}, D_{12}	= Constants in the Redlich-Kister Equation in the Binary System
G	= Gibbs Free Energy
b, d, g	= Parameters of Hydrogen-Bonding Contribution Term, $f^{(3)}$; see Equation (4.12)
f^o	= Fugacity of a Component at standard State
$\hat{f}$	= Fugacity of a Component in the Solution
$f_B^{(0)}$, $f_B^{(1)}$	= Dimensionless Terms of Equation (2.2), the Pitzer-Curl Correlation of Second Virial Coefficients
$f^{(0)}$, $f^{(1)}$, $f_T^{(2)}$	= Dimensionless Terms of Equation (2.19), the Tsonopoulos Correlation of Second Virial Coefficients
$f^{(2)}$, $f^{(3)}$	= Dimensionless Polar and Hydrogen-Bonding Contribution Terms of Equation (4.5), the New Correlation of Second Virial Coefficient
f_a, f_μ	= Dimensionless Polar Contribution Terms of Equation (2.5), the O'Connell-Prausnitz Correlation of Second Virial Coefficient
k_{ij}	= Characteristic Binary Constant, see Equation (2.23)
n^D	= Refractive Index of Sodium Light
N	= Number of Data
p^o	= Vapor Pressure, Torr
P	= Total Pressure, Torr
R	= Gas Constant

T	= Absolute Temperature, K
V^o	= Molar Volume of Pure Component, $cm^3 mol^{-1}$
V	= Volume, cm^3
x	= Mole Fraction in Liquid Phase
y	= Mole Fraction in Vapor Phase
z	= Compressibility
$\alpha_0, \alpha_1, \alpha_2$	= Parameters in Equation (4.10)
ρ	= Density, g cm^{-3}
μ	= Dipole Moment, Debye
$\mathcal{P}$	= Parachor
γ	= Activity Coefficient
ω	= Acentric Factor
ω_H	= Acentric Factor of Homomorph
δ_{12}	= $2B_{12}-B_{11}-B_{22}$
η	= Association Factor

SUPERSCRIPTS

L	= Liquid Phase
V	= Vapor Phase

SUBSCRIPTS

c	= Critical Property
E	= Excess Property
i, j	= Component Identification
R	= Reduced Property
1, 2	= Component Identification
12	= Mixture Identification

CHAPTER 1

INTRODUCTION

Methacrylate esters of higher alcohols are produced commercially by either direct esterification or the ester interchange reaction between the lower methacrylates and higher alcohols. In the preparation of ethyl methacrylate the vapor-liquid equilibrium data for the binary mixture ethanol - methyl methacrylate (MMA) are useful in the design of a distillation column for separating the mixture. However, these data have not yet been reported in the literature. The purpose of the present work is to establish isothermal vapor-liquid equilibrium data for the mixture at 313.15, 323.15 and 333.15K by means of a modified Dvorak and Boublik (1) recirculation still.

In order to analyze and correlate vapor-liquid equilibrium data, it is necessary to take the non-ideal behavior of vapor phase into account. For isothermal data and at subcritical temperature, up to a pressure of about 15 atm, the effect of vapor phase imperfection can be reliably calculated using only the second virial coefficients of the pure components and the cross second virial coefficients of the binary mixtures concerned (4). Several empirical methods for predicting the second virial coefficients have been developed (Pitzer and Curl (1957) (5), O'Connell and Prausnitz (1967) (6), Tsonopoulos (1974) (3)), but all of these correlations are not satisfactory in some aspects. For example, the value of one or two of the parameters must be obtained empirically; methods are only applicable in a narrow temperature range; or the results are simply not accurate enough to be acceptable. Because of these weaknesses,

a new empirical correlation for the second virial coefficients of pure polar compounds was developed in this study.

CHAPTER 2

LITERATURE SURVEY

The purpose of this chapter is to give a brief review of literature covering those points which are of interest to this study, i.e., methods for the direct experimental determination of vapor-liquid equilibrium and empirical correlations for the second virial coefficients.

2.1 Experimental Methods

The direct experimental determination of vapor-liquid equilibrium means that samples of the liquid and vapour which are in true equilibrium are separated and the concentrations of both phases are determined analytically.

In their work entitled "Vapor-Liquid Equilibrium" Hala et al. (7) presented a bibliography for experimental methods, which can be classified into the following groups:

1. Distillation Method
2. Static Method
3. Dew and Bubble-Point Method
4. Flow Method
5. Circulation Method

2.1.1 Distillation Method

In this oldest method, a small amount of liquid is distilled off from the boiling flask which contains a large

charge. During such distillation, a large amount of liquid sample is required and only a very small sample of condensate is allowed to be withdrawn for analysis. This method is very simple but has marked disadvantages and causes large errors in determining the equilibrium temperature, pressure and composition. At present, it is rarely used.

2.1.2 Static Method

In this method, the liquid sample is charged into a closed evacuated equilibrium cell which is agitated at constant temperature until the equilibrium is reached between the vapor and the liquid. Then the samples of the two phases are withdrawn and analyzed.

The main disadvantage of this method is that of pressure changes in the equilibrium cell during sampling, causing disturbance to the equilibrium.

2.1.3 Dew and Bubble-point Method

This method employs an apparatus similar to the static method, but omitting the analyses of the compositions in two phases. A mixture of known composition is introduced into an evacuated equilibrium cell of variable volume which is maintained at constant temperature.

By varying the volume of the equilibrium cell, the system pressure, at which condensation commenced and is completed, is observed. The dew point and bubble point

pressures are measured directly. From these data, the saturation curves of the two phases at constant temperature can be plotted against composition.

One great advantage with this method is that in the determination of the equilibrium diagrams, it is not necessary to take samples of liquids or vapors for analysis. However, the dew and bubble points are not easily defined very sharply, hence highly refined precision instrument has to be used to detect the occurence of vapor or liquid sensitively.

2.1.4 Flow Method

The flow method is used to measure equilibrium data in systems of limited miscibility in the liquid phase. A steady stream of vapor mixture is passed through equilibrium cell where it is cooled and partially liquified. Then the vapor which is in equilibrium with the condensate, is separated and removed for analysis. The samples are withdrawn and analyzed continuously.

It is obvious that during passing of the vapor mixture, there are pressure drops which will affect the equilibrium. Hence the main difficulties of this method are in the maintenance of constant system pressure and temperature during rapid condensation.

2.1.5 Circulation Method

This method is the most widely used. Vapor-liquid equilibrium data are obtained by continuously circulating the vapor formed by the vaporization of the liquid through the system and bringing it back into contact with the liquid until no further change in the composition of either phase can be detected. In the meantime,

condensed vapor and liquid are kept separate to allow the removal of samples for analysis.

This method is convenient to use both in the region of medium and low pressures.

Even though there are various equilibrium stills with simple circulation, they differ significantly from one another in their construction details.

According to the manner of circulation of the phases, these stills can be classified into two groups:

1. Stills with circulation of vapor phase
2. Stills with circulation of the liquid and vapor phases

The most typical stills of these two groups are those of Othmer (8), Jones, Schoenborn and Colburn (9), and Gillespie (10).

The Othmer still and the Jones still belong to the first group. In the Othmer still, the vapor produced by boiling the liquid mixture in an insulated still is removed, condensed and the overflow of condensate is returned to the still. An immersion heater is used to provide turbulent mixing and boiling.

The Jones still operates in a similar manner. But the overflow condensate is vaporized outside the still before it makes contact with the liquid phase contained therein again.

A Cottrell pump is used in one family of Gillespie still for the purpose of recirculating both the liquid and the vapor phases. The liquid mixture in the still is boiled by an internal heater form vapor bubbles that thoroughly mix with the liquid

mixture to ensure quiet and steady boiling.

The evolved vapors carry a flow of liquid with them into the cottrell pump from which this mixture spurts into the equilibrium chamber. Equilibrium is assumed to have been attained as the contact phases separate after leaving the upper end of cottrell pump. The overflow condensate then returns to the base of cottrell pump and makes contact with the liquid in the still. The conditions in the cottrell pump are ideal for obtaining the desired equilibrium between the phases.

Following a systematic study, Dvorak and Boublik (11) stated that intense stirring is necessary both in the liquid and in the condensate receivers. Accordingly, they proposed an apparatus which is suitable even for systems having a very high relative volatility. Two additional modifications were made by Boublikova and Lu (1): the circulation loop in the evacuated chamber was shortened to reduce the pressure drop, a well for an electrical heater was made in the boiling vessel. (Details of design are presented in Chapter 5.)

So far it has not been possible to construct a still which would yield thermodynamically consistent data for all systems. The relative merits of the various types of still were summarized and discussed by Gillespie (10) and Hala et al. (7).

2.2 Empirical Correlations of the Second Virial Coefficient

Experimental determination of second virial coefficients (B) for all systems is a formidable proposition; it is a usual practice to predict these data by the use of suitable correlations.

Correlations for second virial coefficients can be obtained from statistical mechanical formulas using an expression for the pair intermolecular potential energy (16), or by empirical or semi-empirical methods. The most popular method has been the last, since the computation is usually the easiest (although not always the most accurate).

In 1957, Pitzer and Curl (5) developed a very successful empirical correlation of the B of the nonpolar gases. Because of the soundness and reliability of this correlation, it was used as the basis to develop a correlation of the B of polar gases by O'Connell and Prausnitz (6) and by Tsonopoulos (3). Along this line, a predictive method for the B of polar gases is developed in this study. These three correlations are presented in the following sections. Other correlations (13)(14)(15), which have not originated from the Pitzer-Curl correlation are not as accurate as the above correlations, so they are not considered here.

2.2.1 The Correlation of Pitzer and Curl

By extending the theory of corresponding states originally proposed by van der Waals (17), Pitzer and Curl (15) used critical temperature (T_c), critical pressure (P_c) and an additional parameter called acentric factor (ω) which is a macroscopic measure of the effect of acentricity, i.e., the non-spherical nature of intermolecular forces, to correlate the B of pure nonpolar gases characterized by zero dipole moment.

The definition of ω is given below:

$$\omega_i = -\log_{10}\left(\frac{P_i^o}{P_{c_i}}\right)_{T_{R_i=0.7}} - 1.000 \qquad (2.1)$$

where P^o_i is the vapor pressure of component i at reduced temperature $T_{R_i}=0.7$. P_{c_i} is the critical pressure of component i. The values of ω can be evaluated directly from the above equation. Fluids consisting of spherical molecules, for example Ar, Kr, have an acentric factor equal to zero, the quantum gases, for example, He, H_2 have negative ω's and everything else has a positive value of ω. Acentric factors of substances can be found in the compilation of Reid, Sherwood and Prausnitz (1977) (18).

The Pitzer-Curl correlation provides good predictions for the B of nonpolar gases. In the reduced dimensionless form, it is:

$$\frac{P_{c_i} B_{ii}}{R T_{c_i}} = f_B^{(0)} + \omega_i f_B^{(1)} \qquad (2.2)$$

where R is the gas constant.

The function $f_B^{(0)}$ gives the reduced second virial coefficients for simple fluids ($\omega_i=0$) while $f_B^{(1)}$ is a correlation function which is multiplied by ω_i, gives the effect of acentricity on the second virial coefficient. The two functions $f_B^{(0)}$ and $f_B^{(1)}$ were determined from experimental data for a number of nonpolar or slightly polar substances. Highly polar substances such as ammonia, nitriles or alcohols were not included.

The empirically determined functions are:

$$f_B^{(0)} = 0.1445 - \frac{0.330}{T_{R_i}} - \frac{0.1385}{T_{R_i}^2} - \frac{0.0121}{T_{R_i}^3} \qquad (2.3)$$

$$f_B^{(1)} = 0.073 + \frac{0.46}{T_{R_i}} - \frac{0.50}{T_{R_i}^2} - \frac{0.097}{T_{R_i}^3} - \frac{0.0073}{T_{R_i}^8} \qquad (2.4)$$

Pitzer and Curl did not extend their correlation to mixtures by defining mixing rules for the parameters in Equations (2.3) and (2.4) to estimate the cross second virial coefficient B_{ij}.

2.2.2 The Correlation of O'Connell and Prausnitz

The O'Connell and Prausnitz method (6), uses the Pitzer-Curl correlation to calculate the B_{ii} for pure, nonpolar gases. They also use the Pitzer-Curl correlation as the basis for their correlation for polar gases. In place of ω_i, they use ω_{H_i}, the acentric factor of the polar compound's homomorph (19), i.e., a nonpolar compound having approximately the same size and shape as the polar compound, to present the effect of acentricity on the B. By examining the B of 41 polar gases, (10 alcohols, 6 ethers, an aldehyde, ketones, 6 esters, 7 amines, 4 heterocyclic and 4 other polar gases), they established two empirically determined functions for the B of polar gases, f_μ for the polar effect induced by the dipole moments among molecules, and f_a, an "association" function for compounds which exhibit special forces, such as hydrogen bonds.

For pure polar gases, the correlation has the form:

$$\frac{P_{c_i} B_{ii}}{R T_{c_i}} = f_B^{(0)} + \omega_{H_i} f_B^{(1)} + f_\mu - \eta_i f_a \qquad (2.5)$$

where the association constant η_i is an empirically determined quantity which reflects the tendency of compound i (e.g., an alcohol) to associate with itself to form dimers.

The empirical function f_μ depends on the reduced temperature, T_R, and on μ_R, the reduced dipole moment, defined by

$$\mu_{R_i} = \frac{10^5 \mu_i^2 P_{c_i}}{T_{c_i}^2} \qquad (2.6)$$

in which μ_i is the dipole moment of pure component i in Debye units, the critical pressure in atmospheres, and the critical temperature in degree Kelvin. The function f_μ was determined from experimental data for 17 polar fluids which do not exhibit specific chemical forces.

For $\mu_{R_i} > 4$, it is given by

$$\begin{aligned} f_\mu = {} & -5.237220 + 5.665807(\ln \mu_{R_i}) \\ & -2.133816(\ln \mu_{R_i})^2 + 0.2525373\ (\ln \mu_{R_i})^3 \\ & + \frac{1}{T_{R_i}}[5.769770 - 6.181427\ (\ln \mu_{R_i}) \\ & + 2.283270(\ln \mu_{R_i})^2 - 0.2649074(\ln \mu_{R_i})^3] \end{aligned} \qquad (2.7)$$

For the compounds with $\mu_{R_i} < 4$, f_μ is set to be zero. The association function f_a is given by:

$$f_a = \exp[6.6\ (0.7 - T_{R_i})] \qquad (2.8)$$

The values for μ_{H_i}, μ_{R_i}, and η_i for some components are presented in Tables(4-1), (4-3), and (4-6).

The two polar terms, f_μ and f_a in this correlation are set equal to zero for $T_{R_i} \geq 0.95$.

To estimate cross second virial coefficient B_{ij}, O'Connell and Prausnitz proposed the following mixing rules for the various parameters in the above correlation equations.

For the case where i and j are both nonpolar gases, Equations (2.1), (2.2), (2.3) and (2.4) give values of B_{ij}, where $P_{c_{ij}}$ replaces P_{c_i}, $T_{c_{ij}}$ replaces T_{c_i}, and ω_{ij} replaces ω_i. The mixing rules have the forms:

$$T_{c_{ij}} = (T_{c_i} T_{c_j})^{1/2} \tag{2.9}$$

$$\omega_{ij} = 0.5(\omega_i + \omega_j) \tag{2.10}$$

$$P_{c_{ij}} = 4\, T_{c_{ij}} \left[\frac{P_{c_i} V_{c_i}}{T_{c_i}} + \frac{P_{c_j} V_{c_j}}{T_{c_j}} \right] / (V_{c_i}^{1/3} + V_{c_j}^{1/3})^3 \tag{2.11}$$

For the case where i is a polar substance, and j is nonpolar, Equations (2.1), (2.2), (2.3) and (2.4) are used for B_{ij} where Equation (2.9) is used for $T_{c_{ij}}$. For ω_{ij}, the mixing rule is:

$$\omega_{ij} = 0.5(\omega_{H_i} + \omega_j) \tag{2.12}$$

Equation (2.11) is used for $P_{c_{ij}}$.

For the case where both components i and j are polar, Equation (2.5) is used for B_{ij}, where T_{c_i} is replaced by $T_{c_{ij}}$

from Equation (2.9), ω_{H_i} is replaced by $\omega_{H_{ij}}$:

$$\omega_{H_{ij}} = 0.5(\omega_{H_i}+\omega_{H_j}) \tag{2.13}$$

P_{c_i} is replaced from (2.11), where the reduced dipole moment $\mu_{R_{ij}}$ is given by:

$$\mu_{R_{ij}} = \frac{10^5 \mu_i \mu_j P_{c_{ij}}}{T^2_{c_{ij}}} \tag{2.14}$$

Finally, η_i is replaced by η_{ij} according to

$$\eta_{ij} = 0.5(\eta_i+\eta_j) \tag{2.15}$$

For cross second virial coefficients of nonpolar compounds, this correlation based on the above mixing rules works well if the components are similar in size. However, for extremely different molecules, the predicted values are somewhat too negative.

In fact, the O'Connell-Prausnitz correlation has been used widely (for example, in two important monographs on computer calculation for vapor-liquid equilibria: Prausnitz et al. 1967 (20), Renon et al. (1971) (21)). Nevertheless, several drawbacks contained in their method are:

1. Euband and Smith (22) have stated that the homomorph concept shall be limited to organic compounds. However, O'Connell and Prausnitz applied this concept to inorganic compounds, (e.g. methane was considered as the homomorph of both water and ammonia; propane the homomorph of sulfur dioxide) thus leading to unsatisfactory results.

2. The homomorph concept introduces another difficulty. Which critical constants should be used in Equations (2.3) and (2.4) - those of the homomorphs or those of the polar compounds? Inconsistently, O'Connell and Prausnitz use the polar compound's critical constants, but not its acentric factor. This results in the overcorrection of the values of B for polar gases.

3. The association factor is strictly an empirical correlation factor. Some substances which could be expected to associate (e.g., H_2O and NH_3) do not have association constants. On the other hand, some substances which might not actually "associate" have associate constants (e.g., ketones and ethers).

4. The polar terms (2.7) and (2.8) are arbitrarily set to equal to zero for $T_{R_i} \geq 0.95$. This leads to a discontinuity that can frequently be very substantial, as shown in Chapter 4.

2.2.3 The Correlation of Tsonopoulos

By using up to date data of Ar and Kr, Tsonopoulos (3) modified the Pitzer-Curl correlation for nonpolar gases. A slight modification of $f_B^{(0)}$ in Equation (2.3) made it possible to fit all the B data of simple fluids (ω=0) to within 1% error. The modified $f_B^{(0)}$ is

$$f^{(0)} = f_B^{(0)} - \frac{0.000607}{T_{R_i}^8} \qquad (2.16)$$

Tsonopoulos checked $f_B^{(1)}$ against reliable B values for compounds with large acentric factors and then established a modified function $f^{(1)}$ with one term less than $f_B^{(1)}$. The modified $f_B^{(1)}$ has the form:

$$f^{(1)} = 0.0637 + \frac{0.331}{T_{R_i}^2} - \frac{0.423}{T_{R_i}^3} - \frac{0.008}{T_{R_i}^8} \qquad (2.17)$$

Thus,

$$\frac{P_{c_i} B_{ii}}{R T_{c_i}} = f^{(0)} + \omega_i f^{(1)} \qquad (2.18)$$

This equation improves the fit to the B values of nonpolar gases at low reduced temperatures ($T_{R_i} < 0.75$), and was used by Tsonopoulos as a basis for establishing a new correlation for polar gases.

Polar gases considered in his study included alcohols, phenol, water, ketones, ethers, aldehydes, and alkyl nitriles. They were classified into two classes: hydrogen-bonding gases (alcohols, phenol, and water), and non-hydrogen-bonding gases (ketones etc.).

The polar effects of these two classes were treated separately. In order to obviate the need of determining and using homomorphs, Tsonopoulos used the actual acentric factor for all polar gases.

For the non-hydrogen-bonding gases, a one-parameter function was established to account for the polar contribution. By adding this polar contribution term to Equation (2.18) the B values of non-hydrogen-bonding gases were fitted satisfactorily. It has the form:

$$\frac{P_{c_i} B_{ii}}{R T_{c_i}} = f^{(0)} + \omega_i f^{(1)} + f_T^{(2)} \qquad (2.19)$$

where the polar term is given by

$$f_T^{(2)} = \frac{a_{T_i}}{T_{R_i}^6} \qquad (2.20)$$

For each non-hydrogen-bonding gas, parameter a_{T_i} is an average value taken within a lower temperature range (usually at $T_{R_i} \leq 0.95$) in which the individual value of a_{T_i} is determined from the corresponding B value, and does not vary very much with temperature.

A satisfactory correlation between a_{T_i} and μ_{R_i} was established as:

$$a_{T_i} = -2.140\text{x}10^{-4}(\mu_{R_i}) - 4.30\text{x}10^{-21}(\mu_{R_i})^8 \qquad (2.21)$$

In fact, parameter a_{T_i} has a negative value for the non-hydrogen-bonding gas.

The association effect of the hydrogen-bonding gases makes it difficult to express the temperature dependence of the polar contribution to the second virial coefficients; Tsonopoulos developed a two-parameter function for the polar contribution.

The polar term of Equation (2.22) then has the form:

$$f_T^{(2)} = \frac{a_{T_i}}{T_{R_i}^6} - \frac{b_{T_i}}{T_{R_i}^8} \qquad (2.22)$$

Both a_{T_i} and b_{T_i} were assumed to be positive. The B values of eight alcohols, phenol and water were analyzed with equations (2.19) and (2.22).

A constant value of a_{T_i}, 0.0878 is used for all eight alcohols; values of b_{T_i} for eight alcohols are listed in Table (4-8). No further generalization of b_{T_i} for alcohols was made in his study. For water, the a_{T_i} value is 0.0279 and b_{T_i} value is 0.0229. On the contrary, phenol has a negative value for

a_{T_i} and zero value for b_{T_i}.

In general, Tsonopoulos' method provides reliable predictions for the second virial coefficients of hydrogen-bonding gases.

To estimate cross second virial coefficient B_{ij} of mixture, Tsonopoulos presented the following mixing rules. The expressions for ω_{ij} and P_{ij} are the same as those of O'Connell and Prausnitz:

$$\omega_{ij} = 0.5\ (\omega_i + \omega_j) \tag{2.10}$$

$$P_{c_{ij}} = \frac{4\ T_{c_{ij}}\ (P_{c_i} V_{c_i}/T_{c_i} + P_{c_j} V_{c_j}/T_{c_j})}{(V_{c_i}^{1/3} + V_{c_j}^{1/3})^3} \tag{2.11}$$

However, for $T_{c_{ij}}$, Tsonopoulos introduced an empirically determined characteristic constant k_{ij} for each binary mixture to account for the deviation of $T_{c_{ij}}$ from the geometric mean as expressed in Equation (2.9). Thus $T_{c_{ij}}$ is expressed as

$$T_{c_{ij}} = (T_{c_i} T_{c_j})^{1/2}(1-k_{ij}) \tag{2.23}$$

Tsonopoulos suggested that $T_{c_{ij}}$ can be assumed to be the geometric mean of T_{c_i} and T_{c_j} (i.e., $k_{ij}=0$) only when i and j are very similar in size and chemical nature. Values of k_{ij} for nonpolar systems were reported by Chueh and Prausnitz (23).

Equations (2.10), (2.11) and (2.23) are used for nonpolar-nonpolar binary mixtures.

For polar-nonpolar binary mixtures Tsonopoulos assumed that

B_{ij} has no polar term:

$$a_{T_{ij}} = 0$$

$$b_{T_{ij}} = 0$$

For polar-polar binary mixtures, mixing rules for the parameters in the polar term are presented as

$$a_{T_{ij}} = 0.5(a_{T_i} + a_{T_j}) \tag{2.24}$$

$$b_{T_{ij}} = 0.5(b_{T_i} + b_{T_j}) \tag{2.25}$$

With a temperature-independent k_{ij} for each binary mixture this correlation provides much better predictions for B_{ij} than those of the O'Connell-Prausnitz correlation.

However, his correlation still has several shortcomings.

1. Instead of assuming the polar contribution parameter, a_{T_i}, of non-hydrogen-bonding gases to be independent of temperature values of a_{T_i} are obtained as an average value within an arbitrary low temperature range. This approach raises a question whether equation (2.20) is reliable beyond the temperature range as mentioned above.

2. Fixing values of the polar contribution parameter a_{T_i} for alcohols creates difficulties to generalize the parameter b_{T_i} in Equation (2.22).

3. The characteristic constant k_{ij} is an empirically determined value, and therefore is not available for many polar-polar binary mixtures.

CHAPTER 3

THEORETICAL CONSIDERATION

Complete description of vapor-liquid equilibria for a system gives equilibrium composition of both phases as well as temperature and total pressure. In a typical experimental investigation temperature or total pressure is held constant.

Usually chemical processing is operated at low or moderate pressure. Therefore particular attention has been given the subject of vapor-liquid equilibrium at low pressures - up to several atmospheres. Under these conditions certain quite reliable assumptions can be made about the behavior of the vapor phase which allow development of an accurate equation for the calculation of liquid phase activity coefficients from phase equilibrium data. Since the activity coefficients are useful in data reduction for vapor-liquid equilibrium calculations, their calculation and correlation are required.

3.1 Evaluation of Liquid Phase Activity Coefficients at Low and Moderate Pressures

Through the definition of activity coefficient γ_i and some assumptions, Van Ness (24) derived an equation to evaluate the liquid phase activitiy coefficient (γ_i^L) at low and moderate pressures.

By definition:

$$\gamma_i = \frac{f_i}{x_i f_i^o} \tag{3.1}$$

For the liquid phase

$$\gamma_i^L = \frac{f_i^L}{x_i (f_i^o)^L} \tag{3.2}$$

For the vapor phase

$$\gamma_i^V = \frac{f_i^V}{y_i (f_i^o)^V} \tag{3.3}$$

where the superscripts L and V indicate the liquid and vapor phase respectively, and,

f_i = fugacity of component i in the solution

f_i^o = fugacity of pure component i at the standard state (i.e., at the temperature and pressure of the solution).

γ_i = activity coefficient of component i in the solution

x_i = mole fraction of component i in the liquid phase

y_i = mole fraction of component i in the vapor phase

Three assumptions were made by Van Ness to derive the equation:

1. The vapor phase of the mixture, as well as the vapors in equilibrium with the pure components, are adequately described by the virial equation terminated after the second virial coefficient (B), i.e., $Z = 1 + BP/RT$, where R is the gas constant, P is the system pressure, T is the system temperature, and Z is the compressibility.
2. The pure component liquid volumes (V_i^0) are incompressible over the pressure range in question.

3. The standard states for the activity coefficients are the pure components at the same temperature and pressure as those of mixture.

Finally, an equation for liquid phase activity coefficient is found as

$$\log \gamma_i^L = \log \frac{y_i P}{x_i P_i^o} + \frac{(B_{ii}-V_i^o)\ (P-p_i^o)}{2.303\ RT} + \log \gamma_i^V \qquad (3.4)$$

In this equation, the quantitative P_i^o, B_{ii}, V_i^o, P are the vapor pressure, second virial coefficient, liquid molar volume of component i, and the total pressure of the system, respectively.

Thus, for a binary solution at low or moderate pressure, $\log \gamma_i^L$ is expressed by:

$$\log \gamma_i^L = \log \frac{y_i P}{x_i p_i^o} + \frac{(B_{ii}-V_i^o)(P-p_i^o)}{2.303\ RT} + \frac{(1-y_i)^2 p \delta_{12}}{2.303\ RT} \qquad (3.5)$$

in which $\delta_{12} = 2B_{12} - B_{11} - B_{22}$, and B_{12} is the cross second virial coefficient.

In equation (3.5), the second and third terms of the right-hand side represent the departure of the vapor phase from ideal behavior.

In order to obtain values of B_{11}, B_{22}, and B_{12}, for the system studied in this investigation, a new empirical correlation of the second virial coefficient for polar gases was developed (see Chapter 4).

3.2 Correlation of Experimental Liquid Phase Activity Coefficients

A number of integrated forms of the Gibbs-Duhem equation are available for correlating liquid phase activity coefficients for binary mixtures, for example, the Margules equation (25), the Van Laar equation (26), the Redlich-Kister equation (2), and the Wilson equation (27).

The Redlich-Kister equations (2) are commonly used for correlating the liquid phase activity coefficient with the liquid phase composition. These equations were deduced from the relation between the liquid phase activity coefficient (γ_i^L) and molar excess Gibbs free energy (G^E) as described below.

An excess Gibbs free energy is defined as the difference between an actual Gibbs free energy and the Gibbs free energy that would be calculated under the same conditions of T,P and x_i by the equation for an ideal solution. Thus by definition (4):

$$G^E = G \text{ (actual solution at } T,p,x_i) - G \text{ (ideal solution at same } T,p,x_i)$$

or in another form:

$$\frac{G^E}{2.303RT} = \sum_i x_i \log \gamma_i^L \qquad (3.6)$$

For a binary system, equation (3.6) has zero values for $x_1=0$ and $x_1=1$. In this application, the usual convension of $\gamma_1^L=1$ for $x_1=1$ and $\gamma_2^L=1$ for $x_1=0$ is adopted.

Differentiating Equation (3.6) with respect to x_1 gives

$$\log\left(\frac{\gamma_1^L}{\gamma_2^L}\right) = \left[\frac{dG^E/2.303RT}{dx_1}\right]_{T,p,x_2} \qquad (3.7)$$

By taking advantage of the relation between G^E and x_i illustrated above, Redlich and Kister assumed the pressure dependence of G^E can be neglected at low or moderate pressure, and proposed that G^E/RT can be presented by an appropriate power series of the liquid composition (x_i).

The expansion for a binary mixture if given by,

$$\frac{G^E}{2.303RT} = x_1x_2[B_{12} + C_{12}(x_1-x_2) + D_{12}(x_1-x_2)^2 + \ldots] \qquad (3.8)$$

where the empirical parameters B_{12}, C_{12}, D_{12} ... depend on temperature only.

From equation (3.6), liquid phase activity coefficients are expressed as:

$$\log \gamma_1^L = x_2^2\,[B_{12}+C_{12}(3x_1-x_2) + D_{12}(x_1-x_2)(5x_1-x_2) + \ldots] \qquad (3.9)$$

$$\log \gamma_2^L = x_1^2\,[B_{12}+C_{12}(x_1-3x_2) + D_{12}(x_1-x_2)(x_1-5x_2) + \ldots] \qquad (3.10)$$

From equation (3.7), $\log \gamma_1^L/\gamma_2^L$ can be expressed as:

$$\log\ \gamma_1^L/\gamma_2^L = B_{12}(x_2-x_1) + C_{12}(6x_1x_2-1) + D_{12}(x_1-x_2)(8x_1x_2-1) + \ldots \qquad (3.11)$$

The Redlich-Kister equations provide not only a convenient method for representing liquid phase activity coefficients, but also for classifying different types of liquid solutions. According to Redlich, Kister and Turnquist (28), only the first term is

required for nearly ideal solutions. For a solution containing an associated component, such as alcohols and acids, the third term is necessary. However, only when very accurate and extensive data are available, the use of four or more terms is warranted. This is further reported by Ho et al. (29), that three-constant Redlich-Kister equations are adequate for representing liquid phase activity coefficients for most of binary systems.

The values of y_i and p can be calculated using these three-constant equations together with Equation (3.4) by means of the Newton-Raphson method of iteration (30). (A detailed description is presented in Appendix III). Computer programs for evaluating and correlating the vapor-liquid equilibrium data of the system studied are presented in Appendix VIII.

3.3 Thermodynamic Consistency Test of Binary Vapor-Liquid Equilibrium Data Obtained at Isothermal Conditions

At isothermal conditions, the integral form of the Gibbs-Duhem equation can be expressed as

$$\int_{x_1=0}^{x_1=1} \log\left(\frac{\gamma_1^L}{\gamma_2^L}\right) dx_1 = -\int_{p_2^o}^{p_1^0} \frac{V^E}{2.303RT}\, dP \qquad (3.11)$$

where V^E is the excess molar volume.

Observing that:

(a) Values of V^E are small

(b) The range of system pressure is small

Redlich and Kister (2) proposed a very good approximation for the thermodynamic consistency test by simply setting the right-hand

side of Equation (3.11) equal to zero, i.e.,

$$\int_{x_1=0}^{x_1=1} \log\left(\frac{\gamma_1^L}{\gamma_2^L}\right) dx_1 = 0 \qquad (3.12)$$

Equation (3.12) provides what is called the area test of Redlich and Kister. The integral can be evaluated by plotting $\log(\gamma_1^L/\gamma_2^L)$ versus x_1 and then measuring the net area under the curve. The requirement of thermodynamic consistency is met if the net area is very close to zero.

CHAPTER 4

DEVELOPMENT OF A NEW EMPIRICAL CORRELATION FOR SECOND VIRIAL COEFFICIENTS OF POLAR COMPOUNDS

At moderate pressure, the second virial coefficient provides a good measure of the departure of the vapor phase from ideal gas behavior arising from two body interactions. In this study, the second virial coefficients, B, for ethanol and methyl methacrylate are needed. Although values of B for ethanol are available in the literature, no experimental data are reported for methyl methyacrylate (an ester).

The correlation proposed by Tsonopoulos for polar gases, unfortunately did not include esters. For this reason, an attempt was made to develop a generalized empirical correlation for obtaining the second virial coefficient for methyl methacrylate by modifying the Tsonopoulos correlation. The Pitzer-Curl correlation for non-polar gases modified by Tsonopoulos provides a meansfor estimating the polar effects on the second virial coefficients for polar gases, and was used in this study as suggested.

In the present study the following polar compounds: esters, ketones, ethers, acetaldehyde, and alcohols were included in the development of the new correlation.

4.1 The Virial Equation of State

The virial equation (4) gives the compressibility factor as a power series in terms of reciprocal molar volume 1/V:

$$Z = \frac{Pv}{RT} = 1 + \frac{B}{v} + \frac{C}{v^2} \ldots \qquad (4.1)$$

where Z is the compressibility factor, B is the second virial coefficient and C is the third virial coefficient. All of the virial coefficients are independent of pressure or density and are functions of temperature and composition.

At low or moderate pressure, the virial equation of state, truncated at the second virial coefficient:

$$Z = 1 + B/V \tag{4.2}$$

can accurately represent the p-V-T behavior of vapors.

The composition dependence of B for an N-component mixture is given accurately by the following relationship:

$$B_{mix} = \sum_{j=1}^{N} \sum_{i=1}^{N} y_i y_j B_{ij} \tag{4.3}$$

where B_{ii} and B_{jj} are the pure component second virial coefficients, and B_{ij} $(i \neq j)$ is the cross second virial coefficient.

For a binary mixture, B_{mix} becomes:

$$B_{mix} = y_1^2 B_{11} + 2y_1 y_2 B_{12} + y_2^2 B_{22} \tag{4.4}$$

4.2 Development of an Empirical Correlation

It is known that polar compounds are characterized by a non-zero dipole moment μ which shows the effect of electrostatic forces between molecules. The polar compounds considered in this study are alcohols, esters, ketones, ethers and acetaldehyde as listed in Table (4-1). The B values available in the literature for these compounds are listed in Appendix VIII. These compounds are further classified into hydrogen-bonding and non-hydrogen-bonding classes. Hydrogen bonding compounds have

bonding between the hydrogen atom attached to the oxygen atom in one molecule with the oxygen atom of another molecule; this makes their behavior in the vapor phase different and more complex than that of non-hydrogen bonding polar compounds (esters ... etc.). These two classes of compounds are treated separately.

Halm (3) reported that the deviations of the reduced second virial coefficients of polar from non-polar behavior are small at reduced temperature greater than one but increase rapidly with decreasing temperature. The Pitzer-Curl correlation as modified by Tsonopoulos yields excellent estimation of the B values for non-polar compounds. For this reason, it was used for detecting the deviation of second virial coefficients for polar compounds from that of non-polar compounds. The deviation due to the effect of polarity on the compounds can be corrected by an additional function ($f^{(2)}$) of reduced dipole moment and reduced temperature. For hydrogen-bonding polar compounds where both polar effects and hydrogen-bonding effects prevail, the deviations can be accounted for by adding an extra correction function $f^{(3)}$ of reduced temperature to the polar correction function $f^{(2)}$.

As a result, the reduced second virial coefficient for the polar compounds can then be expressed by combining functions $f^{(2)}$ and $f^{(3)}$ with Equation (2.18) as follows:

$$\frac{P_{c_i} B_{ii}}{R T_{c_i}} = f^{(0)} + \omega_i f^{(1)} + f^{(2)} + f^{(3)} \qquad (4.5)$$

Table 4-1

VALUES OF PARAMETERS FOR THE COMPOUNDS USED IN THIS DEVELOPMENT

Substance	T_{c_i}, K [14]	P_{c_i}, atm [14]	ω_i [14]	ω_{H_i} [6]	μ_i [32]	η_i [6]
Dimethyl Ether	400	53.0	0.192	0.152	1.3	0.55
Ethyl Ether	466.7	35.9	0.281	0.252	1.3	0.28
Acetone	508.1	46.4	0.309	0.187	2.8	0.00
Methyl-Ethyl Ketone	535.6	41.0	0.329	0.187	2.8	0.30
Methyl-N-Propyl Ketone	564.0	38.4	0.348	0.278	2.8	0.55
Methyl Isopropyl Ketone	553.4	38.0	0.349		2.8	
Diethyl Ketone	561.0	36.9	0.347		2.7	
Acetaldehyde	461.0	55.0	0.303	0.152	2.7	0.00
Ethyl Formate	508.4	46.8	0.283	0.252	2.0	0.36
N-Propyl Formate	538.0	40.1	0.315	0.297	1.9	0.39
Methyl Acetate	506.8	46.3	0.324	0.215	1.7	0.62
Ethyl Acetate	523.2	37.8	0.363	0.278	1.9	0.50
N-Propyl Acetate	549.4	32.9	0.392		1.8	
N-Butyl Acetate	579.0	31.0	0.417		1.8	
Methyl Propanoate	530.6	39.5	0.352	0.326	1.7	0.49
Ethyl Propanoate	546.0	33.2	0.395		1.8	
Methanol	512.6	79.9	0.599	0.105	1.7	1.21
Ethanol	516.2	43.0	0.635	0.152	1.7	1.00
N-Propanol	536.7	51.0	0.624	0.201	1.7	0.57
N-Butanol	562.9	63.6	0.590	0.252	1.7	0.45
Isopropanol	508.3	47.0	0.666	0.187	1.7	0.65
2-Butanol	536.0	41.4	0.576	0.215	1.7	0.58
Isobutanol	547.7	42.4	0.588	0.215	1.7	0.49
Tert-Butanol	506.2	39.2	0.618	0.201	1.7	0.54

where P_{c_i} = critical pressure of component i

T_{c_i} = critical temperature of component i

ω_i = acentric factor of component i

$$f^{(0)} = 0.1445-0.330/T_{R_i} -0.1385/T_{R_i}^2-0.0121/T_{R_i}^3 - 0.000607/T_{R_i}^8 \quad (2.16)$$

$$f^{(1)} = 0.0637+0.331/T_{R_i}^2 -0.423/T_{R_i}^3-0.008/T_{R_i}^8 \quad (2.17)$$

The numerical values of T_{c_i}, P_{c_i}, ω_i, and μ_i for the compounds investigated in this work are presented in Table (4-1). The development of functions $f^{(2)}$ and $f^{(3)}$ are discussed below.

4.2.1 Non-Hydrogen-Bonding Polar Gases

In this work, eight esters, five ketones, two ethers and acetaldehyde were studied. The data source and the temperature range of the available second virial coefficient data for these compounds are listed in Table (4-2).

The contribution of the non-hydrogen-bonding polar effect, $f^{(2)}$, for each individual compound was obtained by substracting $f^{(0)} + \omega_i f^{(1)}$ from $\frac{P_{c_i} B_{ii}}{RT_{c_i}}$.

When values of $f^{(2)}$ were plotted against $(1/T_{R_i})^C$, the curvature of the resulting curve was reduced by increasing the value of C from unity as illustrated in Figure (4-1) for methyl acetate. It appears that the value of $f^{(2)}$ approaches zero at extremely high temperature, as dictated by the fact that the polar effect diminishes as temperature increases.

Table 4-2

REDUCED TEMPERATURE RANGE AND DATA SOURCE OF SECOND VIRIAL COEFFICIENT FOR NON-HYDROGEN-BONDING POLAR COMPOUNDS

Substance	Number of Data	Reduced Temp. Range	Data Source
Dimethyl Ether	7	0.68-0.81	(33)(36)
Ethyl Ether	28	0.63-0.87	(33)
Acetone	7	0.59-0.71	(33)
Methyl-Ethyl Ketone	5	0.59-0.69	(33)
Methyl N-Propyl Ketone	5	0.59-0.70	(33)
Methyl Isopropyl Ketone	3	0.59-0.66	(34)
Diethyl Ketone	3	0.60-0.67	(34)
Acetaldehyde	16	0.63-1.03	(33)
N-propyl Formate	23	0.50-5.00	(35)
Methyl Acetate	23	0.50-5.00	(35)
Ethyl Acetate	23	0.50-5.00	(35)
N-Propyl Acetate	23	0.50-5.00	(35)
N-Butyl Acetate	23	0.50-5.00	(35)
Methyl Propanoate	23	0.50-5.00	(35)
Ethyl Propanoate	23	0.50-5.00	(35)
Ethyl Formate	23	0.50-5.00	(35)

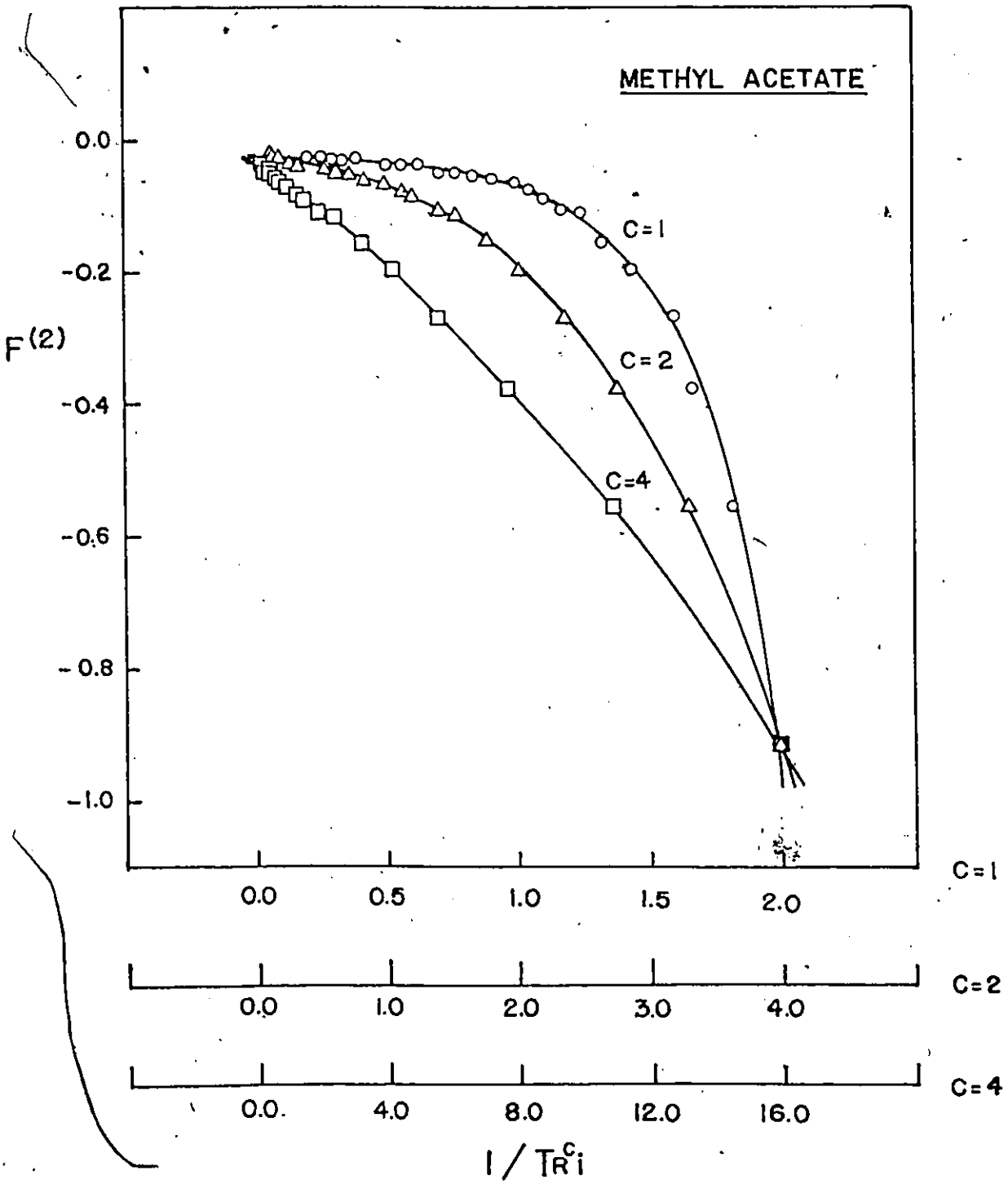

Figure 4-1 Relationship Between $f^{(2)}$ and $1/T_{R_i}^{c}$ for Methyl Acetate

Accordingly, the function $f^{(2)}$ was expressed by:

$$f^{(2)} = a_i/T_{R_i}^{c} \qquad (4.8)$$

In this equation, the quantity of a_i was considered only as a function of reduced dipole moment (μ_{R_i}). Value of μ_{R_i} are listed in Table (4-3). In order to find an optimum value of c which gives the minimum value of the RMS deviation of Equation (4.8), the Golden section search method (37) was employed. In this method, several values of c were assumed within a probable region in which the optimum value c lies, and the corresponding RMS deviations of Equation (4.8) were calculated and compared. Simultaneously, the value of a_i for each c was obtained during the calculation of RMS. By sequentially reducing the region, the optimum c together with a_i were found. The values thus obtained together with the RMS deviations for each compound are listed in Table (4.3).

The values of c vary from 3.1 to 11.0. This large difference caused difficulties in selecting an appropriate value of c. It was then arbitrarily decided to adopt the value of 6 as used by Tsonopoulos Values of a_i were again calculated by means of the least-squares method.

Therefore, Equation (4.8) was:

$$f^{(2)} = a_i/T_{R_i}^{6} \qquad (4.9)$$

Values of a_i and RMS deviations of B using Equation (2.18) and Equations (4.9) are listed in Table (4.4). Figure (4-2) depicts the values of a_i plotted against μ_R for all the non-hydrogen bonding polar compounds studied in this work. Figure (4-2) displays two important characteristics which should be considered in the calculation of a correlating functional form. It demonstrated that $f^{(2)}$ diminishes to zero as μ_R approaches

Table 4-3

VALUES OF μ_{R_i} AND VALUES OF c AND a_i FOR EQUATION (4.8) AND RMS DEVIATION OF B FROM EQUATIONS (2.18) AND (4.8)

Substance	μ_{R_i}	a_i	C_i	RMS* Deviation of B cm^3 mol^{-1}
Dimethyl Ether	56.0	-0.02874	4.2	15.0
Ethyl Ether	27.9	-0.00010	11.0	45.0
Acetone	140.9	-0.02825	6.4	5.5
Methyl-Ethyl Ketone	112.1	-0.03515	4.6	26.4
Methyl N-Propyl Ketone	94.6	-0.00601	9.2	31.7
Methyl Isopropyl Ketone	97.3	-0.02311	4.7	2.3
Diethyl Ketone	85.5	-0.02302	5.6	1.9
Acetaldehyde	188.7	-0.05570	5.8	33.9
Ethyl Formate	72.4	-0.005131	6.7	7.0
N-Propyl Formate	50.0	-0.003056	7.0	10.0
Methyl Acetate	52.1	-0.06021	3.9	28.2
Ethyl Acetate	49.9	-0.01600	5.1	17.2
N-Propyl Acetate	35.3	-0.008189	5.6	15.7
N-Butyl Acetate	30.0	-0.02597	5.0	21.6
Methyl Propanoate	40.6	-0.05149	3.1	21.2
Ethyl Propanoate	36.1	-0.02993	3.2	23.3

*RMS deviation = $\sqrt{\Sigma |B_{cal.}-B_{exp.}|^2/N}$ in which $B_{cal.}$ refers to the calculated values from the correlation, $B_{exp.}$ represents the experimental values and N is the number of data points.

Table 4-4

VALUES OF a_i FOR EQUATION (4.9) AND RMS DEVIATION OF B FROM EQUATIONS (2.18) AND (4.9)

Substance	a_i	RMS Deviation of, B cm^3mol^{-1}
Dimethyl Ether	-0.01651	16.1
Ethyl Ether	-0.00135	47.7
Acetone	-0.03391	11.9
Methyl Ethyl Ketone	-0.01825	38.6
Methyl N-Propyl Ketone	-0.02581	97.8
Methyl Iso-Propyl Ketone	-0.01245	14.9
Diethyl Ketone	-0.01898	7.3
Acetaldehyde	-0.05289	34.0
Ethyl Formate	-0.00780	12.8
N-Propyl Formate	-0.00528	15.4
Methyl Acetate	-0.02060	88.7
Ethyl Acetate	-0.01006	27.0
N-Propyl Acetate	-0.00643	17.7
N-Butyl Acetate	-0.01559	57.0
Methyl Propanoate	-0.01258	91.6
Ethyl Propanoate	-0.00744	68.7

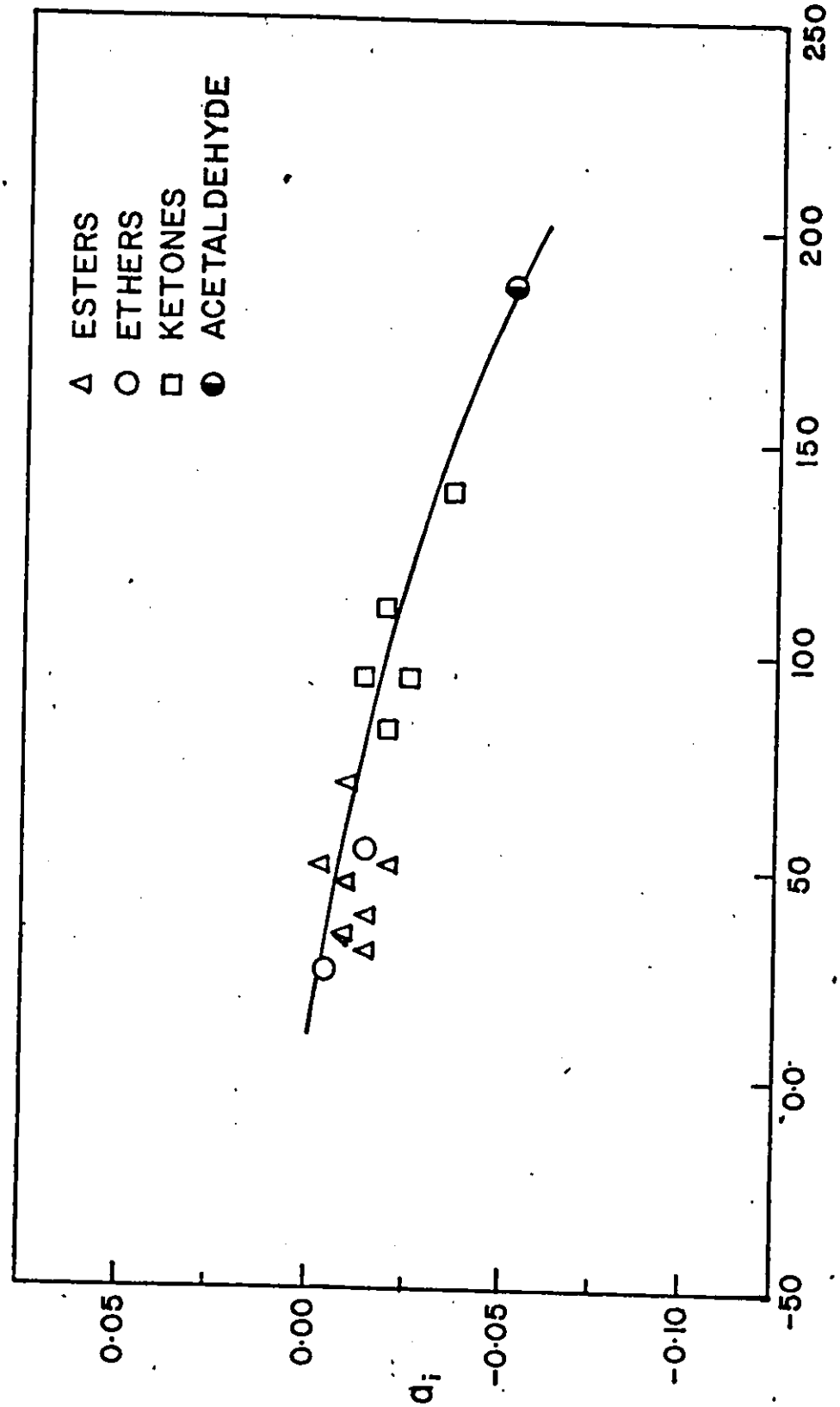

Figure 4-2 Relationship Between a_i and Reduced Dipole Moment for Non-Hydrogen-Bonding polar Substances (—— calculated by Equation (4.10)).

zero, and the representative function should be exponential at higher μ_{R_i} and linear at lower μ_{R_i} as indicated in Figure (4-2). The function chosen to be the best suited is the following:

$$a_i = \alpha_0 \mu_{R_i} + \alpha_1 \, (\exp \alpha_2 \mu_{R_i}) \qquad (4\text{-}10)$$

The optimum value of α_2 for minimizing the RMS deviation of Equation (4.10) was also obtained by means of the Golden section search method (37). It should be mentioned that values of α_0, and α_1 were simultaneously evaluated during the calculation of RMS deviation of Equation (4.10). A good fit of this equation was obtained as shown in Figure (4-2). The obtained values of α_0, α_1 and α_2, are -0.0001799, -0.00002169 and 0.03605, respectively. RMS deviation of this fit is 0.04.

The complete equation for the second virial coefficient of non-hydrogen-bonding polar gases then can be represented by adding the one-parameter function $f^{(2)}$ to Equation (2.18) as shown below:

$$\frac{P_{c_i} B_{ii}}{R T_{c_i}} = f^{(0)} + \omega_i f^{(1)} + f^{(2)} \qquad (4.11)$$

where

$$f^{(2)} = a_i / T_{R_i}^{6} \qquad (4.9)$$

$$a_i = 0.0001799 \, \mu_{R_i} - (0.00002169)(\exp. \, 0.03605 \, \mu_{R_i}) \qquad (4.10)$$

In general, the results obtained from a generalized expression are inferior to those obtained from the expression representing the individual compound. This is also true for the results obtained in this study. This can be seen from

Table (4-4) of this section and Table (4-9) of Section 4.4, particularly for n-butyl acetate, acetone and methyl n-propyl ketone.

The discrepancy observed for these three compounds as depicted in Figures (4-3), (4-4), and (4-5) indicates that the discrepancy tends to increase with decreasing temperature. The results of fitting Equation (4.11) to B values for the compounds studied in this work, will be discussed in Section 4.4.

4.2.2 Hydrogen-Bonding Polar Gases

With hydrogen linked to an electronegative atom (for example O, N) molecules tend to associate with each other by forming hydrogen bonds.

It is generally acknowledged that along with the polar character, alcohols display strong hydrogen bonded association, and show much greater deviations from the perfect gas laws than do non-hydrogen-bonding polar gases. Consequently, the second virial coefficients of alcohols are more negative than those of non-hydrogen-bonding polar gases (at the same corresponding states), thus reflecting the additional effect of hydrogen-bonding. In Table 4-5 the data source and the temperature range of the experimental B values are listed for the eight alcohols.

To study the effect of hydrogen-bonding apart from the effect of polarity, the polar correction function $f^{(2)}$ developed in 4.2.1 was extended to alcohols.

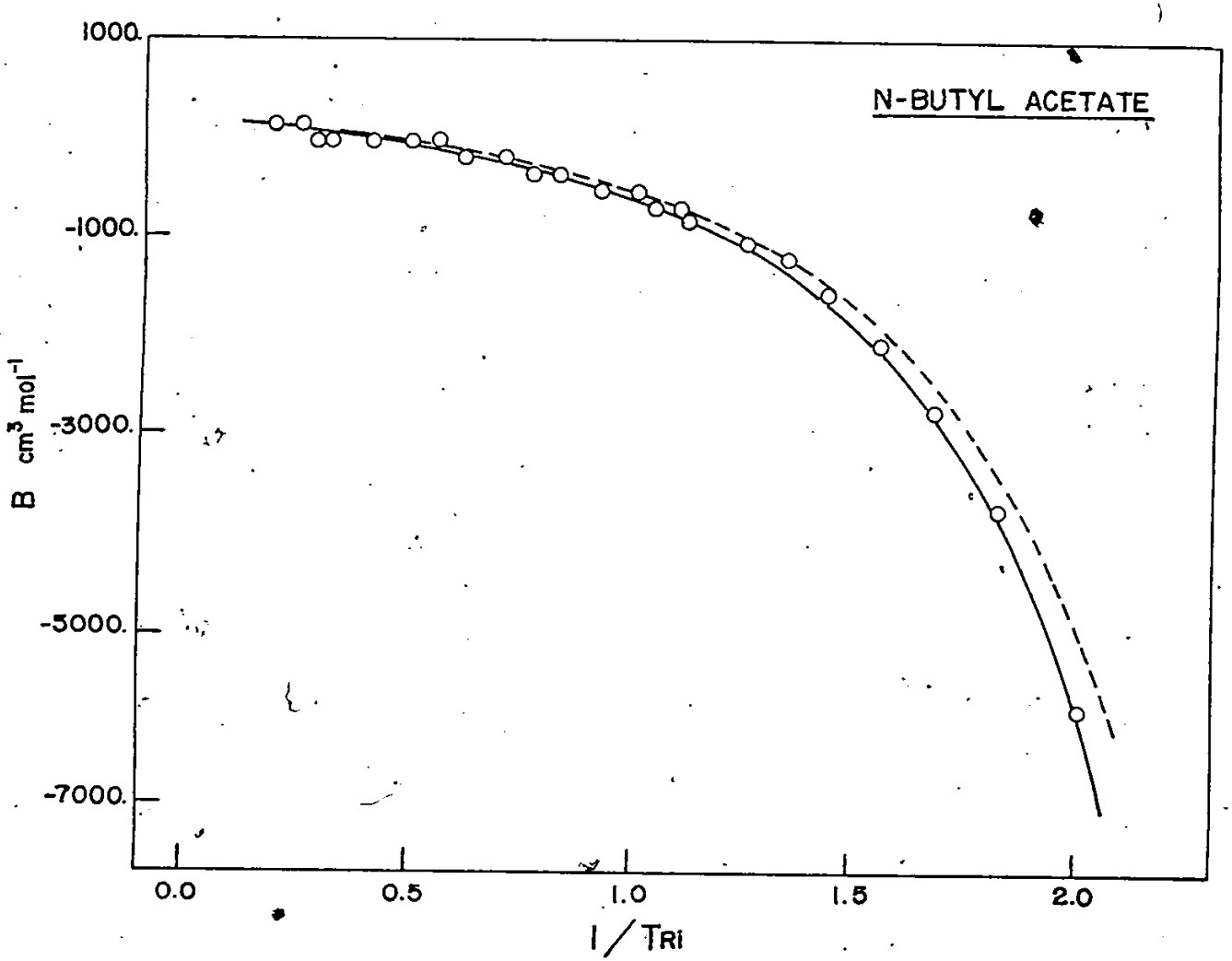

Figure 4-3 Comparisons of Experimental and Calculated Values for N-Butyl Acetate (o Experimental, —— Calculated from Equations (2.18) and (4.8), --- Calculated from Equations (2.18) and (4.9))

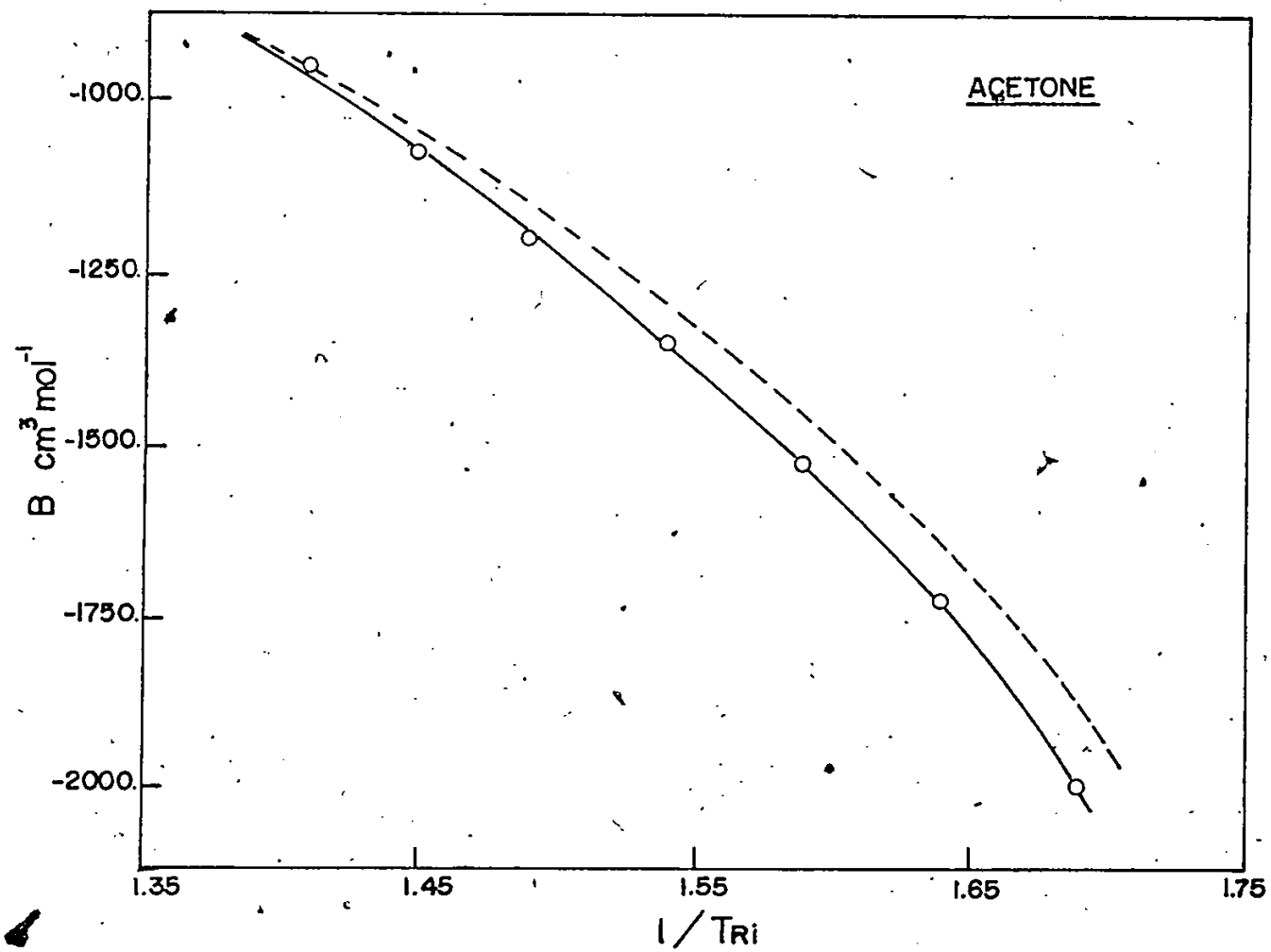

Figure 4-4 Comparisons of Experimental and Calculated Values for Acetone (o Experimental, ——— Calculated from Equations (2.18) and (4.8), ---- Calculated from Equations (2.18) and (4.9))

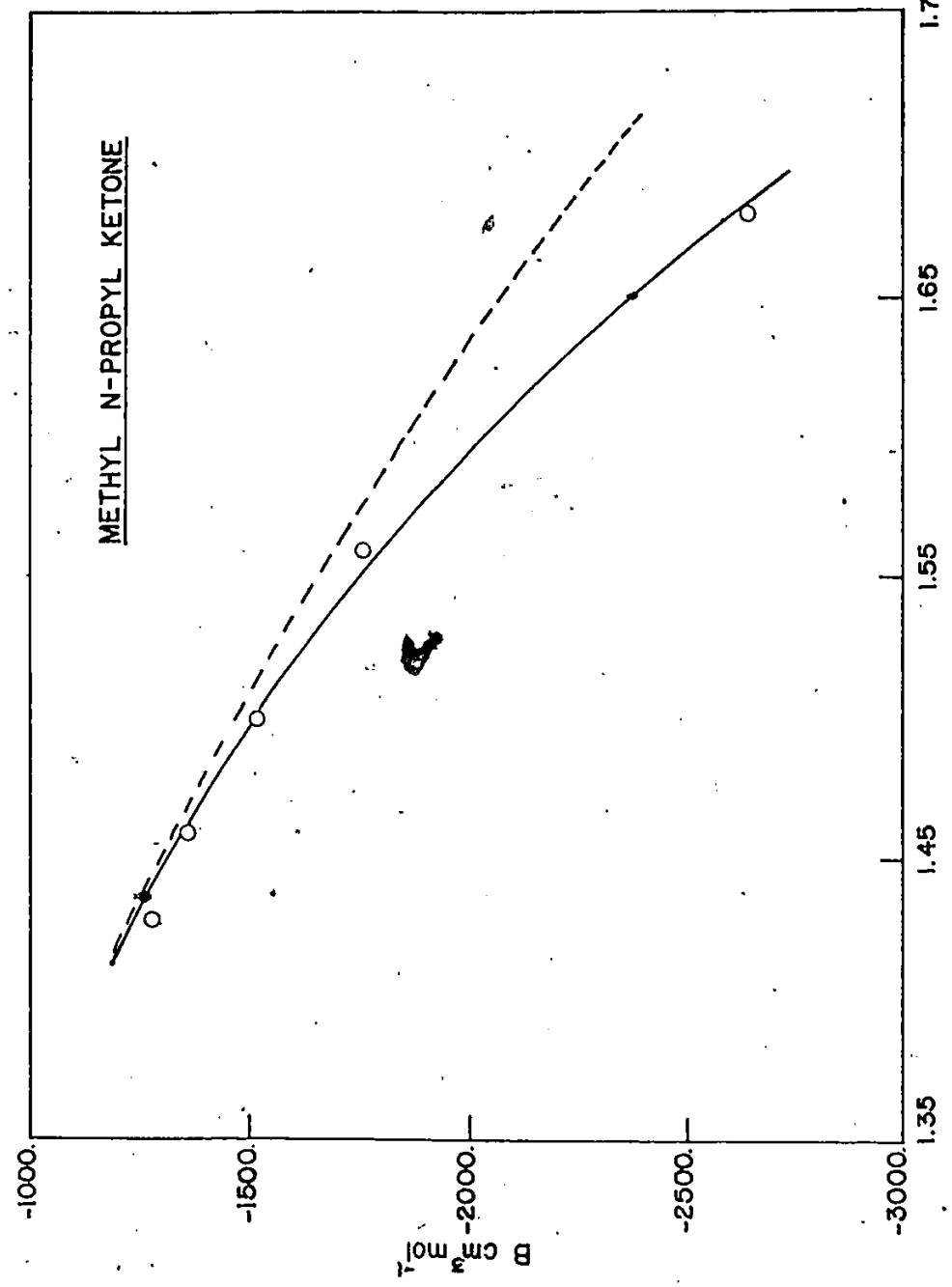

Figure 4-5 Comparisons of Experimental and Calculated Values for Methyl N-Propyl Ketone (o Experimental, ——— Calculated from Equations (2.18) and (4.8), --- Calculated from Equations (2.18) and (4.9))

Table 4-5

REDUCED TEMPERATURE RANGE AND DATA SOURCE OF SECOND VIRIAL COEFFICIENTS FOR HYDROGEN-BONDING POLAR COMPOUNDS

Substance	Number of Data	Reduced Temp. Range	Data Source
Methanol	16	0.58-1.12	(33) (38) (39)
Ethanol	6	0.61-0.76	(33) (38)
N-Propanol	4	0.70-0.79	(33)
N-Butanol	6	0.62-0.78	(33)
Iso-Propanol	12	0.66-0.93	(33)
2-Butanol	4	0.71-0.79	(33)
Iso-Butanol	4	0.72-0.80	(33)
Tert-Butanol	4	0.75-0.84	(33)

Along with this extension, the function $f^{(3)}$ was developed to account for the hydrogen-bonding effect. A similar method as mentioned in 4.2.1 was employed to obtain values of $f^{(3)}$ for each alcohol and further to find an expression for $f^{(3)}$.

In order to evaluate the contribution of $f^{(3)}$ on B, values of $f^{(3)}$ for each of the individual alcohols were obtained in terms of ΔB.

$$\Delta B = B - \frac{RT_{c_i}}{P_{c_i}} \left(f^{(0)} + \omega_i f^{(1)} + f^{(2)}\right)$$

Consequently, the quantity ΔB was plotted against $1/T_{R_i}$ as shown in Figure (4-6). It is shown that ΔB changes more drastically with temperature for $T_{R_i} \leq 0.8$ than for $T_{R_i} > 0.8$. This indicates that the behavior of $f^{(3)}$ is in good agreement with the observed behavior of the temperature dependence of the hydrogen-bonding effect. The figure further displays that it is appropriate to extend the polar correction function $f^{(2)}$ to alcohols to demonstrate their effects. In order to formulate a suitable expression for $f^{(3)}$, methanol was chosen for further analysis because there are more experimental B values reported for this compound. Therefore, values of $f^{(3)}$ for methanol were plotted against $1/T_{R_i}$ in Figure (4-7).

This figure indicates that at higher temperatures ($T_{R_i} > 0.8$), there is a tendency for the curve to approach zero as the temperature increases, and at lower temperatures ($T_{R_i} < 0.8$), the effect of temperature on $f^{(3)}$ is more profound.

According to the above analysis, a typical model of $f^{(3)}$

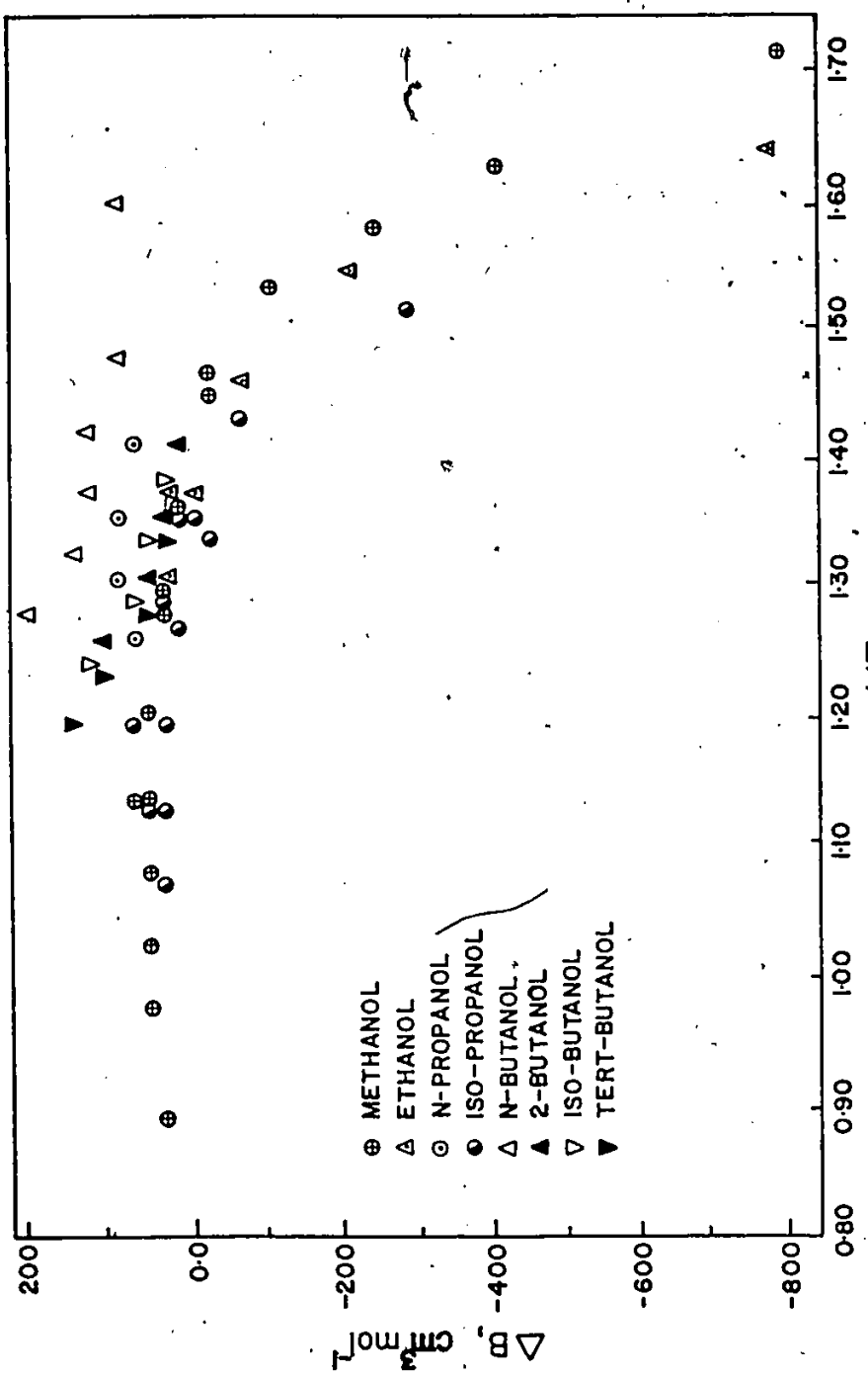

Figure 4-6 Relationship Between ΔB and $1/T_{R_i}$ for Eight Alcohols

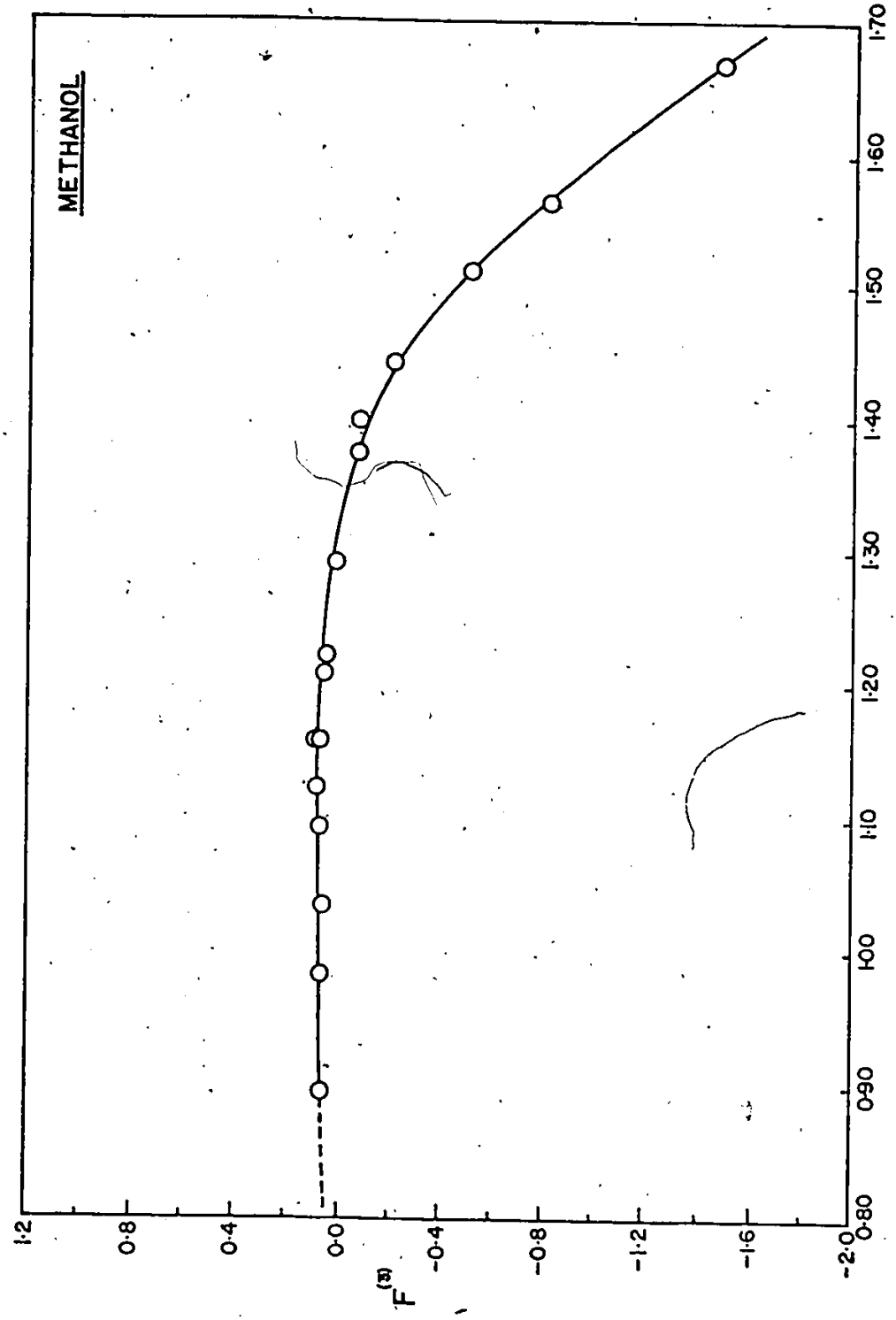

Figure 4-7 Relationship Between $f^{(3)}$ and $1/T_{R_i}$ for Methanol

was developed for each alcohol:

$$f^{(3)} = \frac{b_i}{T_{R_i}} + \left(\frac{1}{T_{R_i}} - \frac{1}{T_{R_c}}\right)\left(d_i \exp\, g_i/T_{R_i}\right) \qquad (4.12)$$

in which b_i, g_i and d_i are constants for each alcohol, and T_{R_c} is the reduced temperature at which the behavior of $f^{(3)}$ starts changing. By using an appropriate value of $1/T_{R_c}$, Equation (4.12) may accurately describe $f^{(3)}$ for all the alcohols, that is, at $T_{R_i} < 0.8$, the exponential term in Equation (4.12) predominates, while at $T_{R_i} \geq 0.8$ the linear term predominates. First of all, a trial-and-error procedure together with the Golden section search method (37) were used to obtain the values of T_{R_c}, b_i, d_i and g_i for methanol. Initially, several possible values of T_{R_c} were estimated from Figure (4-7) and used in the Golden section search method (37). The procedure used in the calculation may be described as following

1) Designate a search interval for g_i
2) Select a value for T_{R_c} in Equation (4.12)
3) Apply the Golden section search method to find a value for g_i which minimizes the RMS deviation of B. Values of b_i and d_i are thus obtained during the calculation.
4) Repeat steps (2) and (3) by using different values of T_{R_c}.

Consequently, several sets of values for T_{R_c}, g_i, b_i, d_i and RMS deviation of B were obtained. The final selection was based on the set which yields the smallest RMS deviation of second virial coefficient. The values of T_{R_c}, g_i, b_i and d_i thus obtained are 1.24, 5.5938, 0.05014 and -0.00023065, respectively.

In Figure (4-7), values of $f^{(3)}$ obtained from the experimental data of B for methanol were plotted along with the curve calculated from the Equation (4.12). The figure indicates that the equation fits the data satisfactorily over the whole temperature range.

Since Equation (4.12) gives an excellent fit of methanol, values of g_i, d_i and b_i for the other seven alcohols were determined by fixing $1/T_{R_c} = 1.24$ (i.e. $T_{R_i}=0.81$). The values of g_i, d_i, b_i and RMS deviation of B obtained from Equations (4.12) and (4.5) for eight alcohols are listed in Table (4-6).

The values of b_i and g_i for n-propanol and C_4 alcohols are much greater than those for the other alcohols. These differences caused difficulties in obtaining a generalized expression for these values.

In order to generalize Equation (4.12), it was hoped that one of the three parameters, b_i, g_i, and d_i be kept constant so that values of the other two parameters might be generalized in terms of some physical properties. Values of b_i, g_i, and d_i for methanol were used as the basis for this attempt.

By a trial-and-error method, it was found that by fixing $d_i=0.00023065$ for all the alcohols, reasonable values of b_i and g_i were obtained. Equation (4.12) was then expressed as

$$f^{(3)} = \frac{b_i}{T_{R_i}} + \left(\frac{1}{T_{R_i}} - 1.24\right)(0.00023065)\exp g_i/T_{R_i} \qquad (4.13)$$

The recalculated values of b_i and g_i are listed together with the RMS deviations of B as obtained from Equations (4.5) and (4.13)

Table 4-6

VALUES OF μ_{R_i}, b_i, d_i, g_i,

AND RMS DEVIATIONS OF B FOR ALCOHOLS

Substance	μ_{R_i}	b_i	d_i	g_i	RMS of B $cm^3 mol^{-1}$
Methanol	87.9	0.05014	-2.3065×10^{-4}	5.5938	15.4
Ethanol	68.3	0.02135	-1.4401×10^{-6}	8.8251	17.6
N-Propanol	51.2	0.02259	2.6124×10^{7}	-13.081	1.8
N-Butanol	39.8	0.1767	-1.7923×10^{-7}	-2.1523	5.4
Iso-Propanol	52.6	0.02603	-2.3110×10^{-7}	8.6906	5.6
2-Butanol	41.6	0.09351	-3.4823×10^{3}	-2.6700	2.3
Iso-Butanol	40.8	0.1006	-6.2145×10^{3}	-6.4277	4.7
Tert-Butanol	44.2	0.06691	-1.8652×10	-2.3252	9.4

Table 4-7

VALUES OF PARAMETERS IN EQUATION 4-13 AND THE PARACHORS

(P) FOR ALCOHOLS

Substance	b_i	g_i	RMS deviation of B $cm^3 mol^{-1}$	P
Methanol	0.05014	5.5938	15.4	88.8
Ethanol	0.07455	5.7764	28.4	126.8
N-Propanol	0.08943	4.4005	8.1	165.0
N-Butanol	0.02339	5.6447	28.7	203.4
Iso-Propanol	0.10540	4.4353	17.0	164.4
2-Butanol	0.06095	5.5199	13.3	201.9
Iso-Butanol	0.06925	5.5812	21.4	202.1
Tert-Butanol	0.07056	5.1979	20.4	201.3

in Table (4-7). It can be seen that the RMS deviations of B obtained are acceptable.

In this work, the parachor, $\mathcal{P}$, which has been shown to characterize the molecular structure (40) is regarded as one of the most promising physical constant to generalize b_i and g_i. Values of parachor for alcohols are listed in Table (4-7).

As shown in Figures 8 and 9, b_i and g_i are plotted against $\mathcal{P}$ respectively. A weak dependence of b_i and g_i on $\mathcal{P}$ was found. These results need to be validated when adequate and reliable data of B are available.

For the time being, the two-parameter hydrogen-bonding correction function $f^{(3)}$ is used to account for the hydrogen-bonding effect of the compounds. A complete expression for the B of hydrogen-bonding polar gases then can be expressed as follows:

$$\frac{P_{c_i} B_{ii}}{R T_{c_i}} = f^{(0)} + \omega_i f^{(1)} + f^{(2)} + f^{(3)} \qquad (4.5)$$

In Figure (4-10), the experimental and calculated values of B for ethanol were plotted against $^1/T_{R_i}$. It indicates that Equations (4.5) and (4.13) give good fit of the experimental values of B.

The comparison of this development with experimental data of B and those obtained by using the methods of O'Connell-Prausnitz (1967) and Tsonopoulos (1974), is discussed in Section 4.4.

4.3 Cross Second Virial Coefficients for Mixtures

The correlation developed here for the second virial coefficients of pure gases, provides a basis for calculating the

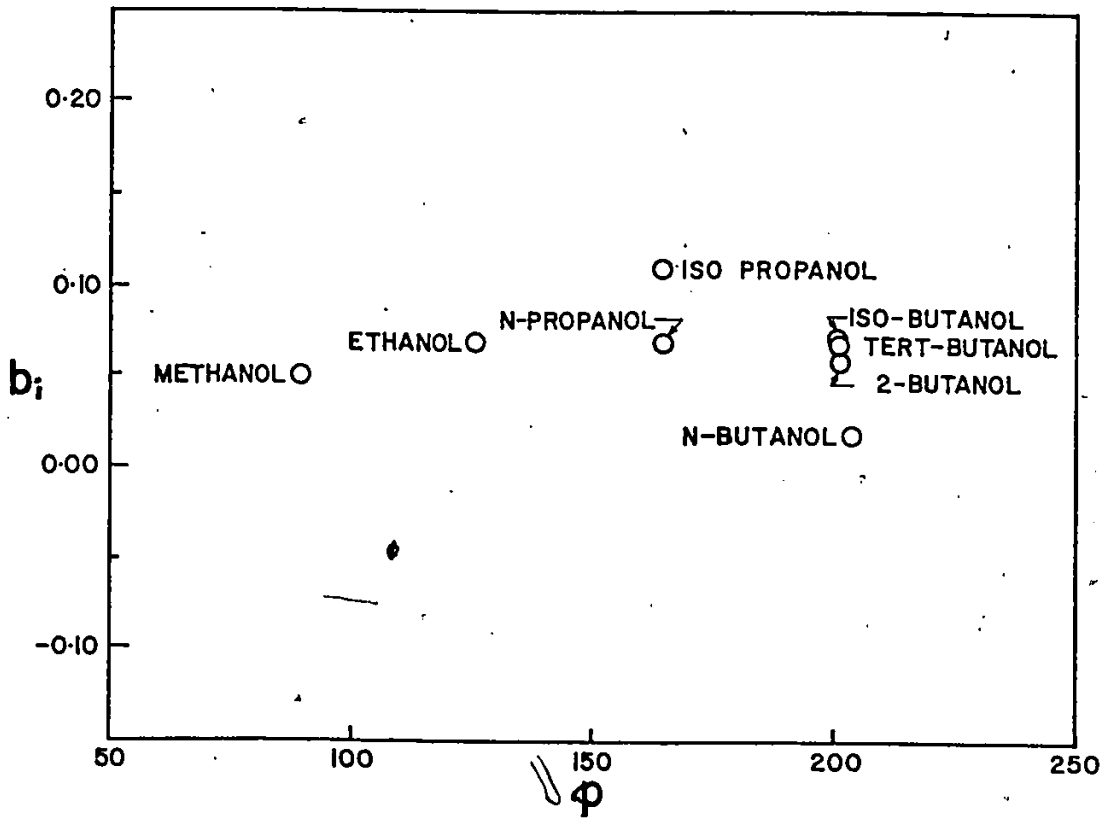

Figure 4-8 Dependence of b_i on Parachor, φ, for Alcohols

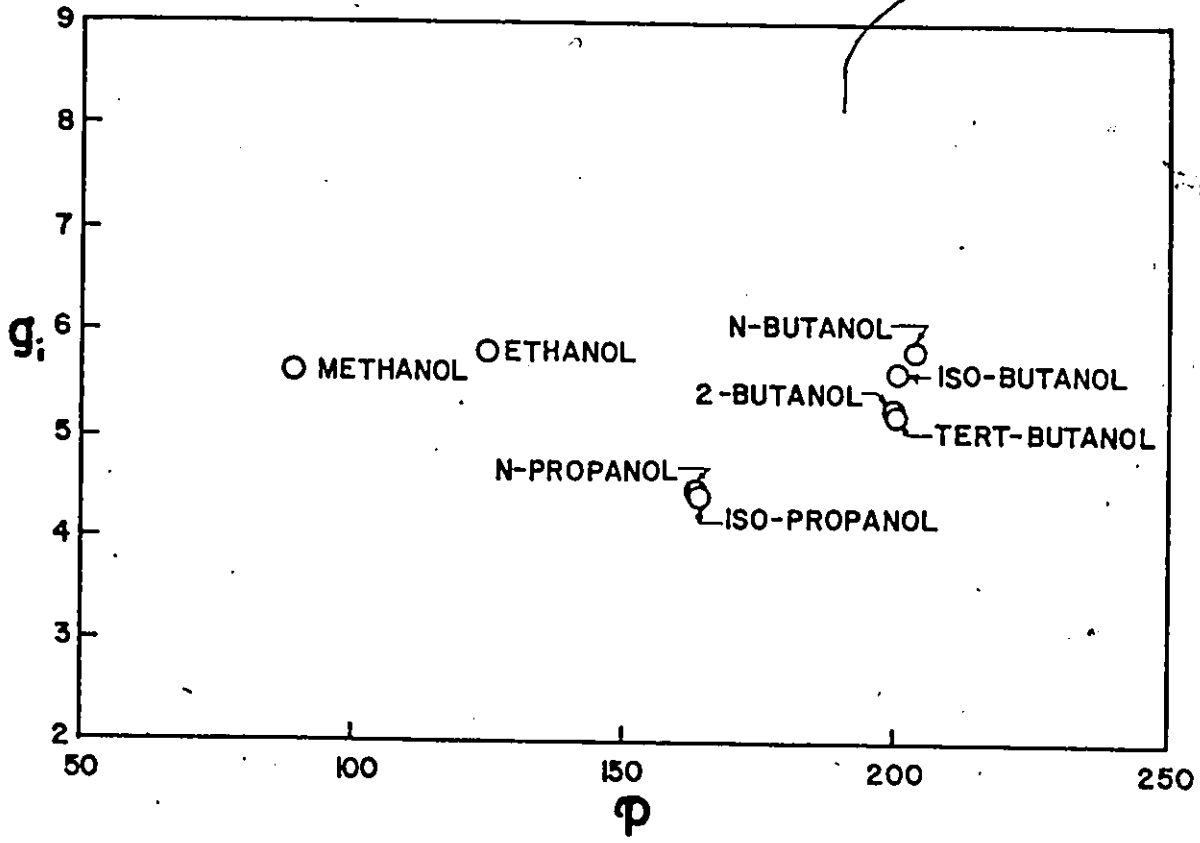

Figure 4-9 Dependence of g_i on Parachor, φ, for Alcohols

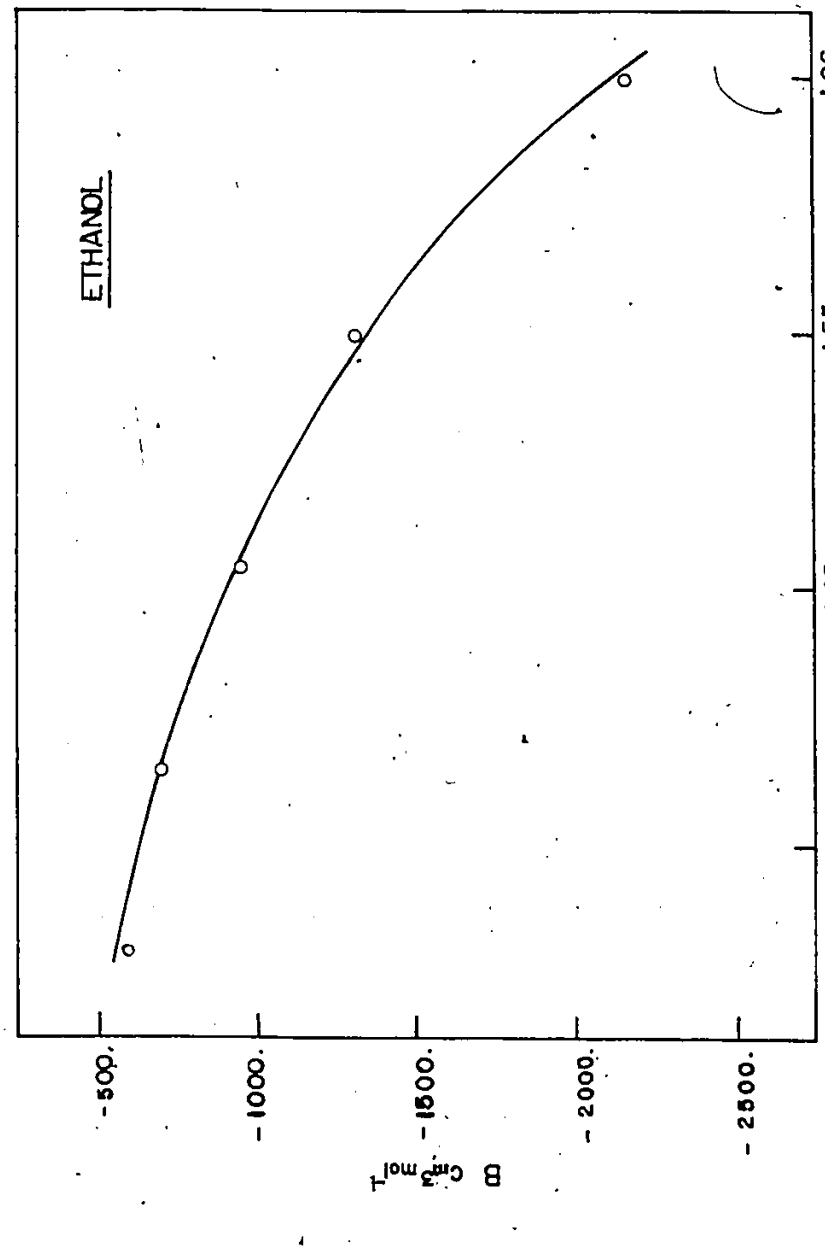

Figure 4-10 Comparison of Experimental and Calculated Values for Ethanol (o Experimental, —— Calculated)

second virial coefficient for polar-polar gaseous mixtures.

The only requirement for extending this correlation to mixtures is to determine suitable mixing rules. The cross second virial coefficient B_{ij} has the same temperature dependence as B_{ii} and B_{jj} have, but the parameters to be used with the present correlation are $P_{c_{ij}}$, $T_{c_{ij}}$, ω_{ij}, a_{ij}, b_{ij}, and g_{ij}.

There are no "universal" mixing rules, but in the absence of experimental data for a given i-j binary mixture mixing rules similar to those suggested by Prausnitz (4) were employed in this study:

$$T_{c_{ij}} = (T_{c_i} T_{c_j})^{1/2} \tag{4.14}$$

$$P_{c_{ij}} = \frac{4\, T_{c_{ij}} (P_{c_i} V_{c_i}/T_{c_i} + P_{c_j} V_{c_j}/T_{c_j})}{(V_{c_i}^{1/3} + V_{c_j}^{1/3})^3} \tag{4.15}$$

$$\omega_{ij} = 0.5\ (\omega_i + \omega_j) \tag{4.16}$$

$$a_{ij} = 0.5(a_i + a_j) \tag{4.17}$$

$$b_{ij} = 0.5(b_i + b_j) \tag{4.18}$$

$$g_{ij} = 0.5(g_i + g_j) \tag{4.19}$$

The suitability of these mixing rules needs to be further examined by the experimental data of B_{ij} for polar-polar binary mixtures

4.4 Comparisons of the Proposed Correlation with Those Proposed by O'Connell and Prausnitz (4) and Tsonopoulos (3).

The correlation proposed by o'Connell and Prausnitz and

by Tsonopoulos and the correlation developed in this study were evaluated in detail to study their relative merits in predicting second virial coefficients of pure polar substances.

Values of parameters used in the O'Connell-Prausnitz correlation and the Tsonopoulos correlation are listed in Tables (4-1) and (4-8), respectively.

The three correlations evaluated here were tested against a data set comprising of 314 experimental points for 24 polar compounds listed in Table (4-1). These 24 compounds include esters, ethers, ketones, alcohols and acetaldehyde.

The results of the evaluation study were summarized in Table (4-9). For convenience in assessing the merits of each correlation for different groups of compounds, the results have been broken down into two classes, that is, non-hydrogen-bonding polar compounds and hydrogen-bonding polar compounds.

The RMS deviations and absolute average deviations between the experimental and calculated B values were employed as the basis for comparison. Although this approach is not sufficient enough for the purpose of statistical analysis, it still offers some insight about the differences among these three correlations.

In the RMS calculations, the expression used was

$$RMS = \sqrt{\Sigma (B_{exp.} - B_{cal.})^2 / N} \qquad (4.20)$$

instead of

$$RMS = \sqrt{\Sigma (B_{exp.} - B_{cal.})^2 / (N-n)} \qquad (4.21)$$

in which, n refers to number of parameters in the correlation.

Table (4-8)

VALUES OF PARAMETERS a_{T_i} and b_{T_i} FOR EQUATION (2.22)

USED IN THE TSONOPOULOS CORRELATION

Substance	a_{T_i}	b_{T_i}
Methanol	0.0878	0.0560
Ethanol	0.0878	0.0560
N-Propanol	0.0878	0.0447
N-Butanol	0.0878	0.0367
Iso-Propanol	0.0878	0.0537
2-Butanol	0.0878	0.0487
Iso-Butanol	0.0878	0.0481
Tert-Butanol	0.0878	0.0508

Nevertheless this difference does not affect the comparison between the proposed correlation and the Tsonopoulos correlation as both correlations contain the same number of parameters. Another reason for adopting Equation (4.20) is that in some cases the number of available data points is less than the number of parameters of the generalized expression. The number of parameters used in the correlations of O'Connell and Prausnitz is larger than that of the proposed correlation. The calculated RMS deviations obtained by means of Equation (4.20) for the O'Connell and Prausnitz correlation should be less than observed by means of Equation (4.21). The RMS deviations obtained from Equation (4.20) for the O'Connell and Prausnitz correlation are generally larger than those obtained from the proposed and the Tsonopoulos correlations. Therefore, the selection of Equation (4.20) for calculating RMS deviations does not affect the conclusion of the comparison.

For non-hydrogen-bonding polar gases, the Tsonopoulos correlation is not applicable to esters, since the polarity constants (a_{T_i}) used in the correlation are only available for ethers, ketones and acetaldehyde. Likewise, the empirical parameters (association constants) used in the O'Connell-Prausnitz correlation are not available for some of the compounds shown in Table (4-1). As a result, it is not possible to have overall comparison for these three correlations. It is shown in Table (4-9) that the new correlation gives satisfactory estimations for the 16 non-hydrogen-bonding polar compounds. In prediction of B for ketones, ethers, and acetaldehyde, the deviations of the new

correlation are almost the same as those of Tsonopoulos correlation. However, the O'Connell-Prausnitz correlation gives the largest deviations among the three correlations.

The experimental and calculated B values for ethyl ether and ethyl acetate were plotted in Figures (4-11) and (4-12), respectively. It is shown in Figure (4-11) that at lower temperatures, the new correlation gives better fit to the B values of ethyl ether than the other two correlations. The O'Connell-Prausnitz correlation seems to over-correct the B values in the lower temperature range. In Figure (4-12), the new correlation fits the B values of ethyl acetate excellently over the whole temperature range from T_{R_i}=0.5 to T_{R_i}=5.0. While the O'Connell-Prausnitz correlation only gives good fit in the range between T_{R_i}=0.5 and T_{R_i}=0.95. However, the discontinuity at T_{R_i}=0.95 is because the polar correction terms in this correlation are set to zero for $T_{R_i} \geq 0.95$. The Tsonopoulos correlation is not applicable for ethyl acetate.

With respect to the available data of alcohols, the new correlation gives very accurate prediction of B. As shown in Table (4-9), the deviation of the new correlation for each alcohol falls within the experimental error range of B (i.e. $\pm$2%). However, the Tsonopoulos correlation also gives good results even though its deviations are somewhat larger than those obtained from the new correlation.

The O'Connell-Prausnitz correlation gives very poor results for alcohols, the deviations of this correlation are several

Table 4-9

COMPARISONS OF THREE CORRELATIONS WITH EXPERIMENTAL DATA FOR PURE POLAR SUBSTANCES

Non-Hydrogen-Bonding Substance	THIS WORK		TSONOPOULOS		O'CONNELL & PRAUSNITZ	
	RMS Deviation of B	Average Absolute* Deviation of B	RMS Deviation of B	Average Absolute* Deviation of B	RMS Deviation of B	Average Absolute* Deviation of B
Dimethyl ether	28.1	5.31	22.6	4.36	30.1	5.08
Ethyl ether	50.1	5.80	54.1	6.44	85.3	7.20
Aceton	74.3	4.34	47.5	2.56	241.1	12.6
Methyl ethyl ketone	71.4	2.99	111.7	5.75	105.8	7.45
Methyl n-propyl ketone	195.1	6.35	156.9	3.96	299.0	18.5
Methyl isopropyl ketone	127.7	6.61	183.4	9.68		
Diethyl ketone	63.5	3.34	13.2	0.72		
Acetaldehyde	34.6	3.21	47.8	4.11	91.4	10.6
Ethyl formate	72.1	8.65			33.6	21.3
N-propyl formate	59.5	8.08			29.4	24.3
Methyl acetate	93.7	40.5			54.1	47.7
Ethyl acetate	14.0	20.0			44.5	38.6
N-propyl acetate	17.7	13.7				
N-butyl acetate	205.5	17.5			80.0	146.2
Methyl propanoate	44.9	74.6				
Ethyl propanoate	53.1	28.2				
Hydrogen-Bonding Substance						
Methanol	15.4	1.46	26.2	2.76	205.3	33.9
Ethanol	28.4	2.25	62.9	5.19	222.0	18.0
N-propanol	8.1	1.05	15.1	1.72	22.0	2.22
N-butanol	28.7	2.68	61.4	5.52	117.0	7.94
Iso-propanol	17.0	2.16	22.2	3.64	127.2	6.45
2-butanol	13.3	1.54	14.7	1.70	51.4	4.82
Iso-butanol	21.4	2.64	23.2	2.80	96.7	9.13
Tert-butanol	20.5	2.53	33.2	4.48	72.2	7.94
Ave.**	19.1	2.04	32.4	3.48	114.2	11.2

* Average absolute deviation $= \frac{\Sigma|B_{cal.} - B_{exp.}|}{B_{exp.}} \times 100\%$.

** Over-all average values of RMS deviations or average absolute deviations for alcohols.

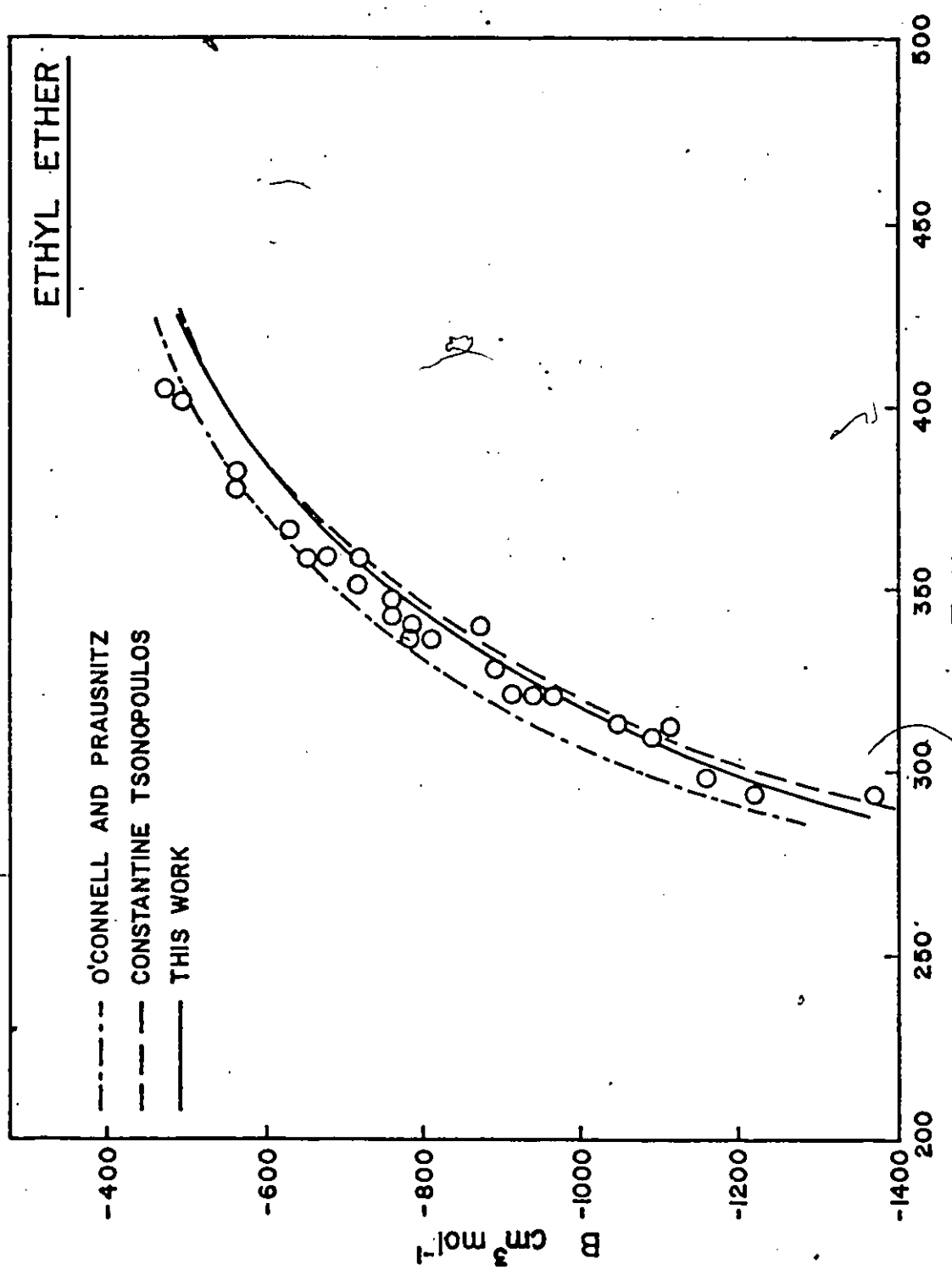

Figure 4-11 Comparisons of Calculated Results Obtained from Three Correlations with Experimental Data for Ethyl Ether. (O Experimental)

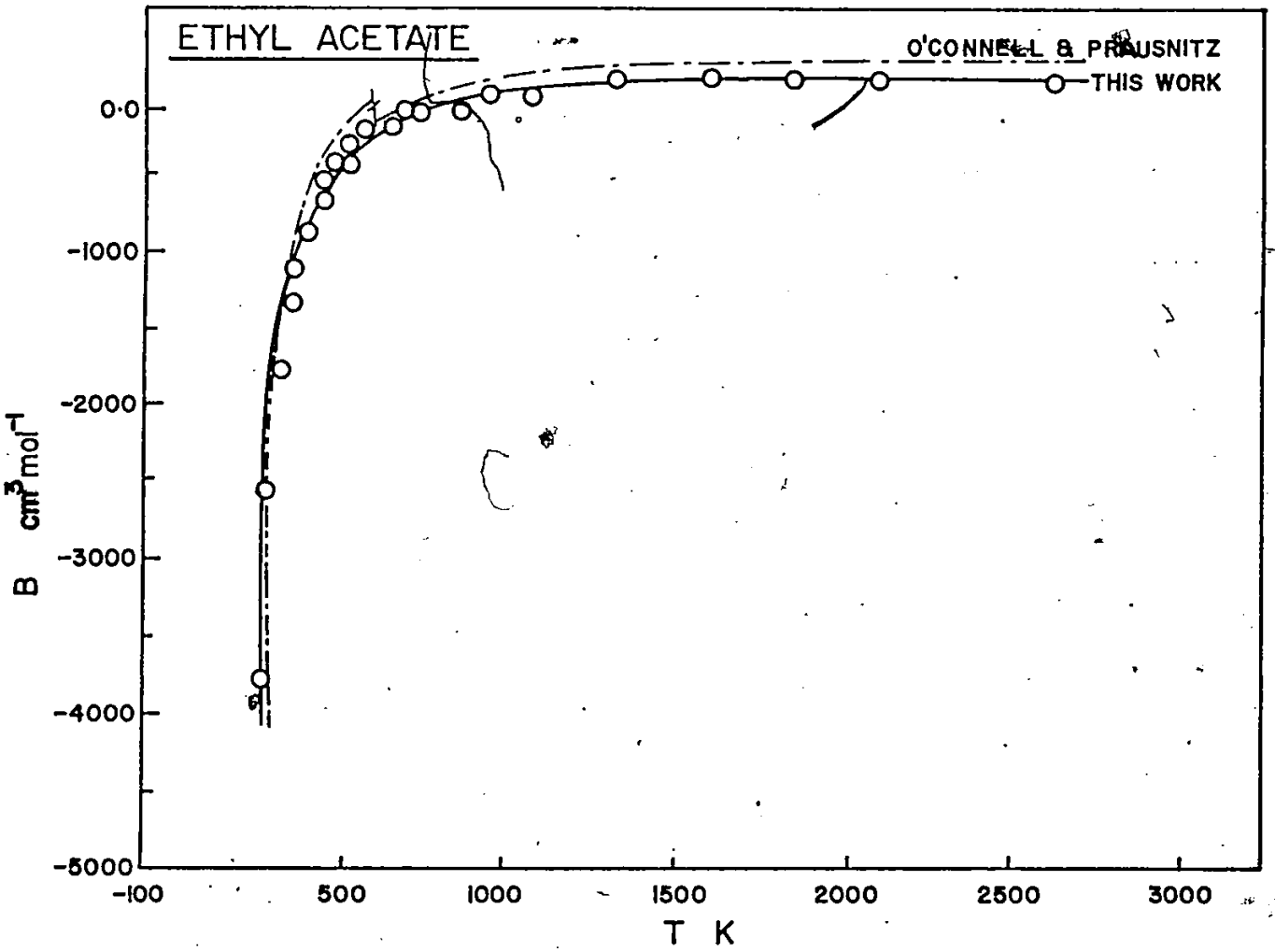

Figure 4-12 Comparisons of Calculated Results Obtained from Two Correlations with Experimental Data for Ethyl Acetate. (O Experimental)

times larger than those obtained from the new correlation and the Tsonopoulos correlation. A good example of the fit of the new correlation is illustrated in Figure (4-13) for methanol - for which we have the most extensive information. For comparison, the results from the O'Connell-Prausnitz correlation and the Tsonopoulos correlation were also plotted. It is shown that the new correlation provides an excellent fit to the data over the whole temperature range, and is somewhat more accurate than the fit provided by the Tsonopoulos correlation. While, the O'Connell-Prausnitz correlation leads to serious errors. The discontinuity in the correlation at $T_{R_i}=0.95$ is -298 $cm^3 mol^{-1}$.

4.5 Discussion and Conclusions

The values of B for methanol were used in the development of Equations (4.12) and (4.13) for representing the contribution of the hydrogen bonding effect to the B values. This choice may not be the best as it is often found that the first compound of a homologous series may differ considerably from the general behavior of the remaining series. Further justification of the proposed expression should be made when more data for second virial coefficients become available.

The calculated values of B for methyl methylacrylate by means of the proposed correlation may not be as good as desired because the correlation is a generalized one; not restricted to esters. The effect of the possible variation of B values for methyl methacrylate on the calculation of the liquid phase activity coefficients will be discussed in Chapter 6.

An empirical correlation for predicting second virial coefficients for pure polar compounds has been developed by using 314 data points of 24 polar compounds. The proposed mixing rules for estimating second virial cross coefficients need to be further examined by experimental data of B_{ij} for polar-polar binary mixtures.

In general, the present method seems to be better than those proposed by o'Connell and Prausnitz and by Tsonopoulos. It offers a good framework for further improvements.

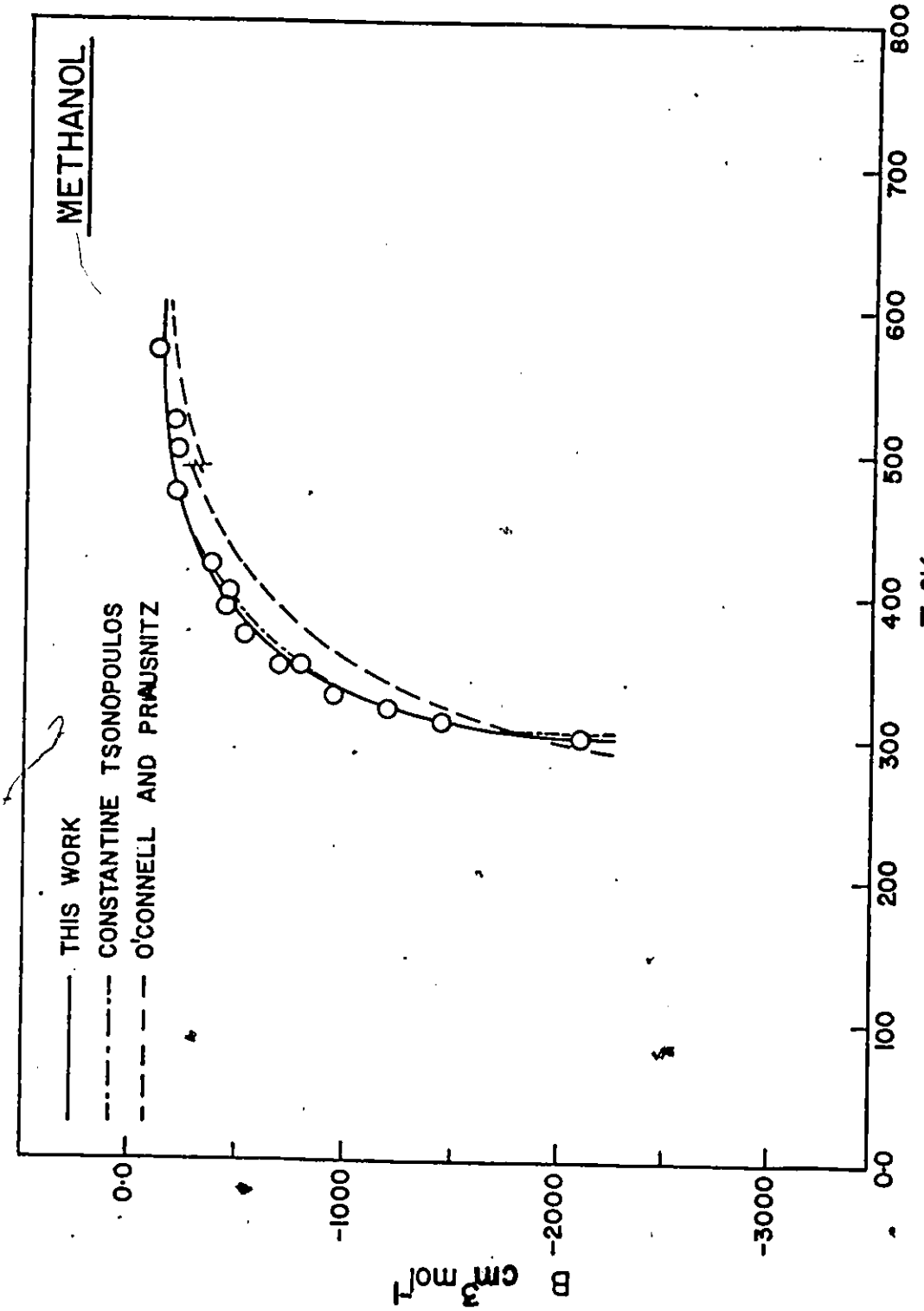

Figure 4-13 Comparisons of Calculated Results Obtained from Three Correlations with Experimental Data for Methanol. (0 Experimental)

CHAPTER 5

EXPERIMENTAL DETAILS

5.1 Materials

Aldrich analyzed grade MMA, containing 65 PPM hydroquinone monomethyl ether, supplied by Aldrich Chemical Company Inc., and absolute alcohol supplied by Canadian Industrial Alcohols and Chemicals Ltd. were used without further purification. The purity of both liquids as determined by gas chromatographic analyses was estimated to be 99.9% minimum. (The analytical results are reported in Appendix I). Physical constants of these materials are given in Table (5-1). The vapor pressure data available in the literature for pure methyl methacrylate are generally not in good agreement (41). The values obtained in this work were preferred to the literature values.

5.2 Apaparatus

5.2.1 Equilibrium Still

In this work, vapor-liquid equilibrium data were studied by means of a modified Dvorak and Boublik still which was originated from the family of the Gillespie still and has been described previously (1). Details of the design are shown in Figure (5-1). The still was made by pyrex glass.

The Cottrell pump (K) together with the recirculation loop ensured that equilibrium was achieved. The long

Table 5-1

PHYSICAL CONSTANTS OF PURE COMPONENT LIQUIDS

n^D refractive index of sodium light; ρ density and p^o, vapour pressure; V^o, molar volume

Component	n^D (298.15K) Obs.	n^D (298.15K) Lit.	ρ (298.15)/g cm^{-3} Obs.	ρ (298.15)/g cm^{-3} Lit.
Ethanol	1.35914	1.35914[42]	0.78523	0.78522[44]
Methyl methacrylate	1.41198	1.4120[43]	0.9379	0.9375[45] 0.9380[46]

	p^o Torr. 313.15K Obs.	313.15K Lit.	323.15K Obs.	323.15K Lit.	333.15K Obs.	333.15K Lit.
Ethanol	134.37	134.32[47]	221.49	221.20[47]	352.36	351.83[47]
Methyl methacrylate	75.88	75.2[48]	119.45	115.2[48]	181.91	178.6[48]

	V^o cm^{3}mol^{-1} 313.15K	323.15K	333.15K
Ethanol	59.66[44]	60.36[44]	61.09[44]
Methyl methacrylate	108.79[45]	110.20[45]	116.68[45]

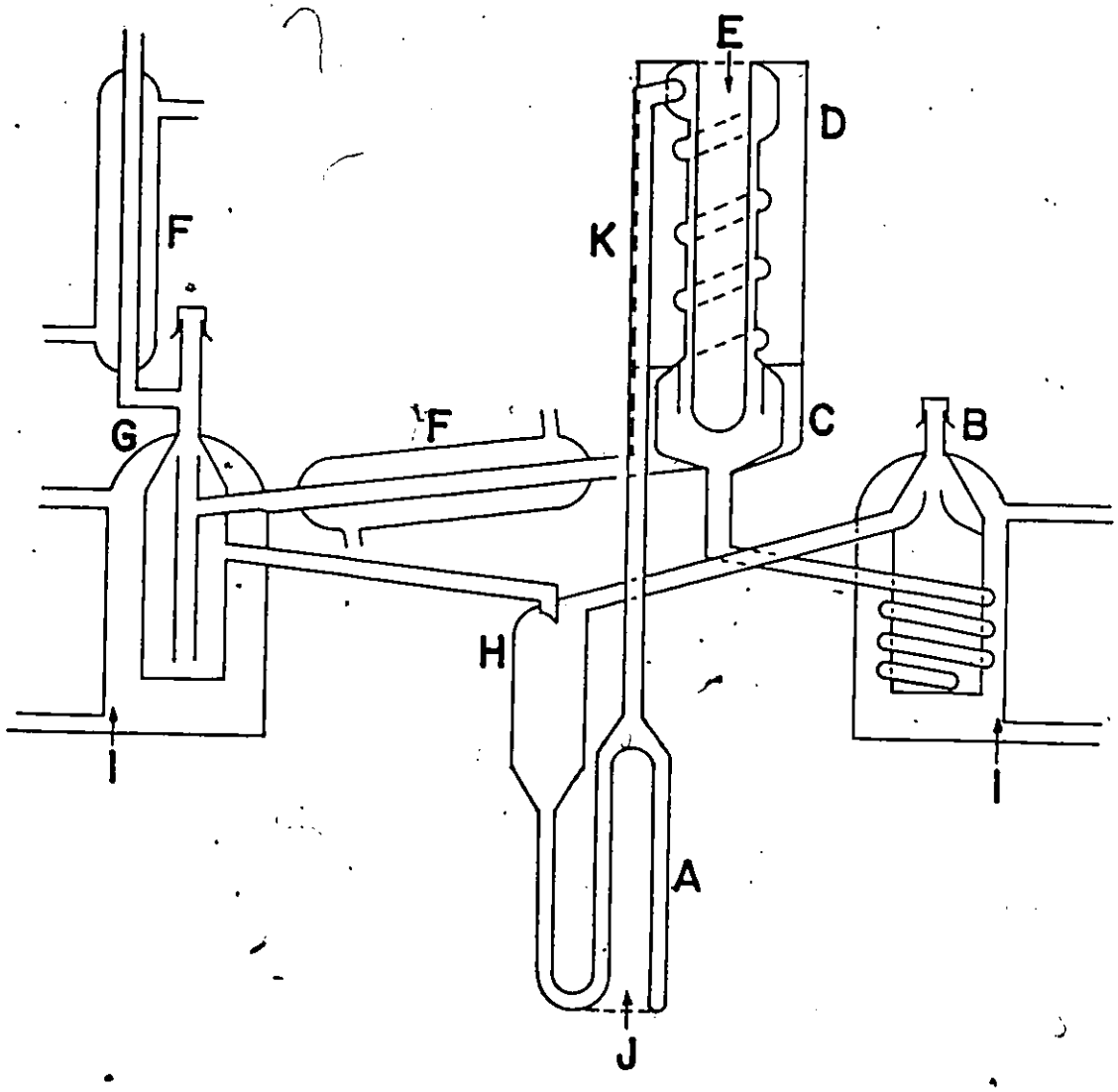

Figure 5-1 Schematic Diagram of the Modified Dvorak and Boublik Still
A boiling vessel, B liquid reservoir, C vapor and liquid separator, D evacuated chamber, E thermometer well, F condensor, G condensate reservoir, H mixing vessel, I cooling jacket, J heater well, K Cottrell pump

thermometer well (E) ensured good temperature measurement. Magnetic stirrers were placed in the liquid reservoir and the condensate reservoir, as stirring prevents any possible density gradient occurring in the reservoirs. The total amount of liquid required in the still is about 120 ml.

5.2.2 Acessory Equipment Used With Still

They are divided into two parts.

a) Temperature Measurement Device

Temperature measurement was made with a quartz thermometer, Hewlett-Packard Model 2801A, which was checked at the triple point of water. The accuracy in temperature measurements is estimated to be $\pm$ 0.01K at higher concentration of ethanol in the liquid, but to be $\pm$ 0.02K at lower concentration of ethanol. The difference in the estimated accuracy is due to the large change in P with x in the lower ethanol concentration region.

For isothermal operation, the desired temperatures 313.5, 322.15 and 333.15K were obtained and regulated by adjusting the total pressure of the system.

b) Pressure Measurement Device

A Texas Instrument Pressure Gauge (Type 144-01) together with a Bourdon Capsule (0 to 174 Kpa) was used to measure the pressure of the still. This gauge was calibrated by measuring the vapor pressure of demineralized and distilled water at different temperature using a Swietoslawski type ebulliometer (7), and checked by a mercury manometer in conjunction with a cathetometer. System pressure was controlled by a two-liquid monostate.

The accuracy of pressure measurement is estimated to be ± 0.05 Torr.

5.2.3 Equipment for Quantitative Analysis

Refractometer

A Baush and Lomb Abbe-3L precision refractometer equipped with a sodium lamp was used to determine the refractive indices of the compositions of the condensed vapor and liquid samples. The calibration values and curve which were obtained by measuring the refractive indices of mixture with known composition are reported in Appendix II. The error in the determined composition is estimated to be less than ± 0.002 mole fraction.

5.3 Experimental Procedure

5.3.1 Test of the Equilibrium Still

Before this study, a series of runs were performed on the system methanol-methyl methacrylate at 313.15, 323.15 and 333.15K, the results were in complete agreement with those of Ishikawa and Lu (41). Besides, the total vapor pressures of methanol and ethanol were measured from 303.15K to 348.15K. The results agree well with the vapor pressures calculated from the Antonine equation constants reported in the literature (47).

5.3.2 Determination of Total Pressures for the Binary Systems

a) Preparation of the Binary Liquid Mixture

For the very first run, the still was usually filled with the more volatile component, and then certain amounts of content

at both reservoirs were withdrawn and replaced by the same amount of the less volatile component for the successive runs.

b) Experimental Procedure

The boiling vessel, the liquid reservoir and the condensate reservoir were charged with the desired mixture at the beginning of each run. Pressure was adjusted manually to obtain the desired temperature in the equilibrium chamber.

The boiling of the liquid was continued for 2½ hours at the desired temperature to ensure attainment of equilibrium, and then after recording the system pressure and temperature, discontinued by a sudden increase of pressure to the atmosphere. Samples of the liquid and the condensed vapor were taken and their refractive indices were measured. Equilibrium temperature was maintained within $\pm$ 0.005K for liquid solutions rich in the more volatile component, and otherwise maintained within $\pm$ 0.02K.

An attempt was made to detect the possible occurrence of polymerization of MMA throughout this work. There was no change of density of pure MMA after boiling for 5 hours, and no manifestation of haziness or turbidity was observed when the boiled monomer was subject to the solvent test of Luskin (43). In determination of vapor-liquid equilibrium data, pure ethanol was used as the initial solution in one series of runs while pure MMA in another. The results obtained from both series are in good agreement. It appears that the volatility of the shipping inhibitor is adequate for preventing the polymerization of MMA in the condensed vapor.

CHAPTER 6

RESULTS AND DISCUSSION

The experimentally determined values of P, T, x_i and y_i together with liquid phase activity coefficients γ_i^L evaluated from Equation (3.5) and the corresponding Gibbs free energy G^E evaluated from Equation (3.6) at each of the three temperatures studied (313.15, 323.15 and 333.15K) are listed in Table (6-1). The second virial coefficients (B_{11} and B_{22}) and the cross second virial coefficients (B_{12}) for the ethanol - MMA system were calculated by the correlation developed in Chapter 4. At the temperatures 313.15, 323.15 and 333.15K the values obtained for B_{11} are -2116, -1662, and -1342, for B_{22}, -2543, -2258, and -2021; and for B_{12}, -1860, -1639, and -1456 cm^3mol^{-1}, respectively.

As discussed in Chapter 4, the B values for ethanol calculated from the generalized correlation are acceptable. However, the validity of the predicted B values for methyl methacrylate cannot be directly confirmed because there is no data available in the literature. An attempt was made to estimate the possible variations of B_{22} (for MMA), and its effect on the calculation of γ_1^L and γ_2^L.

The reduced temperature range of B values used to develop the proposed correlation is from 0.5 to 5.0. It was found that the deviations between the calculated and the literature results of B increase with decreasing temperature, and the maximum deviation is about 35% at T_{R_i}=0.5. Based on this result,

calculations were made by varying the B_{22} value (for MMA) at 323.15K by ± 20%, ± 40%, and ± 50%. These values were then used in Equation (3.5) to evaluate γ_1^L and γ_2^L. The results were then compared with those obtained previously.

The variations of the γ_1^L values are less than those of the γ_2^L values, and the greatest variation of γ_2^L is ± 0.44% when B_{22} value is varied by ±50%, but reduced to ± 0.18% when B_{22} value is varied by ± 20%. On the right-hand side of Equation (3.5), the contribution of the last two terms, which contain the second virial coefficients is much less important than that of the first term. Because only the B_{22} value is varied, γ_1^L is only affected slightly by the third term, however, γ_2^L is affected by both of the last two terms.

These calculated results indicate that even with a variation of 50% in the second virial coefficient of methyl methacrylate, the changes in the calculated γ^L values are negligible.

The thermodynamic consistency of the data was tested by the area test of Redlich and Kister (2) as shown in Figures (6-1) to (6-3). The net area obtained is less than 1% of the total area for each of the isotherms.

The values of γ_i^L and G^E were correlated by means of the three-constant Redlich-Kister Equations (3.9), (3.10) and (3.8). The parameters B_{12}, C_{12} and D_{12} were determined by the least-squares method and the values obtained are listed below:

Redlich-Kister parameters

	313.15	323.15	333.15
B_{12}	0.5273	0.4987	0.4722
C_{12}	0.0041	0.0098	0.0134
D_{12}	0.0213	0.0156	0.0108

To illustrate the agreement obtained, the calculated and the experimental values of log (γ_1^L/γ_2^L), log γ_1^L, log γ_2^L and G^E at three temperatures are compared in Figures (6.1) to (6.9). In addition, the calculated values of y_i, P at given T and x_i which were obtained by means of the Newton-Raphson method are compared with the experimental values in Figures (6-10) to (6-13). In Table (6-2), the calculated values of y_1, P, γ_1^L, and G^E are listed together with the experimental values of x_1. Values of the average absolute deviations between the calculated and the experimental G^E, γ_1^L, γ_2^L, y and P are listed in Table (6-3).

An azeotrope exists in the binary mixture at the three temperatures studied. The calculated azeotropic compositions and pressures at these temperatures agree well with those values obtained graphically as shown in Table (6-4).

Table 6-1

ISOTHERMAL VAPOR-LIQUID EQUILIBRIUM RESULTS FOR ETHANOL (1) + METHYL METHACRYLATE (2): p, TOTAL PRESSURE; x, LIQUID MOLE FRACTION; y, VAPOR MOLE FRACTION; γ_1^L ACTIVITY COEFFICIENT; AND G^E, EXCESS GIBBS FREE ENERGY

P/Torr.	x_1	y_1	γ_1^L	γ_2^L	G^E/J mol^{-1}
			T = 313.15K		
141.15	0.9400	0.9000	1.0051	3.0905	128.64
144.29	0.8898	0.8448	1.0186	2.6669	324.07
146.32	0.8320	0.7958	1.0405	2.3322	456.38
147.31	0.7598	0.7498	1.0808	2.0109	590.63
146.42	0.6388	0.6890	1.1746	1.6513	789.28
143.75	0.5243	0.6420	1.3098	1.4166	799.90
140.07	0.4252	0.6043	1.4822	1.2629	785.01
134.04	0.9331	0.5501	1.7653	1.1472	706.81
127.79	0.2388	0.5038	2.0112	1.0918	608.53
127.20	0.2338	0.5000	2.0294	1.0880	599.11
118.01	0.1569	0.4323	2.4290	1.0423	453.59
117.07	0.1524	0.4260	2.4450	1.0401	441.43
104.33	0.0912	0.3218	2.7557	1.0226	293.67
101.27	0.0793	0.2960	2.8309	1.0174	256.24
87.31	0.0320	0.1543	3.1597	1.0038	105.42
			T = 323.15K		
230.55	0.9380	0.9068	1.0069	2.8816	193.54
234.51	0.8873	0.8528	1.0180	2.5440	325.18
236.83	0.8285	0.8070	1.0418	2.2118	456.90
237.38	0.7558	0.7620	1.0818	1.9204	587.84
235.03	0.6360	0.7028	1.1735	1.5908	727.51
229.83	0.5210	0.6528	1.3021	1.5811	785.03
223.16	0.4238	0.6120	1.4583	1.2461	770.25
212.38	0.3115	0.5593	1.7276	1.1281	680.60
201.46	0.2388	0.5078	1.9432	1.0819	587.14
200.68	0.2338	0.5053	1.9675	1.0762	576.28
184.04	0.1530	0.4270	2.3251	1.0363	429.26
159.03	0.0832	0.2970	2.5870	1.0166	253.03
137.48	0.0330	0.1543	2.9307	1.0045	107.30

T = 333.15K

363.91	0.9360	0.9118	1.0054	2.7241	191.50
368.35	0.8870	0.8638	1.0171	2.4089	316.83
370.66	0.8252	0.8170	1.0405	2.1037	450.79
370.31	0.7540	0.7723	1.0756	1.8571	574.04
364.78	0.6535	0.7143	1.1671	1.5404	709.72
355.15	0.5183	0.6630	1.2903	1.3404	762.68
343.66	0.4220	0.6200	1.4354	1.2251	747.49
325.40	0.3136	0.5643	1.6677	1.1212	661.65
306.55	0.2353	0.5088	1.8903	1.0705	559.34
307.46	0.2375	0.5115	1.8882	1.0708	562.63
279.99	0.1560	0.4285	2.1980	1.0329	416.01
244.28	0.0872	0.3063	2.4597	1.0145	253.82
208.83	0.0349	0.1560	2.6840	1.0013	98.84

Table 6-2

CALCULATED RESULTS OF y_1, P, γ_1^L, γ_2^L and G^E, TOGETHER WITH EXPERIMENTAL VALUES OF x_1

P/Torr.	x_1	y_1	γ_1^L	γ_2^L	G^E/J mol^{-1}
		T = 313.15K			
140.82	0.9400	0.9022	1.0052	3.0150	185.13
144.01	0.8898	0.8453	1.0172	2.6533	319.54
146.66	0.8320	0.7963	1.0393	2.3221	452.12
147.02	0.7598	0.7503	1.0794	2.0031	585.70
146.23	0.6388	0.6930	1.1798	1.6279	733.42
143.61	0.5243	0.6481	1.3209	1.3912	788.99
139.88	0.4252	0.6088	1.4913	1.2467	772.59
133.18	0.3113	0.5543	1.7672	1.1294	679.78
126.75	0.2388	0.5070	2.0075	1.0761	578.73
126.22	0.2338	0.5032	2.0265	1.0730	570.53
116.12	0.1569	0.4282	2.3678	1.0332	423.96
115.40	0.1524	0.4226	2.3911	1.0314	414.17
103.52	0.0912	0.3241	2.7533	1.0114	267.45
100.70	0.0793	0.2982	2.8351	1.0087	235.92
87.33	0.0320	0.1565	3.2048	1.0014	100.68
		T = 323.15K			
229.86	0.9380	0.9080	1.0052	2.8364	186.84
233.87	0.8873	0.8543	1.0170	2.5114	319.04
236.22	0.8285	0.8067	1.0388	2.2091	450.00
236.86	0.7558	0.7615	1.0779	1.9181	579.89
234.49	0.6360	0.7047	1.1740	1.5772	719.82
229.32	0.5210	0.6581	1.3097	1.3571	770.75
222.60	0.4238	0.6175	1.4676	1.2255	751.82
210.90	0.3115	0.5602	1.7183	1.1182	659.85
199.82	0.2388	0.5098	1.9349	1.0690	559.96
198.92	0.2338	0.5057	1.9518	1.0661	551.91
181.21	0.1536	0.4225	2.2655	1.0286	401.75
158.18	0.0832	0.3018	2.6252	1.0085	236.65
137.18	0.0330	0.1552	2.9466	1.0014	99.36

T = 333.15K

363.29	0.9360	0.9132	1.0052	2.6758	188.02
367.74	0.8870	0.8643	1.0161	2.3954	312.65
370.11	0.8252	0.8163	1.0380	2.1088	445.68
369.78	0.7540	0.7729	1.0749	1.8490	570.03
364.40	0.6335	0.7153	1.1675	1.5332	705.77
354.87	0.5183	0.6672	1.2974	1.3284	752.82
343.21	0.4220	0.6251	1.4453	1.2070	731.87
324.13	0.3135	0.5670	1.6690	1.1101	643.48
304.39	0.2353	0.5098	1.8805	1.0611	537.33
305.03	0.2375	0.5117	1.8739	1.0623	540.80
276.53	0.1560	0.4250	2.1533	1.0267	393.15
243.04	0.0872	0.3071	2.4530	1.0084	237.88
209.44	0.0349	0.1584	2.7319	1.0014	100.79

Table 6-3

DEVIATIONS BETWEEN THE CALCULATED AND EXPERIMENTAL VALUES
$\Sigma |\Delta X| / N$

X	313.15K	323.15K	333.15K
G_L^E/J mol^{-1}	16.0	14.8	11.3
γ_1^L	0.0137	0.0129	0.0113
γ_2^L	0.0174	0.0148	0.0122
y^2	0.0029	0.0023	0.0019
P/Torr.	0.61	0.99	1.13

Table 6-4

AZEOTROPIC DATA FOR THE ETHANOL (1) - METHYL METHACRYLATE (2) SYSTEM

Temperature K	Azeotropic Composition mole fraction of ethanol		Azeotropic Pressure Torr.	
	exp.	calc.	exp.	calc.
313.15	0.738	0.739	370.99	370.31
323.15	0.769	0.769	237.50	236.89
333.15	0.799	0.799	370.99	370.31

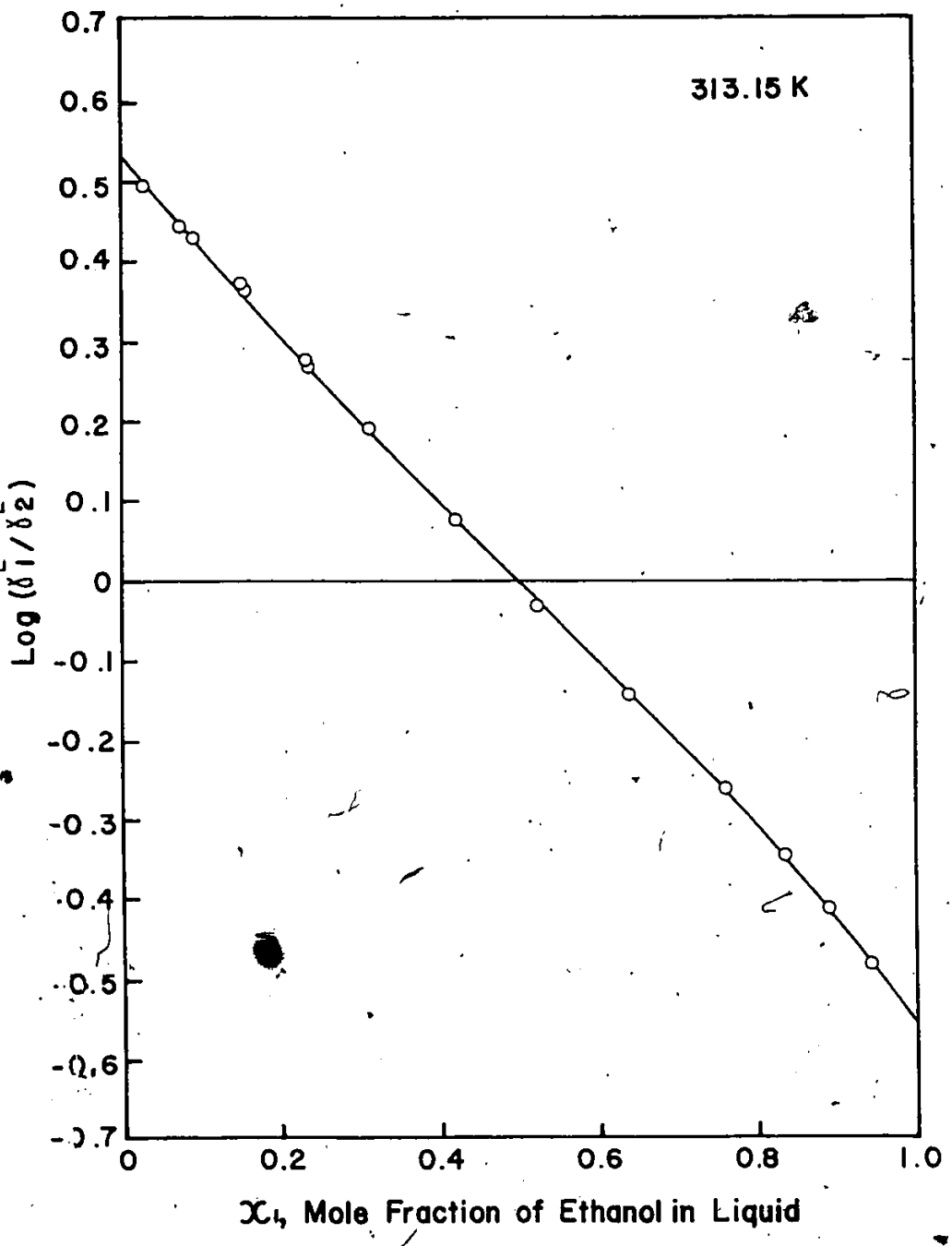

Figure 6-1 Thermodynamic Consistency Test of Vapor-Liquid Equilibrium Data for Ethanol (1) - Methyl Methacrylate (2) System at 313.15K

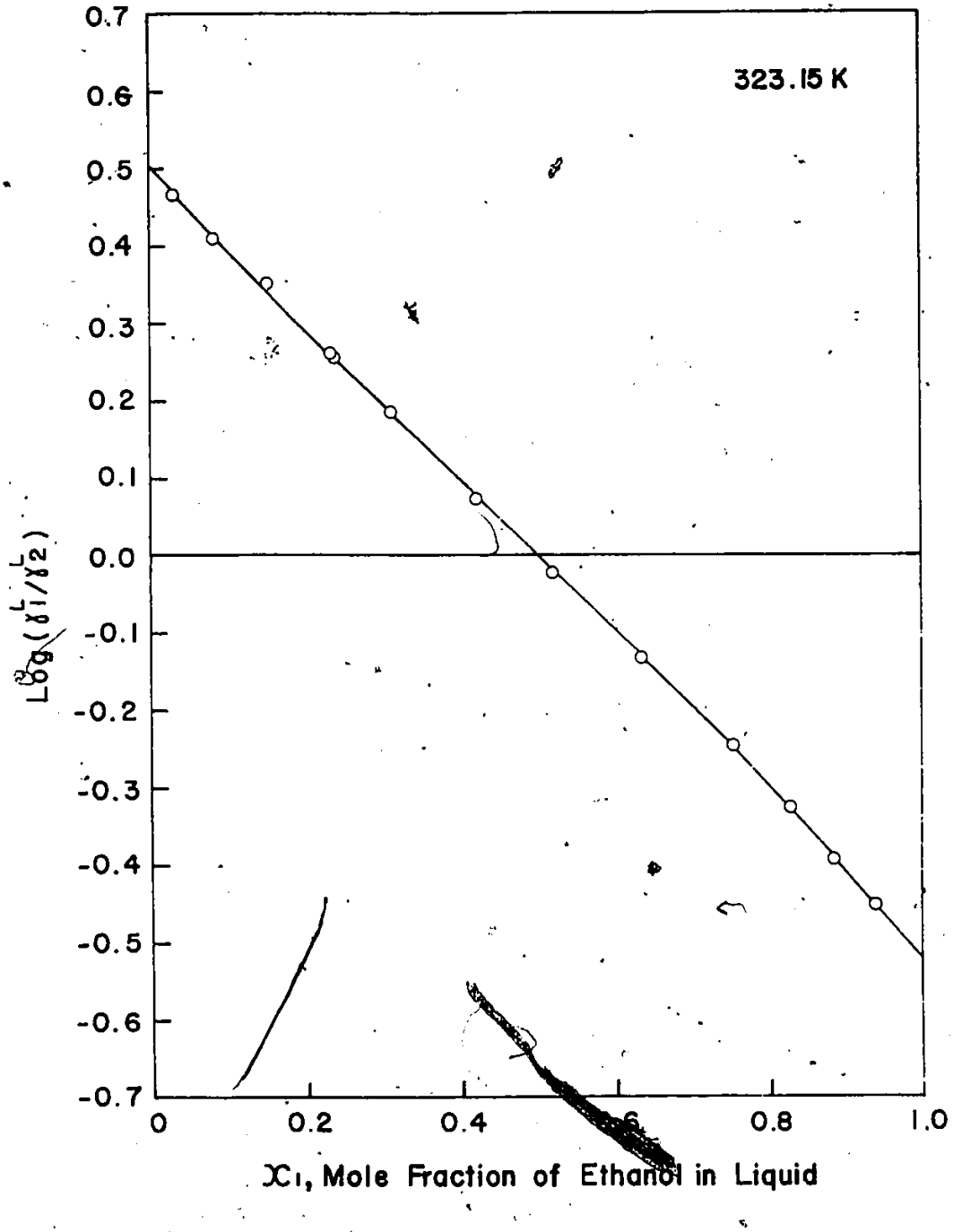

Figure 6-2 Thermodynamic Consistency Test of Vapor-Liquid Equilibrium Data for Ethanol (1) - Methyl Methacrylate (2) System at 323.15K

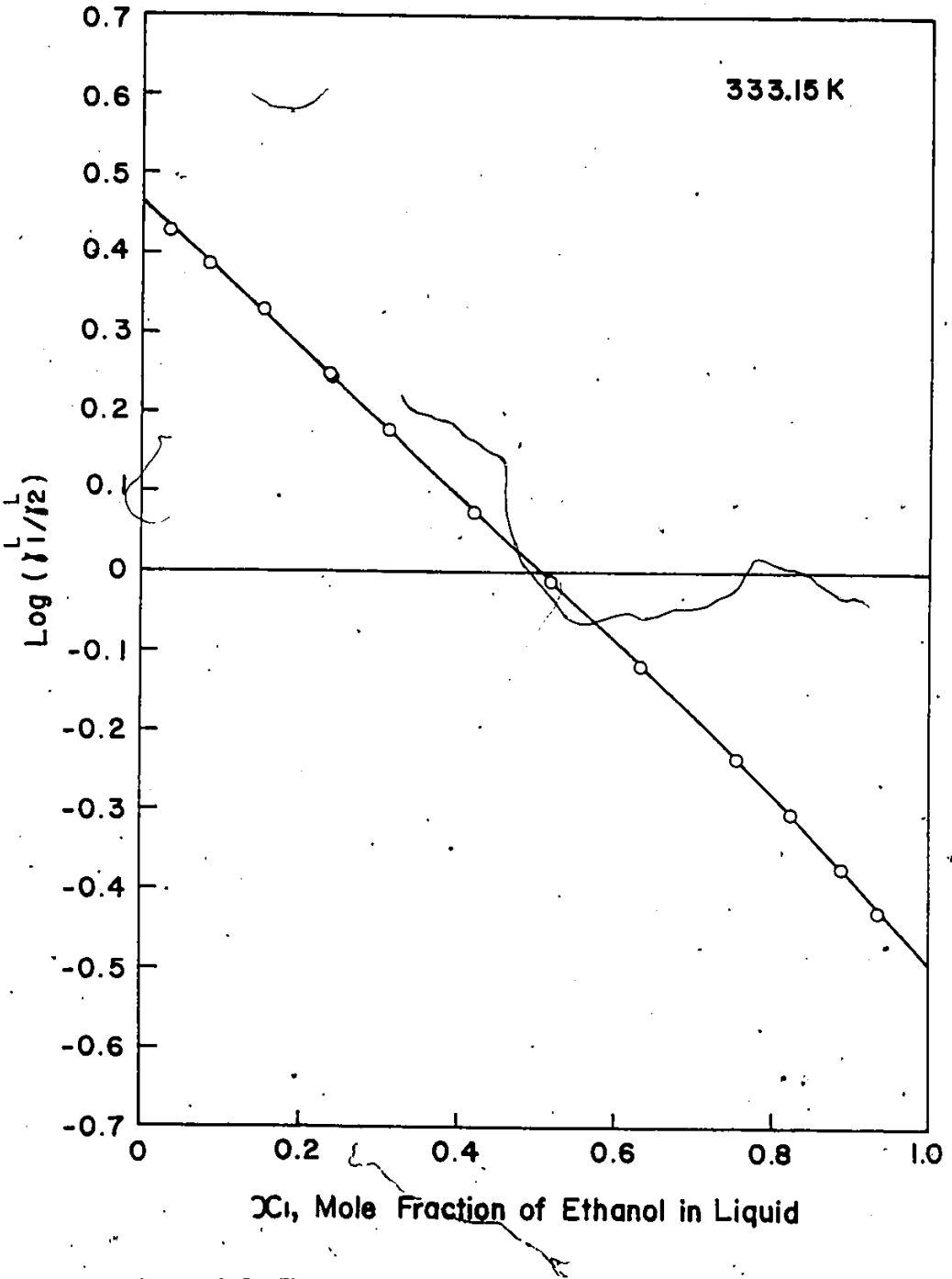

Figure 6-3 Thermodynamic Consistency Test of Vapor-Liquid Equilibrium Data for Ethanol (1) - Methyl Methacrylate (2) System at 333.15K

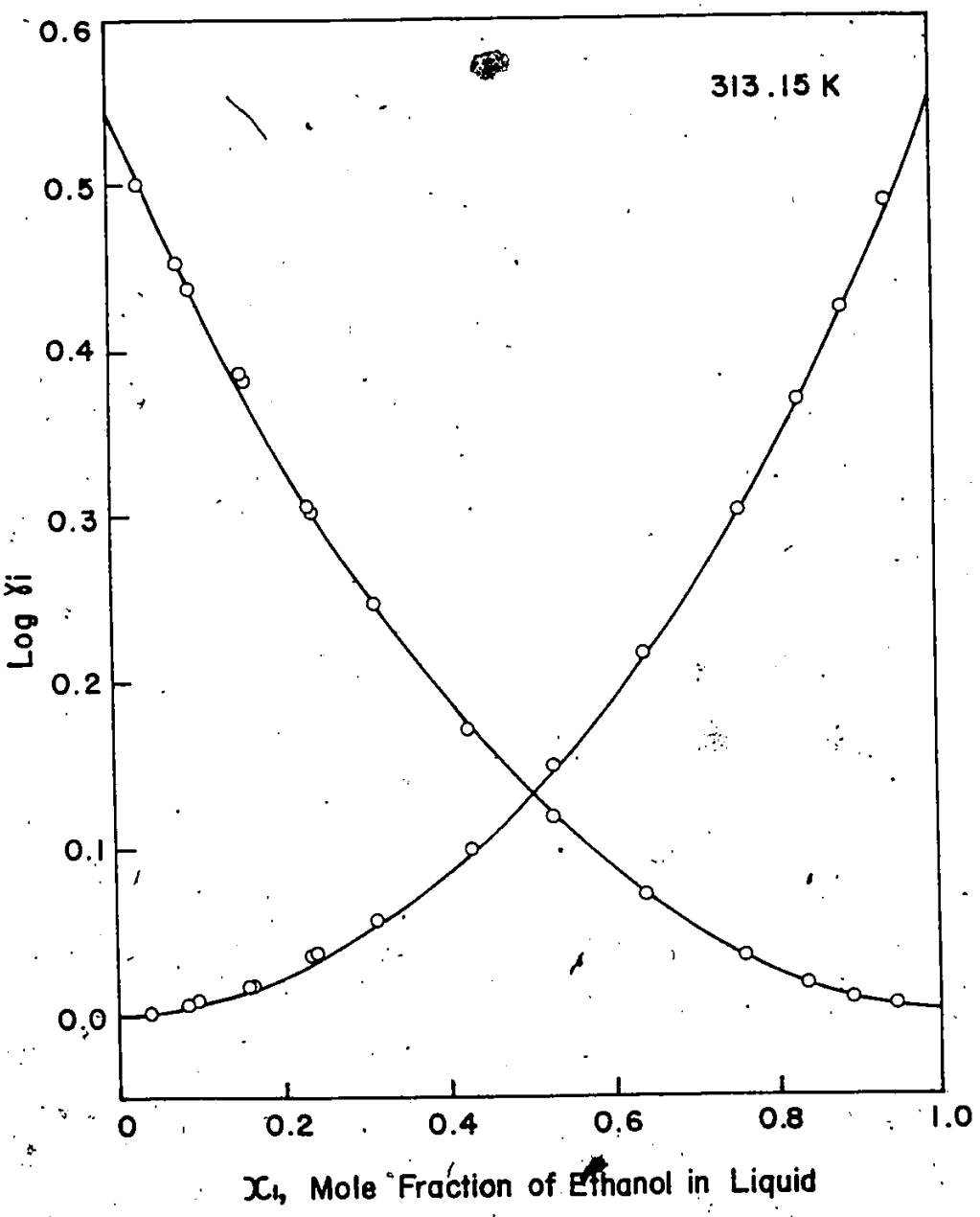

Figure 6-4 Comparison of Calculated and Experimental γ_i^L Values for Ethanol (1) - Methyl Methacrylate Methacrylate (2) System at 313.15K. (0, Experimental, - Calculated)

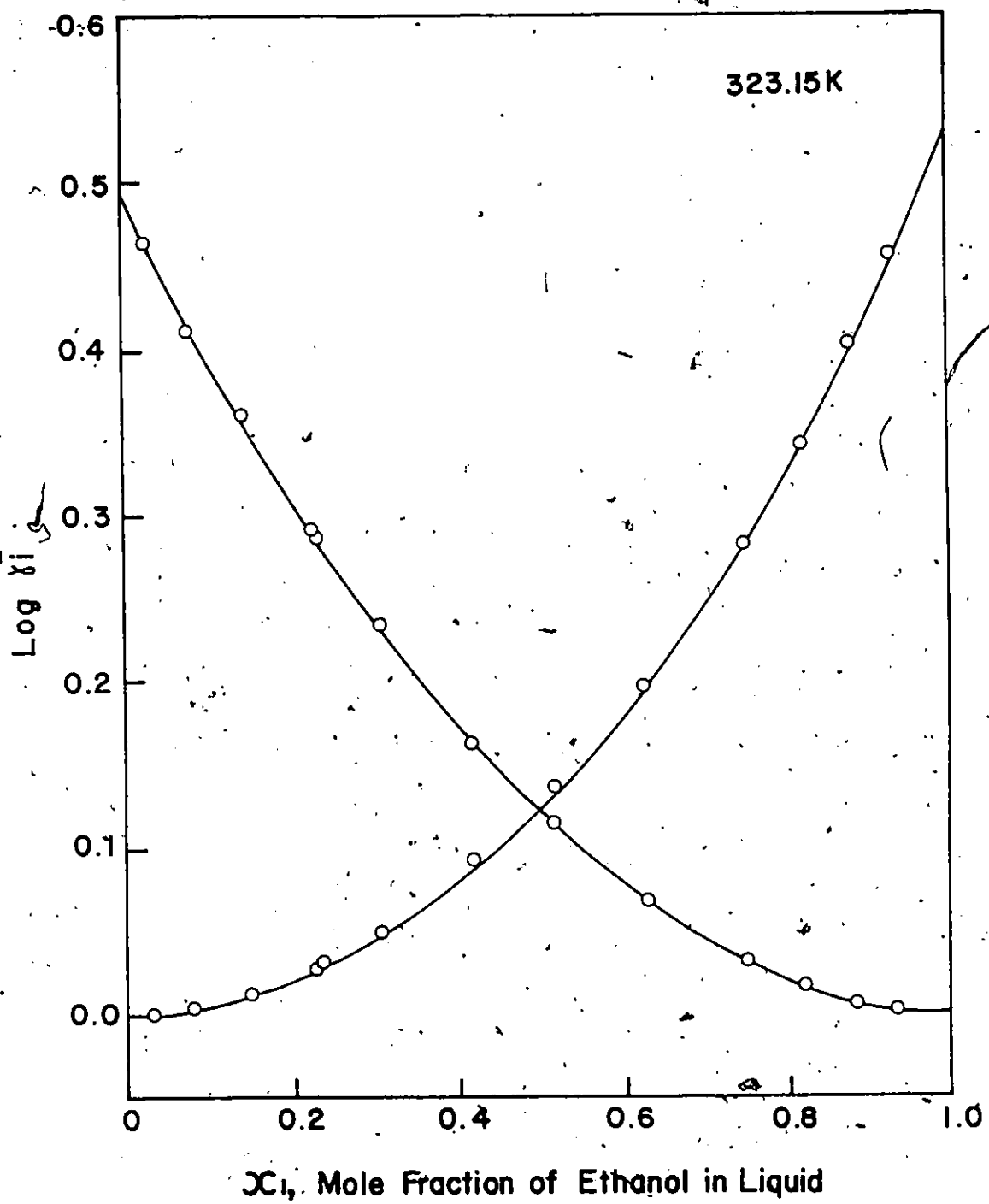

Figure 6-5 Comparison of Calculated and Experimental γ_i^L Values for Ethanol (1) - Methyl Methacrylate (2). System at 323.15K. (0, Experimental, - Calculated)

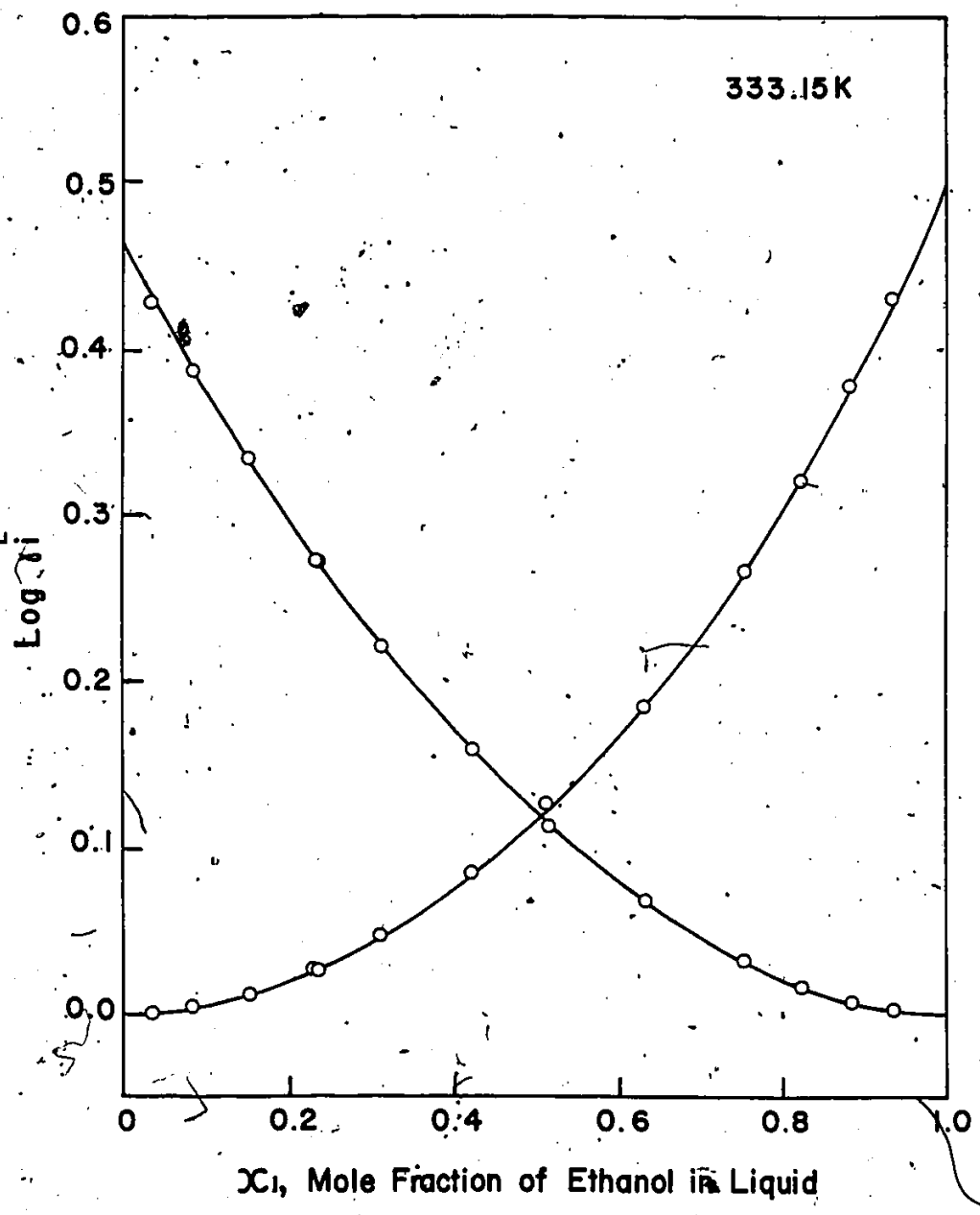

Figure 6-6 Comparison of Calculated and Experimental γ_i^L Values for Ethanol (1) - Methyl Methacrylate (2) System at 333.15K. (0, Experimental, - Calculated)

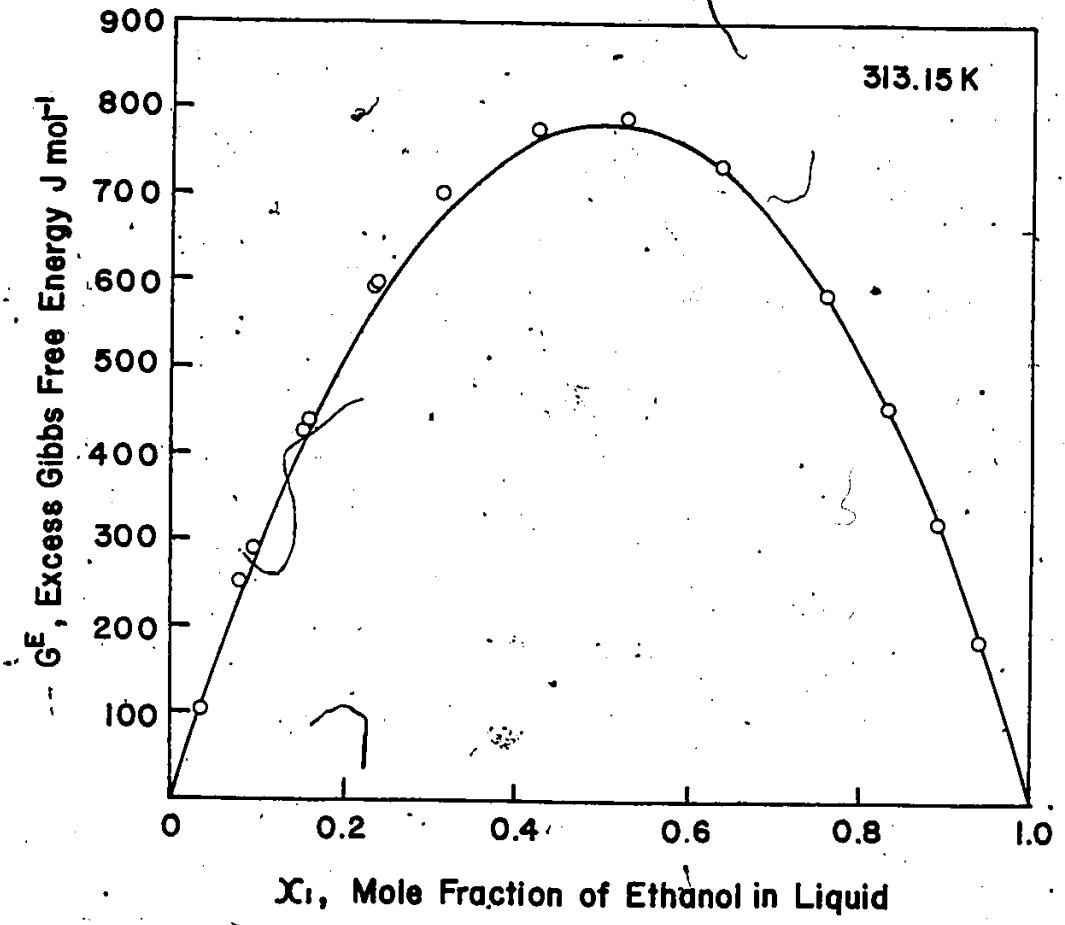

Figure 6.7 Excess Gibbs Free Energy for Mixtures of Ethanol (1) - Methyl Methacrylate (2) System at 313.15K. (0, Experimental, - Calculated)

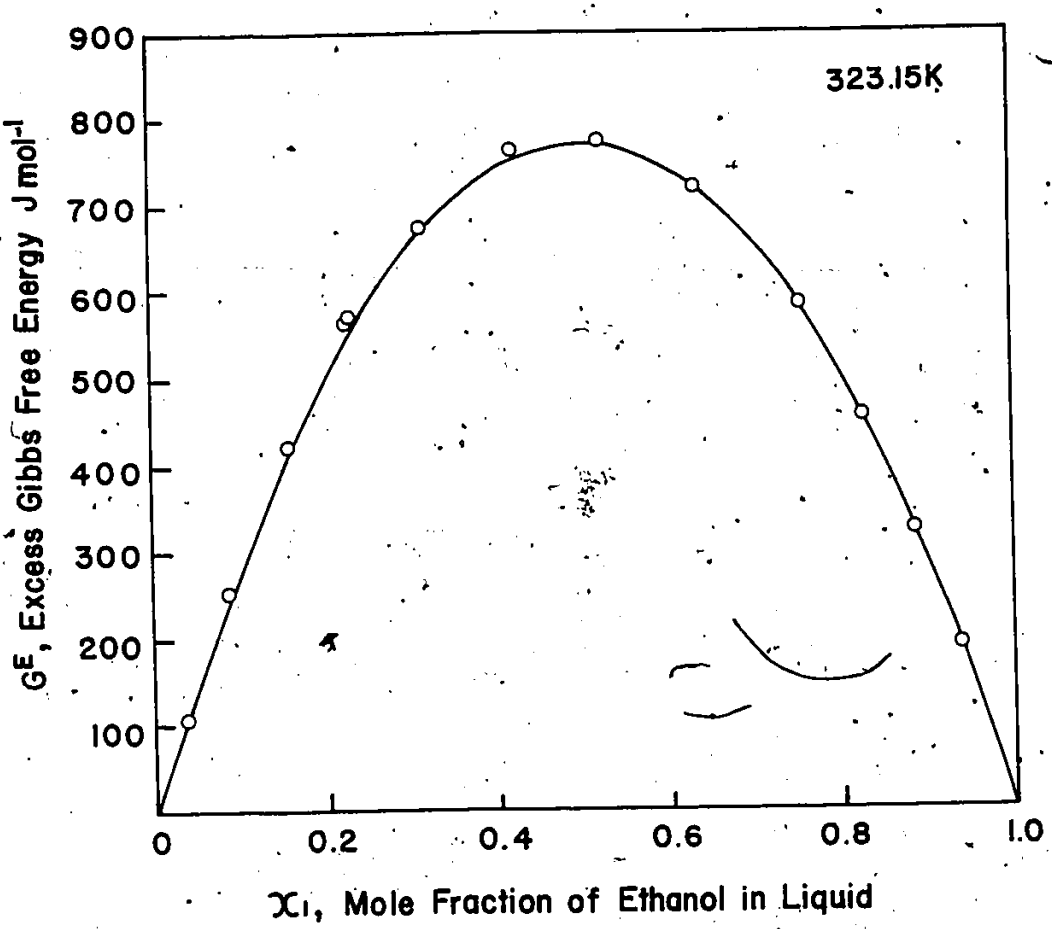

Figure 6-8 Excess Gibbs Free Energy for Mixtures of Ethanol (1) - Methyl Methacrylate (2) System at 323.15K. (0, Experimental, - Calculated)

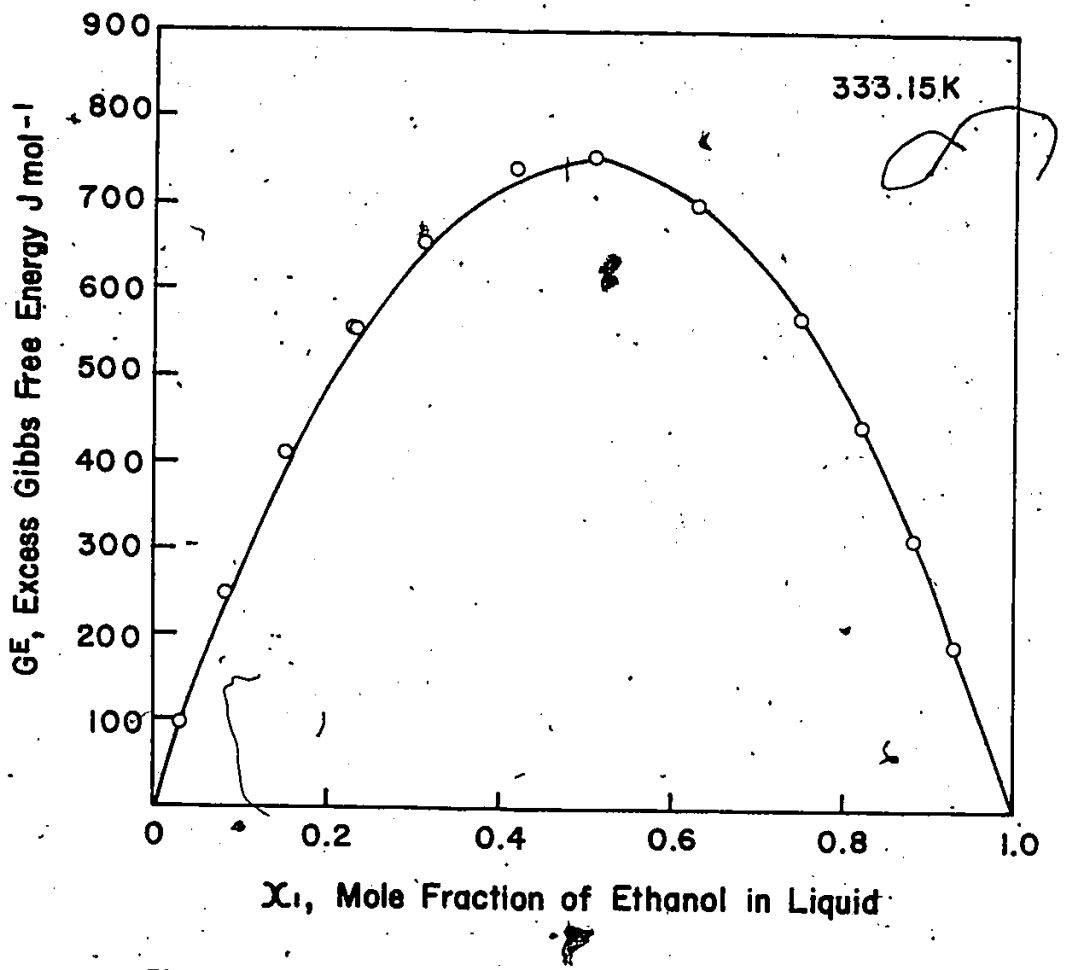

Figure 6-9 Excess Gibbs Free Energy for Mixtures of Ethanol (1) - Methyl Methacrylate (2) System at 333.15K. (0, Experimental, Calculated)

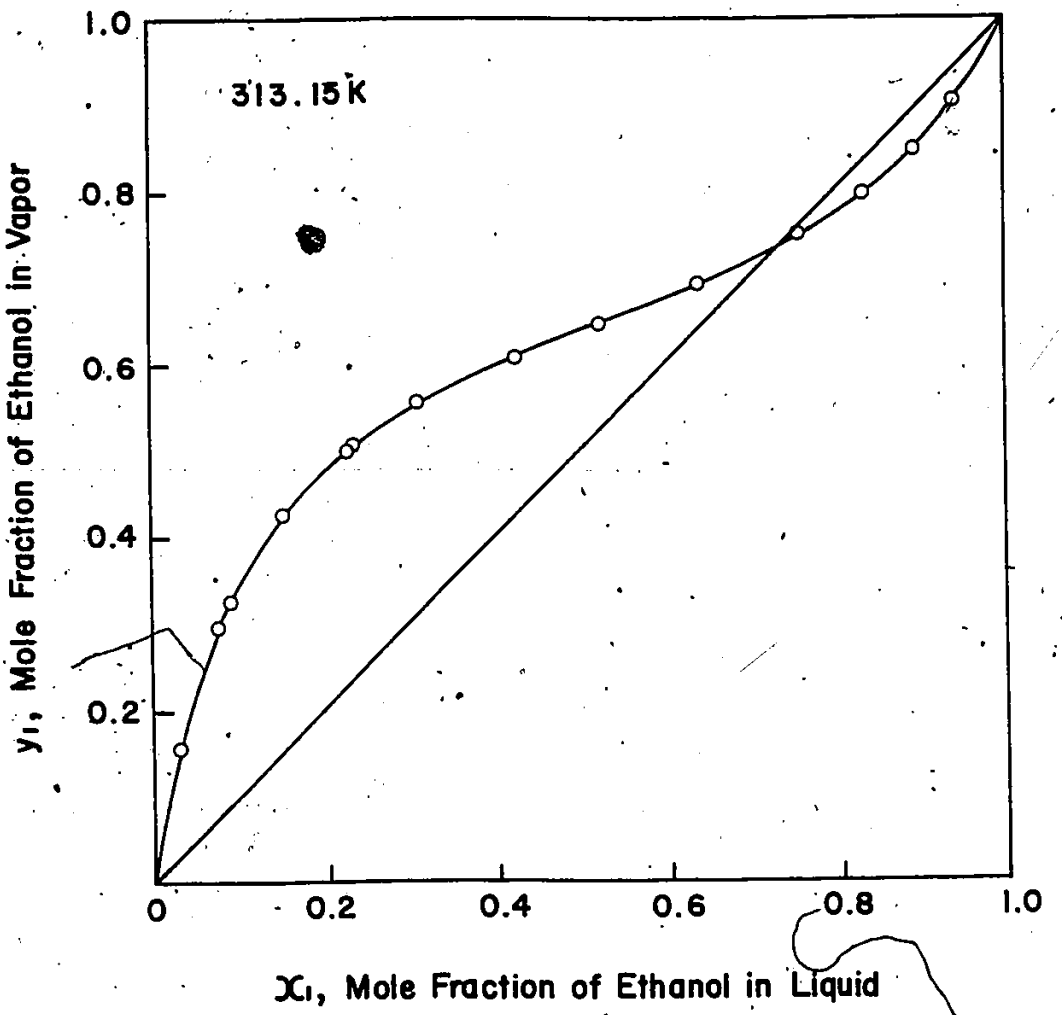

Figure 6-10 Comparison of Calculated y values with Experimental Data for Ethanol (1) - Methyl Methacrylate (2) System at 313.15K. (0, Experimental, - Calculated)

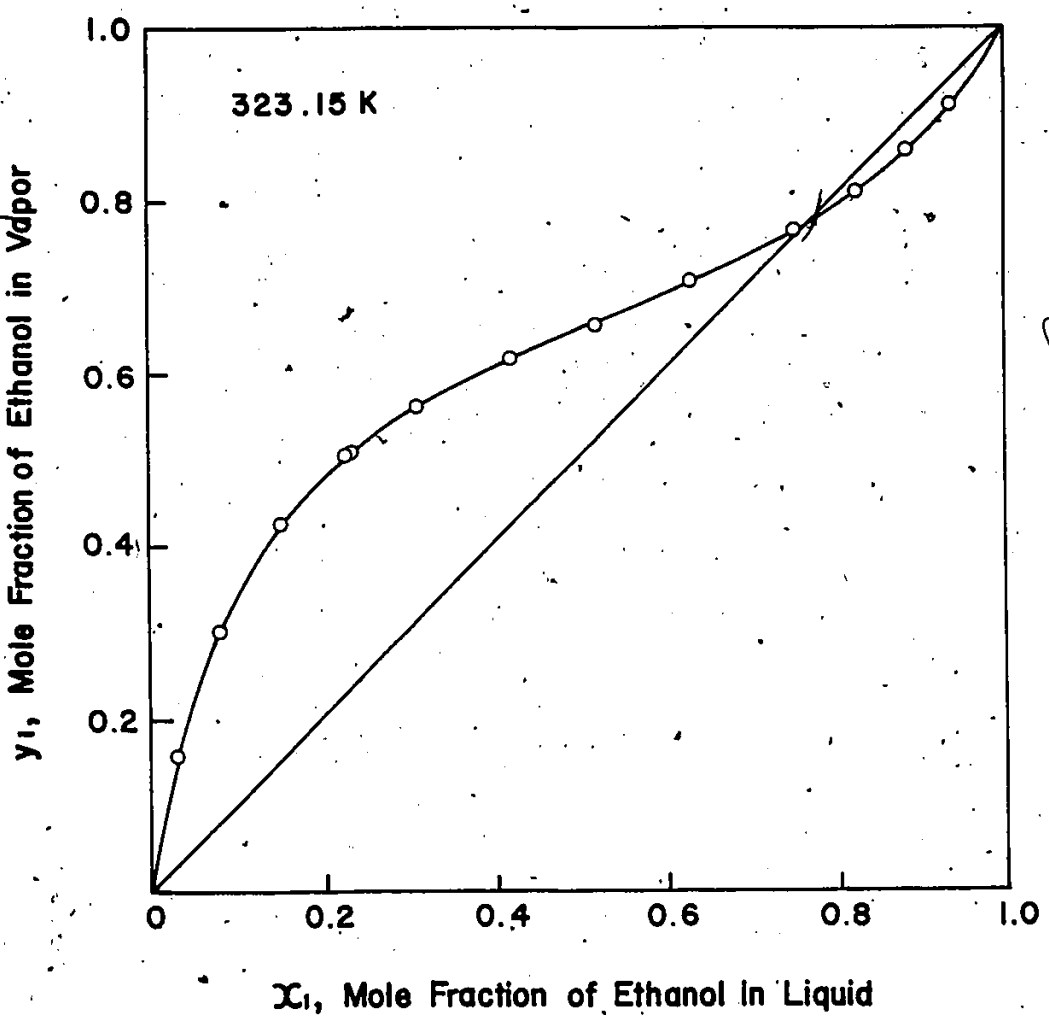

Figure 6-11 Comparison of Calculated y Values with Experimental Data for Ethanol (1) - Methyl Methacrylate (2) System at 323.15K. (0, Experimental, - Calculated)

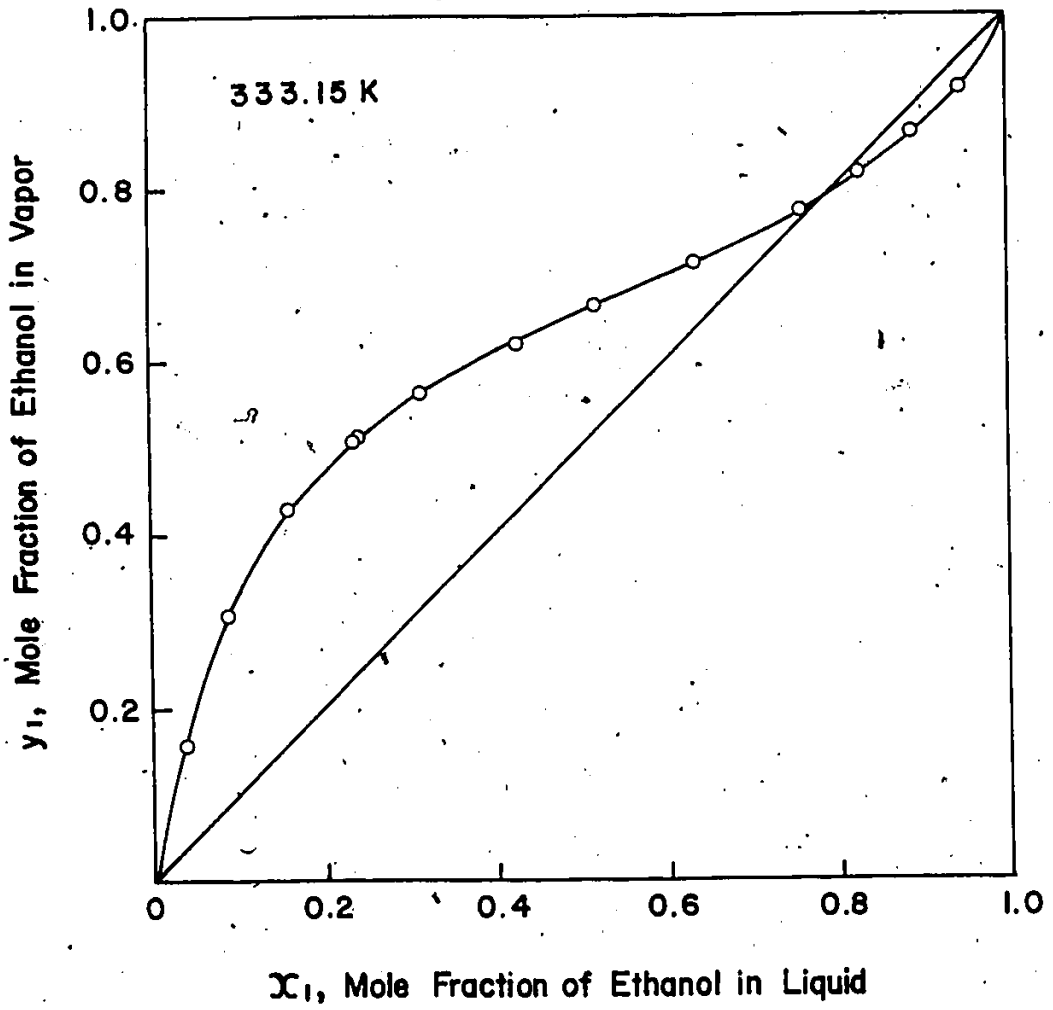

Figure 6-12 Comparison of Calculated y Values with Experimental Data for Ethanol (1) - Methyl Methacrylate (2) System at 333.15K. (0, Experimental, - Calculated)

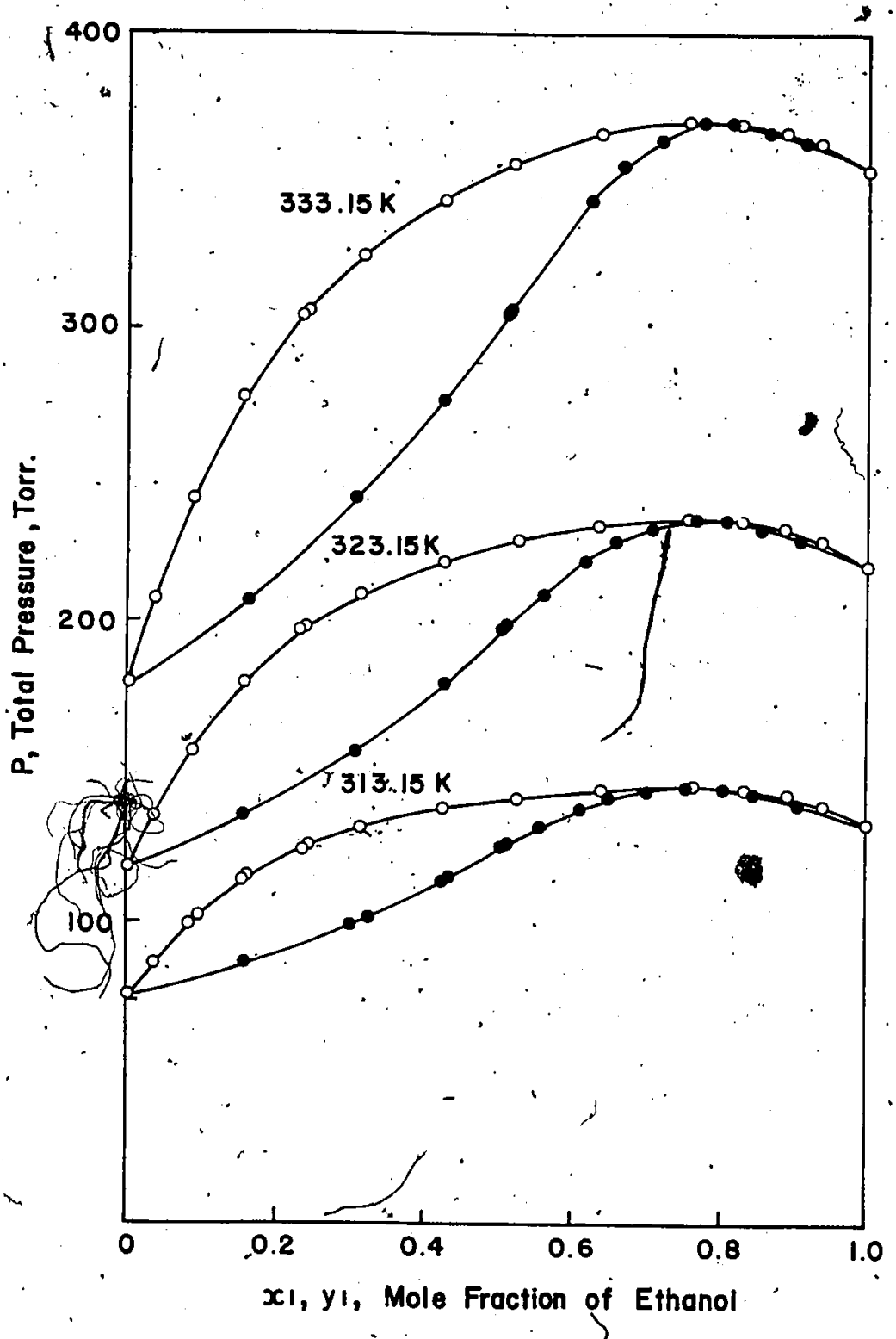

Figure 6-13 Comparison of Calculated p and y with Experimental Data for Ethanol (1) - Methyl Methacrylate (2) System at 313.15, 323.15 and 333.15K. (0, ●, Experimental, - Calculated)

CHAPTER 7

CONCLUSIONS

Isothermal vapor-liquid equilibrium data measured for the ethanol-methyl methacrylate system at 313.15, 323.5 and 333.15K are thermodynamically consistent. A useful empirical correlation for the prediction of second virial coefficients for polar gases has been established and used in this study for the evaluation of the B values for ethanol and methyl methacrylate. The calculated and the experimental values of γ_i^L, G^E, y_i and P are found to be in good agreement. A binary azeotrope exists at all three temperatures and its ethanol concentration increases with increasing temperature.

REFERENCES

1. Boublikova, L. and Lu, B.C.-Y., J. Appl. Chem., 2, 631 (1969).

2. Redlich, O., and Kister, A.T., Ind. Eng. Chem. 40, 345 (1948).

3. Tsonopoulos, C., AICHE J. 20, 263 (1974).

4. Prausnitz, J.M. Molecular Thermodynamics of Fluid-Phase Equilibria, Prentice-Hall Englewood Cliffs, N.J. (1969), Chapter 5.

5. Pitzer, K.S., and R.F. Curl, Jr., J. Am. Chem, Soc., 79, 2369 (1957).

6. O'Connell, J.P., and J.M. Prausnitz, Ind. Eng. Chem. Process Design Develop., 6, 245 (1967).

7. Hala, E., Pick, J., Fried, V. and Vilim, O., "Vapor-Liquid Equilibrium", 2nd ed., Pergamon Press (1967).

8. Othmer, D.F., Ind. Eng. Chem., 20, 143 (1968).

9. Jones, C.A., Schoenborn, E.M., and Colburn, A.P., Ind. Eng. Chem., 35, 666 (1943).

10. Gillespie, D.T.C., Ind. Eng. Chem. Anal. Ed., 18, 575 (1946).

11. Dvorak, K. and Boublik, T., Coll. Czech. Chem, Commun. 28, 1249 (1963).

12. Cottrell, F.G., J. Am. Chem. Soc., 41, 721 (1919).

13. Black, C., Ind. Eng. Chem., 50, 392 (1958).

14. Hayden, J.G. and J.P. O'Connell, Ind. Eng. Chem., Process Des. Dev., No. 3, 14, 200 (1975).

15. Ramanathan, R.T., and R.P. Danner, A.I.Ch.E.J., No. 5, 23, 685 (1977).

16. Hirschfelder, J.O., Curtiss, C.F., Bird, R.B. "Molecular Theory of Gases and Liquids," Wiley, New York, N.Y., (1964).

17. Leland, T.W., Jr., and P.S. Chappelear, Ind. Eng. Chem., 60, No. 7, 15 (1968).

18. Reid, R.G., Prausnitz, J.M. and Sherwood, T.K. "The Properties of Gases and Liquids." McGraw-Hill, 3rd. ed.

New York, (1977).

19. Bondi, A., Simkin, O.J., A.I.Ch.E.J. 3, 473 (1957).

20. Prausnitz, J.M., C.A. Eckert, R.V. Orye and J.P. O'Connell. "Computer Calculations for Multicomponent Vapor-liquid Equilibria," Prentice-Hall, Englewood Cliffs, N.J. (1967).

21. Renon, H., L. Asselineau, G. Cohen, and C. Raimbault, "Computer Calculations for Vapor-liquid and Liquid-Liquid Equilibria," Technip, Paris, (1971) in French.

22. Eubank, P.T., and Smith, J.M., A.I.Ch.E.J. 8, 117 (1962).

23. Chueh, P.L., and J.M. Prausnitz, Ind. Eng, Chem. Fundamentals, 6, 492 (1967).

24. Van Ness H.C., "Classical Thermodynamics of Non-Electrolyte Solutions." Macmilland Co. New York, (1964).

25. Margules, M., Anz. Akad. Wiss. Wien., Math-Naturw Kl., II 104, 1243 (1895).

26. Van Laar, J; Z. Physik, Chem., 72, 723 (1910).

27. Wilson, G.M., J. Am. Chem. Soc., 86, 127 (1964).

28. Redlich, O., Kister, A.T., and Turnquist, A.T., Chem. Eng. Progr., Symposium Ser. No. 2, 48, 49 (1952).

29. Ho, J.C.K., Boshto, and B.C.-Y. Lu, Cand. J. Chem. Eng., 39, 205 (1961).

30. Stark, P.A. "Introduction to Numerical Methods," Macmillan, New York (1970).

31. Halm, R.L., Ph.D. Thesis, Department of Chemical Engineering, Syracuse University (1968).

32. McClellan, A.L., "Tables of Experimental Dipole Moments," W.H. Freeman, San Francisco (1963).

33. Dymond, J.H., and E.B. Smith, "The Virial Coefficients of Gases," Clarendon Press, Oxford (1969).

34. Hauthal, W.H. and H. Sackmann. Proc. 1st. Intern. Conf. Calarimetry Thermodynamics (Warsaw) 625 (1969).

35. Thermodynamics Research Center Data Project, Texas A&M University.

36. Haworth, W.S. and L.E. Sutton, Trans. Faraday Soc. 67, 2907 (1971).

37. Forsythe, G.E., M.A. Malcoln and C.B. Moler, "Computer Methods for Mathematical Computation." Prentice-Hall, Inc., Englewood Cliffs, N.J. (1977).

38. Knoebel, D.H., and W.C. Edmister, J. Chem. Eng. Data, 13, 312 (1968).

39. Kell, G.S., and G.E. McLaurin, J. Chem. Phys., 51, 4345 (1969).

40. Quayle, O.R., Chem. Rev., 53, 439 (1953).

41. Ishikawa, T., and B.C.-Y. Lu., Fluid Phase Equilibria, 3, 23 (1979).

42. Dreisbach, R.R., Physical Properties of Chemical Substances. Dow Chemical Co.: Midland, Mich. (1953).

43. Luskin, L.S., High Polymers Vol. XXIV Vinyl and Diene Monomers, Part 1, p. 165, Willey-Interscience: New York, (1970).

44. Timmermans, J., " Physics-Chemical Constants of Pure Organic Compounds." Elsevier: Amsterdam, (1950).

45. Matheson, M.S., Auer, E.E., Bevilacqua, E.B., Mart, E.J.: J. Am. Chem. Soc. 71, 497 (1949).

46. Brockhaus, A., Jenckel, E., Makromol. Chem. 18/19, 262 (1956).

47. Boublik, T., Fried, V., Hala, E., "The Vapor Pressure of Pure Substances", Elsevier, Amsterdam (1973).

48. Stull, D.R., "Vapor-Pressure of Pure Substances", Organic Compounds Ind. Eng. Chem. 39, 517 (1947).

APPENDIX I

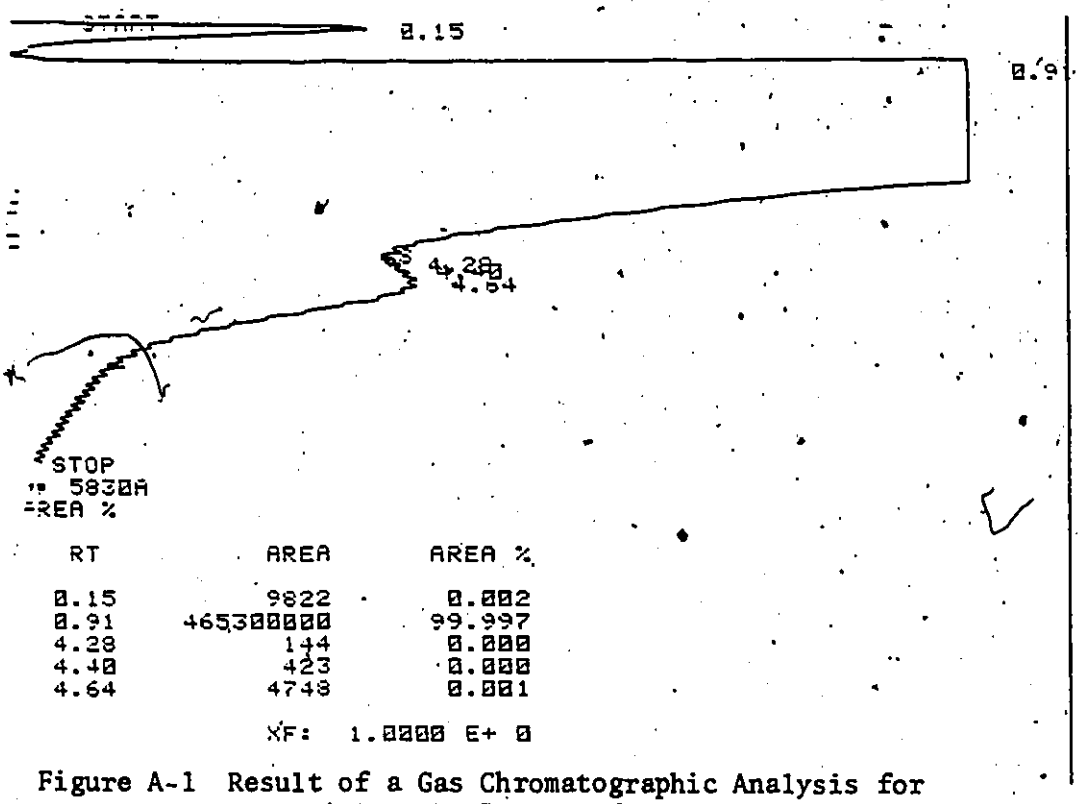

5830A
AREA %

RT	AREA	AREA %
0.15	9822	0.002
0.91	4653000000	99.997
4.28	144	0.000
4.40	423	0.000
4.64	4748	0.001

XF: 1.0000 E+ 0

Figure A-1 Result of a Gas Chromatographic Analysis for Determining the Purity of Ethanol

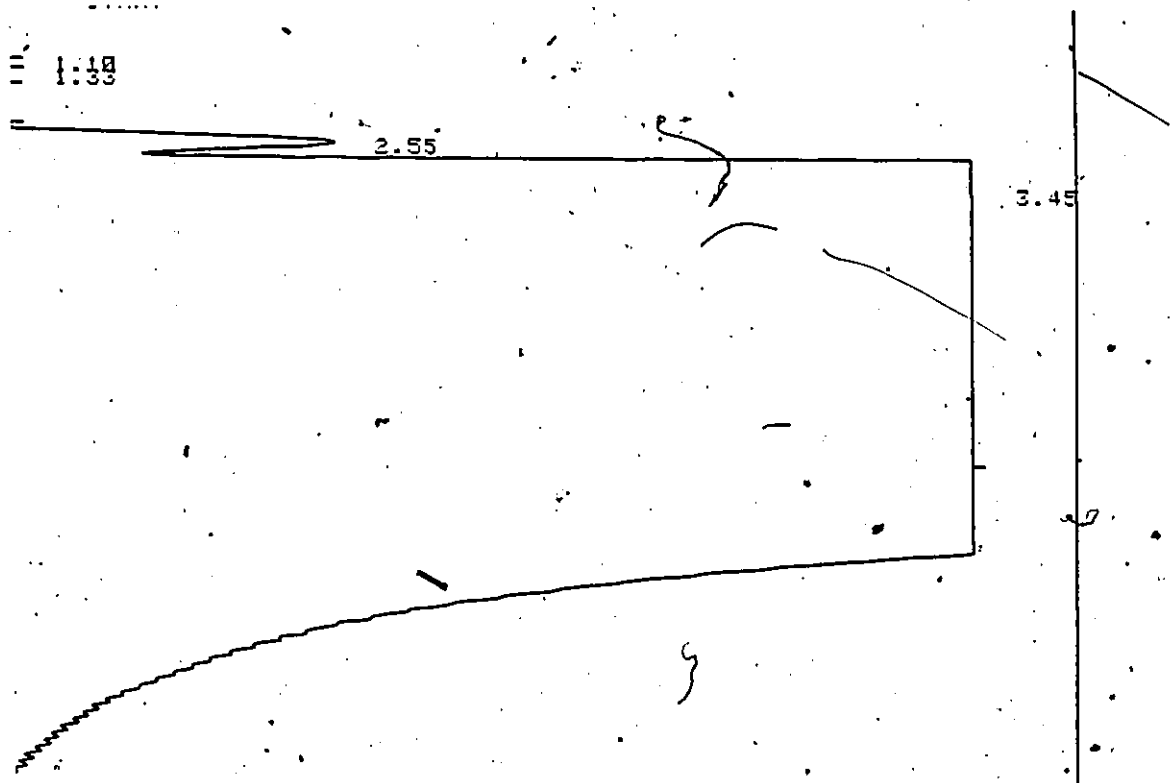

5830A
AREA %

RT	AREA	AREA %
1.10	609	0.000
1.33	1622	0.000
2.55	24570	0.004
3.45	6090000000	99.996

XF: 1.0000 E+ 0

Figure A-2 Result of a Gas Chromatographic Analysis for Determining the Purity of MMA

APPENDIX II

Table A-1

CALIBRATION OF COMPOSITION - REFRACTIVE INDEX
FOR SYSTEM ETHANOL (1) - MMA (2).

Run	Mole Fraction of Ethanol x_1	Refractive Index (n^D) at 25°C
1	0	1.41194
2	0.0074	1.40945
3	0.1242	1.40807
4	0.2045	1.40532
5	0.3044	1.40159
6	0.4140	1.39708
7	0.5031	1.39301
8	0.6045	1.38778
9	0.7044	1.38207
10	0.8015	1.37566
11	0.8965	1.36836
12	0.9484	1.36442
13	1.000	1.35915

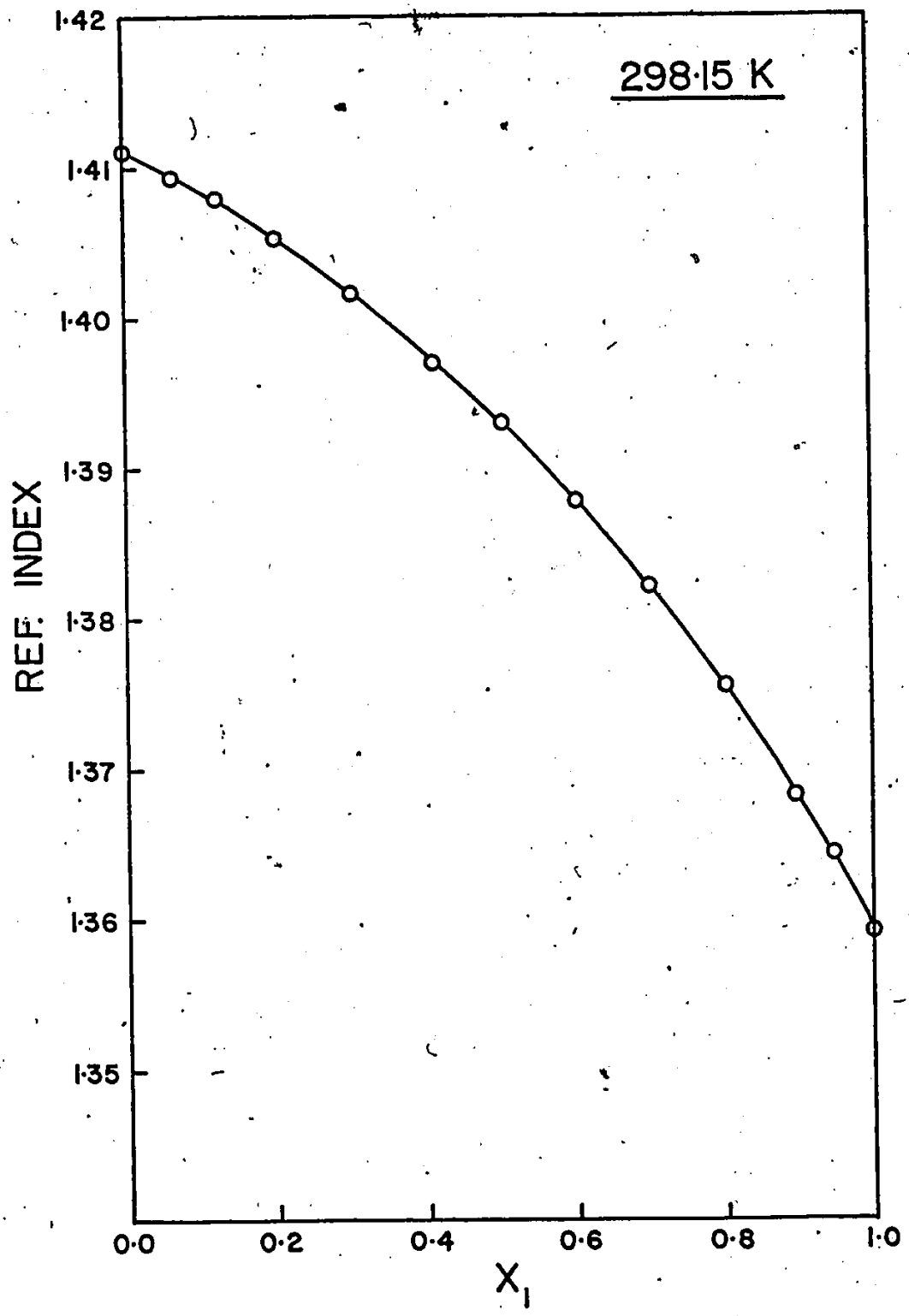

Figure A-3 Calibration Curve for Composition - Refractive Index for the System Ethanol (1) - MMA (2) at 298.15K

APPENDIX III

Calculation of y_i and P

Using equation (3.5) for the two components and constants obtained from Equation (3.8), at given T and x_i, values of y_i and P are calculated by means of the Newton-Raphson method of iteration (30) as described below:

For two components, we can have two non-linear equations in the form of Equation (3.5), while the relationship of $y_1 + y_2 = 1$ is introduced into Equation (3.5). Thus Equation (3.5) can be expressed for the two components as:

$$\log \gamma_1^L = \log \frac{y_1 P}{x_1 p^0} + \frac{(B_{11}-V_1^0)(P-p_1^0)}{2.303\ RT} + \frac{(1-y_1)^2 P}{2.303\ RT} \quad \text{(A3.1)}$$

$$\log \gamma_2^L = \log \frac{(1-y_1)P}{(1-x_1)p^0} + \frac{(B_{22}-V_2^0)(P-p_1^0)}{2.303\ RT} + \frac{y_1^2 P}{2.303\ RT} \quad \text{(A3.2)}$$

While y_1 and P will be treated as variables.

These two equations are simplified as:

$$f_1(y_1, P) = 0 \quad \text{(A3.3)}$$

$$f_2(y_1, P) = 0 \quad \text{(A3.4)}$$

For solving functions f_1 and f_2, we may take an initial guess for a pair of y_1 and P starting from the

experimental data say (y_1, p_1) with reference to an x_1 and T. To set the next approximation, the following approach is established:

At (k+1)th approximation, functions $f_1(y_{k+1}, P_{k+1})$ and $f_2(y_{k+1}, p_{k+1})$ can be expressed in terms of the functions and its derivative at (y_k, P_k) by expending a two-dimension Taylor series:

$$f_1(y_{k+1}, P_{k+1}) = f_1(y_k, P_k) + (y_{k+1}-y_k) \frac{\partial f_1(y_k,P_k)}{\partial y_k} + (P_{k+1}-P_k) \frac{\partial f_1(y_k,P_k)}{\partial p_k} + \ldots \quad \text{(A3.5)}$$

$$f_2(y_{k+1}, p_{k+1}) = f_2(y_k, p_k) + (y_{k+1}-y_k) \frac{\partial f_2(y_k, p_k)}{\partial y_k} + (p_{k+1}-p_k) \frac{\partial f_2(y_k, p_k)}{\partial p_k} + \ldots \quad \text{(A3.6)}$$

Suppose that y_{k+1} and p_{k+1} are both very close to the actual roots so that the values of $f_1(y_{k+1}, P_{k+1})$ and $f_2(y_{k+1}, P_{k+1})$ are almost equal to zero. Then Equations (A3-5) and (A3-6) simplify to

$$0 = f_1(y_k, P_k) + h \cdot \frac{\partial f_1(y_k, P_k)}{\partial y_k} + k \cdot \frac{\partial f_1(y_k, P_k)}{\partial P_k} \quad \text{(A3.7)}$$

$$0 = f_2(y_k, P_k) + h \cdot \frac{\partial f_2(y_k, P_k)}{\partial y_k} + k \cdot \frac{\partial f_2(y_k, P_k)}{\partial P_k} \quad \text{(A3.8)}$$

where $h = y_{k+1} - y_k$; $k = P_{k+1} - P_k$

Thus, we can get the (k+1)th approximation from the kth by

$$y_{k+1} = h + y_k \quad \text{(A3.9)}$$

$$P_{k+1} = k + P_k \quad \text{(A3.10)}$$

The values of h and k for each iteration can be obtained by solving Equations (A3.7) and (A3.8). Rearranging, we can get the simultaneous equations:

$$h \frac{f_1(y_k, P_k)}{y_k} + k \frac{f_1(y_k, P_k)}{P_k} = - f_1(y_k, P_k) \quad \text{(A3.11)}$$

$$h \frac{f_2(y_k, P_k)}{y_k} + k \frac{f_2(y_k, P_k)}{P_k} = - f_2(y_k, P_k) \quad \text{(A3.12)}$$

These resulting simultaneous equations can easily be solved for h and k by determinants, provided that the determinant is not zero, i.e.

$$J = \begin{vmatrix} \frac{f_1(y_k, P_k)}{y_k} & \frac{f_1(y_k, P_k)}{P_k} \\ \frac{f_2(y_k, P_k)}{y_k} & \frac{f_2(y_k, P_k)}{P_k} \end{vmatrix} \neq 0 \qquad \text{(A3.13)}$$

Hence

$$h = \frac{\begin{vmatrix} -f_1(y_k, P_k) & \frac{\partial f_1(y_k, P_k)}{\partial y_k} \\ -f_2(y_k, P_k) & \frac{\partial f_2(y_k, P_k)}{\partial P_k} \end{vmatrix}}{J} \qquad \text{(A3-14)}$$

$$k = \frac{\begin{vmatrix} \frac{\partial f_1(y_k, P_k)}{\partial y_k} & -f_1(y_k, P_k) \\ \frac{\partial f_2(y_k, P_k)}{\partial P_k} & -f_2(y_k, P_k) \end{vmatrix}}{J} \qquad \text{(A3.15)}$$

Having found h and k, then we may use equations (A3.9) and (A3.10) to get the next approximation, and repeat. Computing programme for this application is presented in Appendix VII.

APPENDIX VII

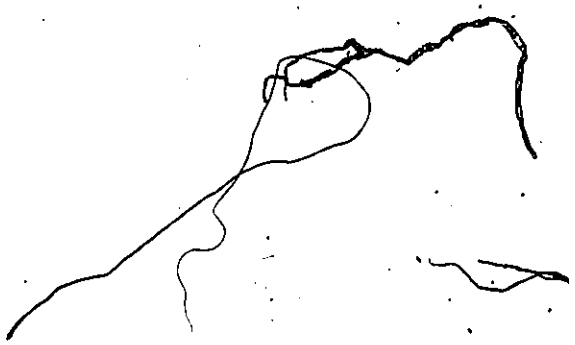

```
      $JOB  [redacted],'YU',TIME=120,PAGES=50
C
C
C     DEPARTMENT OF CHEMICAL ENGINEERING
C
C     JIN-MIN YU
C     ******************************************************************
C     THIS PROGRAM IS USING GOLDEN SECTION SEARCH
C     OF MINIMUM TO FIND OPTIMAL VALUES OF A AND C
C     IN THE EQUATION F(2)=A/TR**C WHICH IS USED
C     IN THE NEW DEVELOPED CORRELATION OF
C     SECOND VIRIAL COEFFIENT FOR THE POLAR CORRECTION
C     TERM.
C     ******************************************************************
C
C
C     ******************************************************************
C     MAIN PROGRAM
C     THIS PROGRAM  IS USING EXPERIMENTAL DATA
C     OF SECOND VIRIAL COEFFIENTS AND CORRESPONDING
C     TEMPERATURES TO CALCULATE VALUES OF F(2)
C     ******************************************************************
      1       IMPLICIT REAL*8(A-H,O-Z)
      2       DIMENSION TC(30),PC(15),W(15),B(30),T(30),BP(30),
             *F0(30),F1(30),F2(200),NDATA(15),
             *       U(15),UR(15),NAME(20),PPP(30),AA(15),E2(30),SU(30),TR(200
      3       DIMENSION PES2(30)
      4       DIMENSION AC(30)
      5       DIMENSION DIF2(30)
      6       DIMENSION BE(30),TK(30)
      7       DIMENSION AR(30),BR(30)
      8       DIMENSION AA0(30),AA1(30),AA2(30)
      9       INTEGER NDATA
     10       EXTERNAL F
     11       TOL=1.0E-5
     12       A=3.0
     13       A=1.0
     14       A=1.5
     15       A=2.5
     16       A=2.0
     17       A=0.0
     18        A=-10.
     19       S=20.
     20       A=-30.
     21       S=30.
     22       S=40.
     23       S=0.0
     24       A=0.0
     25       S=11.
     26       P=82.057
     27       READ,DD,BQ,A2
     28       RR=1.24
     29       CC=6.0
     30       PRINT 897,CC,DD,BQ,A2
     31   897 FORMAT(///3X,'CC=',F10.4,2X,'A0=',F20.10,2X,'A1=',F20.10,2X,'A2=
             *F20.10)
     32       READ,NN
     33       DO 20 I=1,NN
```

```
      READ(5,500) (NAME(K),K=1,20)
  600 FORMAT(20A4)
      READ,NDATA(I),TC(I),PC(I),W(I)
      READ,U(I)
      WRITE(6,500) (NAME(K),K=1,20)
  500 FORMAT(1H1///1X,20A4)
      UR(I)=PC(I)*(U(I)**2)*100000./(TC(I)**2)
      PRINT 707,UR(I)
  707 FORMAT(///2X,'UR=',F10.4)
      PRINT 18,TC(I),PC(I),W(I),U(I)
   18 FORMAT(//2X,'TC=',F10.4,2X,'PC=',F10.4,2X,'W=',F10.4,2X,'U=',
     *F10.4)
      SU(I)=R* TC(I)/PC(I)
      N=NDATA(I)
      PRINT 44,AA(I),BR(I)
   44 FORMAT(//2X,'AA=',F20.10,2X,'BR=',F20.10,2X)
      PRINT 46,AA0(I),AA1(I),AA2(I)
   46 FORMAT(//2X,'AA0=',F10.6,2X,'AA1=',F20.10,2X,'AA2=',F10.6)
      DO 55 K=1,N
   55 READ,T(K),B(K)
      PRINT 7012,N
 7012 FORMAT(//2X,'DATA INPUT =',I5)
      SUMS=0.0
      SUMP=0.0
      DO 30 M=1,N
      BP(M)=(B(M)*PC(I))/(R*TC(I))
      TR(M)=T(M)/TC(I)
      F0(M)=0.1445-0.330/(TR(M))-0.1385/(TR(M)**2)-0.0121/(TR(M)**3)
     *-0.000607/(TR(M)**8)
      F1(M)=0.0637+0.331/TR(M)**2-0.423/TR(M)**3-0.008/TR(M)**8
      F2(M)=BP(M)-F0(M)-W(I)*F1(M)
      TK(M)=1./TR(M)
      PRINT 909,T(M),TR(M),B(M),BE(M),PES2(M)
  909 FORMAT(5X,5F15.4)
      TR(M)=TK(M)
   30 CONTINUE
      Z=FMIN(A,S,F,TOL,F2,TR,N)
      PRINT 1,Z
    1 FORMAT(3H Z=,F12.5)
   20 CONTINUE
      STOP
      END
C*************************************************************************
C
C     GOLDEN SECTION SEARCH OF MINIMUM
C
C*************************************************************************
C
C     AN APPROXIATION  X  TO THE POINT WHERE  F  ATTAIN'S A MINIMUM UN
C
      FUNCTION FMIN(AX,BX,F,TOL,F2,TR,N)
      IMPLICIT REAL*8(A-H,O-Z)
      DIMENSION F2(200),TR(200)
C  THE INTERVAL (AX,BX) IS DETERMINED.
C
C  AX    LEFT ENDPOINT OF INITIAL
```

```
C    DX  RIGHT ENDPOINT
C
C
C  C IS THE SQUARED INVERSE OF THE GOLDEN RATIO
C
      QQQQ=5.00
      C=0.5*(3.-DSQRT(QQQQ))
C
C  EPS IS APPROXIMATELY THE SQUARE ROOT OF THE RELATIVE MACHINE
CN PRECISION.
C
      EPS=1.00
   10 EPS=EPS/2.00
      TOL1=1.0+EPS
      IF(TOL1.GT.1.00)  GO TO 10
      EPS=DSQRT(EPS)
C
C  INITIALIZATION
C
      A=AX
      B=BX
      V=A+C*(B-A)
      W=V
      X=V
      E=0.0
      FX=F(F2,TR,X,N)
      FV=FX
      FW=FX
C
C  MAIN LOOP STARTS HERE
C
   20 XM=0.5*(A+B)
      TOL1=EPS*DABS(X)+TOL/3.0
      TOL2=2.0*TOL1
C
C  CHECK STOPPING CRITRION
C
      IF(DABS(X-XM) .LE. (TOL2-0.5*(B-A)))  GO TO 90
C
C  IS GOLDEN-SECTION NECESSARY
      IF(DABS(E) .LE. TOL1) GO TO 40
C
C  FIT PARABOLA
C
      R=(X-W)*(FX-FV)
      Q=(X-V)*(FX-FW)
      P=(X-V)*Q-(X-W)*R
      Q=2.00*(Q-R)
      IF(Q .GT. 0.0) P=-P
      Q=DABS(Q)
      R=E
      E=D
C
C  IS PARABOLA ACCEPTABLE
C
   30 IF(DABS(P) .GE. DABS(0.5*Q*R)) GO TO 40
      IF(P .LE. Q*(A-X)) GO TO 40
      IF(P .GE. Q*(B-X)) GO TO 40
C
C  A PARABOLIC INTERPOLATION STEP
```

```
      C
  109       D=P/Q
  110       U=X+D
      C
      C FMUST NOT BE EVALUATED TOO CLOSE TO AX OR BX
      C
  111        IF((U-A) .LT. TOL2) D=DSIGN(TOL1,XM-X)
  112       IF((B-U) .LT. TOL2) D=DSIGN(TOL1,XM-X)
  113       GO TO 50
      C
      C GOLDEN-SECTION STEP
      C
  114    40 IF(X .GE. XM) E=A - X
  115       IF(X .LT. XM) E=B -X
  116       D=C*E
      C
      C F MUST NOT BE EVALUATED TOO CLOSE TO X
      C
  117    50 IF(DABS(D) .GE. TOL1)U=X+D
  118        IF(DABS(D) .LT. TOL1) U=X+DSIGN(TOL1,D)
  119       FU=F(F2,TR,U,N)
      C
      C UPDATE A,B,V,W,AND X
  120       IF(FU .GT. FX) GO TO 60
  121       IF(U .GE. X) A=X
  122       IF(U .LT. X) B=X
  123      V=W
  124      FV=FW
  125       W=X
  126       FW=FX
  127       X=U
  128       FX=FU
  129       GO TO 20
  130    60 IF(U .LT. X) A=U
  131       IF(U .GE. X) B=U
  132       IF(FU .LE. FW) GO TO 70
  133       IF(W .EQ. X) GO TO 70
  134       IF(FU .LE. FV) GO TO 80
  135       IF(V .EQ. X) GO TO 80
  136       IF(V .EQ. W) GO TO 80
  137       GO TO 20
  138    70  V=W
  139       FV=FW
  140       W=U
  141       FW=FU
  142       GO TO 20
  143    80 V=U
  144       FV=FU
  145       GO TO 20
      C
      C END OF MAIN LOOP
      C
  146    90  FMIN=X
  147       RETURN
  148       END
      C ***************************************************************
      C
      C   THIS  PROGRAM IS USING LEAST-SQUARES METHOD
      C   TO FIND ROOT-MEAN SQUARE DEVIATION OF
      C   F(2)
```

```
C
C ***********************************************************************
      FUNCTION F(F2,TR,CC,N)
      IMPLICIT REAL*8(A-H,O-Z)
      DIMENSION F2(200),TR(200),PP(100),SS(100),PPP(100),
     *FF2(100),DIFF(200)
      SUM=0.0
      SUM1=0.0
      SUM2=0.0
      SUM3=0.0
      DO 66 I=1,N
      PP(I)=TR(I)**CC
      SS(I)=PP(I)**2
      SUM=SUM+PP(I)
      SUM1=SUM1+SS(I)
      SUM2=SUM2+PP(I)*F2(I)
      SUM3=SUM3+F2(I)
   66 CONTINUE
      COBIN=N*SUM1-SUM**2
      Q=SUM3*SUM1-SUM*SUM2
      A=Q/COBIN
      S=N*SUM2-SUM3*SUM
      B=S/COBIN
      A=0.0
      B=SUM3/SUM
      PRINT 55,A,B
   55 FORMAT(4X,'A=',F50.7,2X,'B=',F50.7)
      SSUM=0.0
      DO 666 KK=1,N
      PPP(KK)=TR(KK)**CC
      FF2(KK)=A+B*PPP(KK)
      DIFF(KK)=(F2(KK)-FF2(KK))**2
      SSUM=SSUM+DIFF(KK)
  666 CONTINUE
      F=DSQRT(SSUM/N)
      Y=F
      PRINT 777,Y
  777 FORMAT(15X,'RMS=',F30.7)
      RETURN
      END

\$ENTRY
```

```
$JOB [redacted],'YU',TIME=120,PAGES=50
C ***************************************************************
C
C  DEPARTMENT OF CHEMICAL ENGINEERING
C
C    JIN-MIN YU
C
C    THIS PROGRAM IS USED FOR THE
C    EVALUATION AND CORRELATION OF LIQUID
C    PHASE ACTIVITY COEFFICIENTS AND GIBBS FREE
C    ENERGIES, AT GIVEN TEMPERATURE AND LIQUID
C    COMPOSITION, TOTAL PRESSURE AND VAPOR
C    COMPOSITIONS ARE CALCULATED BY MEANS
C     OF THE NEWTON-RAPHSON METHOD OF ITERATION
C
C ***************************************************************
C
C JIMMY
C
C
C
      IMPLICIT REAL*8(A-H,O-Z)
2     DIMENSION TC(2),PC(2),VC(2),WW(2),AA(2),BE(2),TT(3),PPT(20),
     *F11(30),FF1(30),F12(30),F13(30),CAMAL1(30),CAMA1(30),X2(30),
     *Y2(30),F21(30),FF2(30),F22(30),F23(30),CAMAL2(30),CAMA2(30),
     *CAMLC1(30),CAMLC2(30),CAMAC1(30),CAMAC2(30),DIFF(30),SDIFF(3
     *PERR(30),PECEN(30),CY1(30),CPT(30),DEGE(30),DEGEC(30),GAP(30
     *VV1(3),VV2(3),X1(30),Y1(30),PT(30),DMM(30),PPP1(3),PPP2(3),
     *PECEN1(30),CTP(30),CCAML(30),CCCAML(30),YAC1(90),
     *PTT(30)
3     DIMENSION U(30),UR(30)
4     READ,NNN
5     READ,80,DD,A2
6     PRINT 9,80,DD,A2
7     8 FORMAT(//2X,'BO=',F20.10,2X,'DD=',F20.10,2X,'A2=',F20.10)
8     DO 11 I=1,2
9     READ,TC(I),PC(I),VC(I),WW(I),AA(I),BE(I)
10    READ,U(I)
11    UR(I)=PC(I)*(U(I)**2)*100000./TC(I)**2
12    AA(I)=(80*UR(I)+DD*DEXP(A2*UR(I)))
13    11 PRINT 29,I,WW(I),AA(I),BE(I)
14    29 FORMAT(////2X,I4,2X,'W=',F10.4,2X,'AA=',F10.4,2X,'BE=',F10.4)
15    DO 12 J=1,NNN
16    READ,N
17    READ,TT(J),PPP1(J),PPP2(J),VV1(J),VV2(J)
18    READ,YA,PPA
19    PA=PPA/760.
20    T=TT(J)+273.15
21    V1=VV1(J)
22    V2=VV2(J)
23    TR1=T/TC(1)
24    TR2=T/TC(2)
25    PP1=PPP1(J)/760.
26    PP2=PPP2(J)/760.
27    TC1=TC(1)
28    TC2=TC(2)
29    PC1=PC(1)
30    PC2=PC(2)
31    VC1=VC(1)
32    VC2=VC(2)
```

```
      VP1=VR(1)
      BE2=BE(2)
      BE1=BE(1)
      AA2=AA(2)
      AA1=AA(1)
      WW2=WW(2)
      WW1=WW(1)
      CALL SECON1(T,TC1,TC2,PC1,PC2,WW1,WW2,AA1,AA2,BE1,BE2,VC1,
     *VC2,TR1,TR2,B1,B2,B12,DEL)
      P=82.057
      PRINT 98
   98 FORMAT('0',2X,'EXPERIMENTAL KAMA')
      DO 13 K=1,N
      READ,X1(K),Y1(K),PPT(K)
      PT(K)=PPT(K)/730.
      F11(K)=Y1(K)*PT(K)/(X1(K)*PP1)
      FF1(K)=DLOG10(F11(K))
      F12(K)=(PT(K)-PP1)*(B1-V1)/(2.303*R*T)
      F13(K)=PT(K)*DEL*((1.-Y1(K))**2)/(2.303*R*T)
      CAMAL1(K)=FF1(K)+F12(K)+F13(K)
      X2(K)=1.-X1(K)
      Y2(K)=1.-Y1(K)
      F21(K)=Y2(K)*PT(K)/(X2(K)*PP2)
      FF2(K)=DLOG10(F21(K))
      F22(K)=(PT(K)-PP2)*(B2-V2)/(2.303*R*T)
      F23(K)=PT(K)*DEL*((1.-Y2(K))**2)/(2.303*R*T)
      CAMAL2(K)=FF2(K)+F22(K)+F23(K)
      CAMA1(K)=DEXP(2.303*CAMAL1(K))
      CAMA2(K)=DEXP(2.303*CAMAL2(K))
      PRINT 6,X1(K),Y1(K),CAMAL1(K),CAMA1(K),CAMAL2(K),CAMA2(K)
    6 FORMAT(2X,6F20.4)
   13 CONTINUE
      PRINT 63
   63 FORMAT('0',2X,'COMPARE TERM 1,2,3,1,2,3')
      DO 62 KM=1,N
      PRINT 64,FF1(KM),F12(KM),F13(KM),FF2(KM),F22(KM),F23(KM)
   64 FORMAT(2X,6F20.4)
   62 CONTINUE
      ODEL1=0.000
      PDEL1=0.000
      ZRMS1=0.000
      PDEL=0.000
      ZRMS=0.000
      CALL CALBCD(N,X1,Y1,CAMAL1,CAMAL2,BB,CC,DD)
      ODEL=0.000
      ODEL2=0.0
      PDEL2=0.0
      ZRMS2=0.0
      PRINT 17
   17 FORMAT(3X,'CAL. CONST. OF P-K EQU. AND. CAL KAMAL.')
      DO 14 M=1,N
      CAMLC1(M)=(X2(M)**2)*(BB+CC*(3.*X1(M)-X2(M))+DD*(X1(M)-X2(M))
     **(5.*X1(M)-X2(M)))
      CAMLC2(M)=(X1(M)**2)*(BB+CC*(X1(M)-3.*X2(M))+DD*(X1(M)-X2(M),
     **(X1(M)-5.*X2(M)))
      CCAML(M)=CAMAL1(M)-CAMAL2(M)
      CCCAML(M)=CAMLC1(M)-CAMLC2(M)
      CAMAC1(M)=10**(CAMLC1(M))
      CAMAC2(M)=10**(CAMLC2(M))
      DIFF(M)=CAMLC1(M)-CAMAL1(M)
```

```
      SDIFF(M)=DIFF(M)**2
      PERS(M)=DIFF(M)*100/CAMAL1(M)
      ODEL=ODEL+DABS(DIFF(M))
      PDEL=PDEL+DABS(PERS(M))
      ZRMS=ZRMS+SDIFF(M)
      DIFF1=CAMAC1(M)-CAMA1(M)
      SDIFF1=DIFF1**2
      PERS1=DIFF1*100/CAMA1(M)
      ODEL1=ODEL1+DABS(DIFF1)
       PDEL1=PDEL1+DABS(PERS1)
      ZRMS1=ZRMS1+SDIFF1
      DIFF2=CAMAC2(M)-CAMA2(M)
      SDIFF2=DIFF2**2
      PERS2=DIFF2*100./CAMA2(M)
      ODEL2=ODEL2+DABS(DIFF2)
      PDEL2=PDEL2+DABS(PERS2)
      ZRMS2=ZRMS2+SDIFF2
   14 PRINT 18,X1(M),Y1(M),CAMLC1(M),CAMAL1(M),PERS(M),CAMLC2(M),
     *CAMAL2(M)
   18 FORMAT(2X,2F15.4,2F16.5,F20.4,2F16.4)
      DRMS2=DABS(ZRMS2)/(N-3)
      RMS2=DSQRT(DRMS2)
      ABSPE2=PDEL2/N
      SODEL2=DABS(ODEL2)/N
      PERSE2=SODEL2
      DRMS1=DABS(ZRMS1)/(N-3)
      RMS1=DSQRT(DRMS1)
      ABSPE1=PDEL1/N
       SODEL1=DABS(ODEL1)/N
      PERSE1=SODEL1
      DRMS=DABS(ZRMS)/(N-3)
      RMS=DSQRT(DRMS)
      ABSPER=PDEL/N
      SODEL=DABS(ODEL)/N
      PERSE=SODEL
      PRINT 16,RMS,PERSE,ABSPER
   16 FORMAT(3X,3F15.4)
      PRINT 229
  229 FORMAT('0','STAND D, PERCENT, ABS P, OF CAMA')
      PRINT 227,RMS1,PERSE1,ABSPE1
  227 FORMAT('0',4X,3F15.4)
      PRINT 230
  230 FORMAT(//2X,' DEVIATIONS OF  R2')
      PRINT 231,RMS2,PERSE2,ABSPE2
  231 FORMAT(//4X,'RMS2=',F12.4,2X,'PERSE2=',F12.4,2X,'ABSPE2=',F12.4)
      CALL CALPY(N,V1,V2,PP1,PP2,PT,X1,Y1,DEL,B1,B2,T,CAMAC1,CAMAC2,
     *CY1,CPT)
      SUM1=0.000
      SUM=0.000
      SSUM1=0.000
      SSUM=0.000
      SSSUM1=0.000
      SSSUM=0.000
      DO 15 L=1,N
      DYY=Y1(L)-CY1(L)
      DPP=PT(L)-CPT(L)
      PECEN(L)=(Y1(L)-CY1(L))*100/Y1(L)
      PECEN1(L)=(CPT(L)-PT(L))*100/PT(L)
      SUM=SUM+(Y1(L)-CY1(L))**2
      SUM1=SUM1+(PT(L)-CPT(L))**2
```

```
      SSUM=SSUM+DABS(DYY)
        SSUM1=SSUM1+DABS(DPP)
      SSSUM=SSSUM+DABS(PECEN(L))
      SSSUM1=SSSUM1+DABS(PECEN1(L))
   15 PRINT 41,X1(L),Y1(L),CY1(L),PECEN(L),PT(L),CPT(L),PECEN1(L)
   41 FORMAT(2X,7F15.4)
      STAND=DABS(SUM)/(N-3)
      DSTAND=DSQRT(STAND)
      CENTA=DABS(SSUM)/N
      APECEN=SSSUM/N
      PSTAND=DABS(SUM1)/(N-3)
      PPSTAN=DSQRT(PSTAND)
      PPECEN=SSSUM1/N
      CENTAP=DABS(SSUM1)/N
      DCENTA=CENTA
      DCENTP=CENTAP
      PRINT 78
   78 FORMAT(2X,'DEVIATION OF CY1(L),,2X,STAND,PERCENT,ABS.PERCENT',
      PRINT 79,DSTAND,DCENTA,APECEN
   79 FORMAT(2X,3F30.4)
      PRINT 54
   54 FORMAT('0',2X,'DEVIATION OF CPT(L),2X,STAND,PECENT,ABS.PECENT'
      PRINT 59,PPSTAN,DCENTP,PPECEN
   59 FORMAT(2X,3F30.4)
      TR=6.3144
      OMS1=0.000
      OMS2=0.000
      OMS3=0.000
      DO 38 JJ=1,N
      DEGE(JJ)=(X1(JJ)*CAMAL1(JJ)+(1.-X1(JJ))*CAMAL2(JJ))*2.303*TR*T
      DEGEC(JJ)=(X1(JJ)*CAMLC1(JJ)+(1.-X1(JJ))*CAMLC2(JJ))*2.303*TR*T
      GAP(JJ)=DEGE(JJ)-DEGEC(JJ)
      OMS1=OMS1+GAP(JJ)**2
      OMS2=OMS2+DABS(GAP(JJ))
      OMM(JJ)=GAP(JJ)*100/DEGE(JJ)
      OMS3=OMS3+DABS(OMM(JJ))
      PRINT 47,X1(JJ),DEGE(JJ),DEGEC(JJ),OMM(JJ)
   47 FORMAT(3X,F12.4,2F20.4,F30.4)
   38 CONTINUE
      GSTAND=OMS1/(N-3)
      SGTAND=DSQRT(GSTAND)
      GCENTA=DABS(OMS2)/N
      CGENTA=GCENTA
      GAPECE=OMS3/N
      PRINT 49,SGTAND,CGENTA,GAPECE
   49 FORMAT(2X,3F20.4)
      PRINT 97
   97 FORMAT('1',2X,'VALUES FOR GRAPH')
      DO 32 KJ=1,N
      CTP(KJ)=CPT(KJ)*760.
   32 PRINT 58,PPT(KJ),CTP(KJ),X1(KJ),CY1(KJ),CCAML(KJ),CCCAML(KJ),
     *DEGEC(KJ),DEGE(KJ)
   58 FORMAT(2X,8F15.4)
      PRINT 818
  818 FORMAT('1',2X,'VALUES FOR REFERENCE',//)
      DO 888 LL=1,N
      PTT(LL)=PPT(LL)*(101325/760)
  888 PRINT 887,PTT(LL),X1(LL),Y1(LL),CAMAC1(LL),CAMAC2(LL),DEGEC(L
  887 FORMAT(2X,F10.2,F9.4,F12.4,F10.4,F10.4,F11.2)
      CALL CALZXP(V1,V2,PP1,PP2,T,YA,PA,DEL,B1,B2,BB,CC,DD,YYAC1,PC
```

```
      12 CONTINUE
         STOP
         END
C*************************************************************
C
C
C     PREDICTION OF THE SECON VIRIAL COEFFIENTS
C      BY USING THE NEW DEVELOPED CORRELATION
C
C
C*************************************************************
      SUBROUTINE SECON1(T,TC1,TC2,PC1,PC2,WW1,WW2,AA1,AA2,BE1,BE2,VC1,
     *VC2,TR1,TR2,B1,B2,B12,DEL)
      IMPLICIT REAL*8(A-H,O-Z)
      R=82.057
      BE1=0.0
      A1=0.02135
      A1=-0.00000144
      A2=5.8251
      A0=0.05014
      A1=-0.00023065
      A2=5.5936
      A0=0.07455
      A1=-0.00023065
      A2=5.7764
      FC01=0.1445-0.330/TR1-0.1385/(TR1**2)-0.0121/(TR1**3)-0.000607/
     *(TR1**8)
      FC11=0.0637+0.331/(TR1**2)-0.423/(TR1**3)-0.008/(TR1**8)
      FC21=AA1/(TR1**6)-BE1/(TR1**8)
      FC21=FC21+A0/TR1+A1*(1./TR1-1.24)*(DEXP(A2/TR1))
      TOTL1=FC01+WW1*FC11+FC21
      B1=R*TC1*TOTL1/PC1
      FC02=0.1445-0.330/TR2-0.1385/(TR2**2)-0.0121/(TR2**3)-0.000607/
     *(TR2**8)
      FC12=0.0637+0.331/(TR2**2)-0.423/(TR2**3)-0.008/(TR2**8)
      FC22=AA2/(TR2**6)-BE2/(TR2**8)
      TOTL2=FC02+WW2*FC12+FC22
      B2=R*TC2*TOTL2/PC2
C*************************************************************
C
C CALCULATION OF THE CROSS SECOND VIRIAL COEFFIENTS
C
C*************************************************************
      BK12=0.0
      TTC12=TC1*TC2
      TC12=DSQRT(TTC12)
      TC12=TTC12*(1.-BK12)
      TR12=T/TC12
      PVC=PC1*VC1/TC1+PC2*VC2/TC2
      RS=1./3.
      VC12=(VC1**RS+VC2**RS)**3
      PC12=4.*TC12*PVC/VC12
      WW12=(WW1+WW2)/2.
      AA12=(AA1+AA2)/2.
      BE12=(BE1+BE2)/2.
      BE12=0.0
      A0=A0/2.
      A2=A2/2.
      FC012=0.1445-0.330/TR12-0.1385/(TR12**2)-0.0121/(TR12**3)-0.00
```

```
     *)/(TR12**8)
      FCM=0.0637+0.331/(TR12**2)-0.423/(TR12**3)-0.008/(TR12**8)
      FCM12=AA12/(TR12**6)-BE12/(TR12**8)
      FCM12=FCM12+A0/TR12+A1*(1./TR12-1.24)*(DEXP(A2/TR12))
      TOTL12=FC012+WW12*FCM+FCM12
      B12=8*TC12*TOTL12/PC12
      DEL=2*B12-B1-B2
      PRINT A,T,B1,B2,B12,DEL
    4 FORMAT('1',4X,3F12.5,2F20.4)
      RETURN
      END
C*************************************************************
C
C CALCULATION OF THE REDLISH-KISTER CONSTANTS,BB,DD,CC
C
C*************************************************************
      SUBROUTINE CALBCD(NJ,X1,Y1,CAMAL1,CAMAL2,BB,CC,DD)
      IMPLICIT REAL*8(A-H,O-Z)
      DIMENSION A(3,4),Z1(30),Z2(30),Z3(30),X1(30),Y1(30),CAMAL1(30),
     *CAMAL2(30),RR(30),X(3)
      A(1,1)=0.000
      A(1,2)=0.000
      A(1,3)=0.000
      A(1,4)=0.000
      A(2,2)=0.000
      A(2,3)=0.000
      A(2,4)=0.000
      A(3,3)=0.000
      A(3,4)=0.000
      DO 20 I=1,NJ
      RR(I)=CAMAL1(I)-CAMAL2(I)
      Z1(I)=1.-2*X1(I)
      Z2(I)=(6.*X1(I)*(1.-X1(I)))-1.
      Z3(I)=(1.-2*X1(I))*(1.-6*X1(I)*(1.-X1(I)))
      A(1,4)=A(1,4)+Z1(I)*RR(I)
      A(2,4)=A(2,4)+Z2(I)*RR(I)
      A(3,4)=A(3,4)+Z3(I)*RR(I)
      A(1,1)=A(1,1)+Z1(I)*Z1(I)
      A(1,2)=A(1,2)+Z1(I)*Z2(I)
      A(1,3)=A(1,3)+Z1(I)*Z3(I)
      A(2,2)=A(2,2)+Z2(I)*Z2(I)
      A(2,3)=A(2,3)+Z2(I)*Z3(I)
      A(3,3)=A(3,3)+Z3(I)*Z3(I)
   20 CONTINUE
      A(2,1)=A(1,2)
      A(3,1)=A(1,3)
      A(3,2)=A(2,3)
      DO 40 K=2,3
      DO 40 M=K,3
      DO 40 J=K,4
   40 A(M,J)=A(M,J)-A(M,K-1)*A(K-1,J)/A(K-1,K-1)
      X(3)=A(3,4)/A(3,3)
      DO 80 K=2,3
       J=4-K
      L=J+1
       X(J)=0.000
      DO 81 M=L,3
   81 X(J)=X(J)+A(J,M)*X(M)
   80 X(J)=(A(J,4)-X(J))/A(J,J)
```

```
      BB=X(1)
      CC=X(2)
      DD=X(3)
       PRINT 11
   11 FORMAT('1','CONSTANT IN R-K EQU.')
      PRINT 12,BB,CC,DD
   12 FORMAT(3X,3F30.4)
      RETURN
      END
C*****************************************************************
C
C     CALCULATIONS OF VAPOR COMPOSITIONS
C     AND TOTAL PRESSURES BY MEANS OF
C     NEWTON-RAPHSON METHOD OF ITERATION
C
C*****************************************************************
      SUBROUTINE CALPY(NN,V1,V2,PP1,PP2,PT,X1,Y1,DEL,B1,B2,T,CAMAC1,
     *CAMAC2,CY1,CPT)
      IMPLICIT REAL*8(A-H,O-Z)
       DIMENSION PT(30),X1(30),Y1(30),CAMAC1(30),CAMAC2(30),ZX1(30),
     *CY1(30),CPT(30),ZAMAC1(30),ZAMAC2(30),DECY1(30),DECPT(50)
       R=82.057
      DO 24 I=1,NN
      ZX1(I)=X1(I)
      ZAMAC1(I)=CAMAC1(I)
      ZAMAC2(I)=CAMAC2(I)
      CY1(I)=Y1(I)
      CPT(I)=PT(I)
       DO 23 J=1,50
      SF11=((CPT(I)-PP1)*(B1-V1))/(R*T)+(CPT(I)*DEL*((1.-CY1(I))**2.))/
     *(T**2)
      SF1=DEXP(SF11)
      F1=SF1-ZAMAC1(I)*ZX1(I)*PP1/(CY1(I)*CPT(I))
      SF21=((CPT(I)-PP2)*(B2-V2))/(T*R)+(CPT(I)*DEL*(CY1(I)**2))/(T**2)
      SF2=DEXP(SF21)
      F2=SF2-ZAMAC2(I)*(1.-ZX1(I))*PP2/((1.-CY1(I))*CPT(I))
      FF1=-2*CPT(I)*DEL*(1.-CY1(I))*SF1/(R*T)+ZAMAC1(I)*ZX1(I)*PP1/
     *((CY1(I)**2)*CPT(I))
      FF2=(B1-V1)*SF1/(R*T)+ZAMAC1(I)*ZX1(I)*PP1/((CPT(I)**2)*CY1(I))
      G1=2*CY1(I)*CPT(I)*DEL*SF2/(R*T)-ZAMAC2(I)*(1.-ZX1(I))*PP2/
     *(((1.-CY1(I))**2)*CPT(I))
      G2=(B2-V2)*SF2/(T*R)+ZAMAC2(I)*(1.-ZX1(I))*PP2/((CPT(I)**2)*
     *(1.-CY1(I)))
       COMIN=FF1*G2-FF2*G1
       Q=-F1*G2+FF2*F2
      S=-F2*FF1+G1*F1
       DECY1(J)=Q/COMIN
       DECPT(J)=S/COMIN
      IF(DABS(F1).LE.0.0000001.AND.DABS(F2).LE.0.0000001) GO TO 22
      IF(I.EQ.50) GO TO 707
        DEMAX1=CY1(I)*0.2
        DEMAX2=CPT(I)*0.2
      IF(DABS(DECY1(J)).GT.DEMAX1) DECY1(J)=DSIGN(DEMAX1,DECY1(J))
      IF(DABS(DECPT(J)).GT.DEMAX2) DECPT(J)=DSIGN(DEMAX2,DECPT(J))
      CY1(I)=CY1(I)+DECY1(J)
      CPT(I)=CPT(I)+DECPT(J)
      GO TO 23
  707 PRINT 505
  505 FORMAT('0','ITERATION NO IS OUT OF RANGE')
```

```
      23 CONTINUE
      22 CONTINUE
         RETURN
         END
C*********************************************************************
C
C     THE CALCULATION OF AZEOTROPIC COMPOSITION AND PRESSURE
C
C*********************************************************************
         SUBROUTINE CALZXP(V1,V2,PP1,PP2,T,YA,PA,DEL,B1,B2,BB,CC,DD,
     *YYAC1,PCA)
         IMPLICIT REAL*8(A-H,O-Z)
         DIMENSION YAC1(90),YAC2(90),CAMLA1(90),CAMLA2(90),CAMAL1(90),
     *CAMAL2(90),PAC(90),DEYAC1(90),DEPAC(90)
         R=82.057
         DO 25 I=1,90
         IF(I.EQ.1) PAC(I)=PA
         IF(I.EQ.1) YAC1(I)=YA
         YAC2(I)=1.-YAC1(I)
         CAMLA1(I)=(YAC2(I)**2)*(BB+CC*(3.*YAC1(I)-YAC2(I))+DD*(YAC1(I)-
     *YAC2(I))*(5.*YAC1(I)-YAC2(I)))
         CAMLA2(I)=(YAC1(I)**2)*(BB+CC*(YAC1(I)-3.*YAC2(I))+DD*(YAC1(I)-
     *YAC2(I))*(YAC1(I)-3.*YAC2(I)))
         CAMAL1(I)=10**CAMLA1(I)
         CAMAL2(I)=10**CAMLA2(I)
         SF11=((PAC(I)-PP1)*(B1-V1))/(R*T)+(PAC(I)*DEL*((1.-YAC1(I))**2))
     *(T*R)
         SF1=DEXP(SF11)
         F1=SF1-CAMAL1(I)*YAC1(I)*PP1/(YAC1(I)*PAC(I))
         SF21=((PAC(I)-PP2)*(B2-V2))/(T*R)+(PAC(I)*DEL*(YAC1(I)**2))/
     *(T*R)
         SF2=DEXP(SF21)
         F2=SF2-CAMAL2(I)*(1.-YAC1(I))*PP2/((1.-YAC1(I))*PAC(I))
         FF1=-2*PAC(I)*DEL*(1.-YAC1(I))*SF1/(T*R)+CAMAL1(I)*YAC1(I)*PP1/
     *((YAC1(I)**2)*PAC(I))
         FF2=(B1-V1)*SF1/(T*R)+(CAMAL1(I)*YAC1(I)*PP1/((PAC(I)**2)*YAC1(I)
         G1=2*YAC1(I)*PAC(I)*DEL*SF2/(R*T)-CAMLA2(I)*(1.-YAC1(I))*PP2/
     *(((1.-YAC1(I))**2)*PAC(I))
         G2=(B2-V2)*SF2/(T*R)+CAMAL2(I)*(1.-YAC1(I))*PP2/((PAC(I)**2)*(1.
     *YAC1(I)))
         CORIN=FF1*G2-FF2*G1
         Q=-F1*G2+FF2*F2
         S=-F2*FF1+G1*F1
         DEYAC1(I)=Q/CORIN
         DEPAC(I)=S/CORIN
         IF(DABS(F1).LE.0.0000001.AND.DABS(F2).LE.0.0000001) GO TO 22
         IF(I.EQ.90) GO TO 30
         DEMAX1=YAC1(I)*0.001
         DEMAX2=PAC(I)*0.001
         IF(DABS(DEYAC1(I)).GT.DEMAX1) DEYAC1(I)=DSIGN(DEMAX1,DEYAC1(I))
         IF(DABS(DEPAC(I)).GT.DEMAX2) DEPAC(I)=DSIGN(DEMAX2,DEPAC(I))
         YAC1(I+1)=YAC1(I)+DEYAC1(I)
         PAC(I+1)=PAC(I)+DEPAC(I)
         PCA=PAC(I+1)*760.
          YYAC1=YAC1(I+1)*1.
      25 CONTINUE
      30 PRINT 27
      27 FORMAT('0',2X,'AZEOTROPIC COMPOSITION AND PRESSURE')
         PRINT 29,T,PCA,YYAC1
```

```
      28 FORMAT('0',2X,F10.2,F20.2,F20.4)
         GO TO 32
      30 PRINT 31
      31 FORMAT('0',' ITERATION NO IS OUT OF RANGE')
      32 RETURN
         END
$ENTRY
```

APPENDIX VIII

B VALUES OF POLAR COMPOUNDS AVAILABLE IN THE LITERATURE

T K	B cm^3mol^{-1}
DIMETHYL ETHER[33][36]	
273.16	-613.
283.25	-531.
294.16	-499.
298.16	-446.
303.15	-457.
313.16	-421.
323.15	-405.
ETHYL ETHER[33]	
293.10	-1386.
295.20	-1226.
298.16	-1165.
300.00	-1160.
308.20	-1084.
313.16	-1046.
313.20	-1107.
320.00	-940.
320.00	-907.
323.20	-950.
323.26	-955.
328.16	-900.
336.20	-794.
336.80	-806.
339.16	-790.
340.00	-880.
343.16	-768.
348.16	-770.
350.40	-713.

T K	B cm^3mol^{-1}
METHYL ETHYL KETONE[33]	
314.61	-1968.
338.69	-1589.
352.54	-1362.
362.58	-1228.
370.57	-1130.
METHYL N-PROPYL KETONE[33]	
334.87	-2635.
360.56	-1760.
375.33	-1540.
386.04	-1377.
394.57	-1280.
METHYL ISOPROPYL KETONE[34]	
367.48	-1408.
346.22	-1702.
327.69	-2060.
DIETHYL KETONE[34]	
375.11	-1516.
353.70	-1854.
335.01	-2268.

T K	B cm^3mol^{-1}
351.00	-714.
358.16	-720.
358.16	-682.
360.00	-660.
368.16	-630.
380.00	-570.
382.30	-564.
400.00	-490.
405.20	-480.

ACETONE[33]

300.00	-2000.
310.00	-1730.
320.00	-1520.
330.00	-1350.
340.00	-1200.
350.00	-1080.
360.00	-960.

ETHYL FORMATE[35]

254.20	-2690.
279.62	-1800.
305.04	-1310.
330.46	-1000.
355.88	-798.
381.30	-654.
406.72	-548.
432.14	-465.
457.56	-401.
482.98	-349.
508.40	-306.
559.24	-239.
610.08	-190.
660.92	-152.
711.76	-123.

T K	B cm^3mol^{-1}

ACETALDEHYDE[33]

288.20	-1461.
293.20	-1295.
297.90	-1234.
298.20	-1206.
303.20	-1125.
308.20	-1050.
313.16	-944.
313.20	-959.
333.16	-765.
345.20	-770.
353.26	-633.
372.90	-530.
373.66	-533.
381.20	-550.
438.20	-320.
476.20	-260.

ETHYL ACETATE[35]

261.60	-3800.
287.76	-2530.
313.92	-1820.
340.08	-1380.
366.24	-1100.
392.40	-894.
418.56	-746.
444.72	-633.
470.88	-544.
497.04	-473.
523.20	-414.
575.52	-324.
627.84	-258.
680.16	-207.
732.48	-168.
837.12	-110.
941.76	-69.

T K	B cm^3mol^{-1}
813.44	-79.
915.12	-48.
1016.80	-26.
1271.00	11.
1525.20	33.
1779.40	47.
2033.60	57.
2542.00	70.

N-PROPYL FORMATE[35]

269.00	-3280.
295.90	-2210.
322.80	-1610.
349.70	-1240.
376.60	-985.
403.50	-807.
430.40	-675.
457.30	-573.
484.20	-493.
511.10	-428.
538.00	-375.
591.80	-292.
645.60	-231.
699.40	-185.
753.20	-148.
860.80	-94.
968.40	-56.
1076.00	-29.
1345.00	16.
1614.00	43.
1883.00	60.
2152.00	73.
2690.00	89.

METHYL ACETATE[35]

253.40	-3190.
278.74	-2130.
304.08	-1550.
1046.40	-40.
1308.00	8.
1569.60	37.
1831.20	55.
2092.80	68.
2616.00	85.

N-PROPYL ACETATE[35]

274.70	-4500.
302.17	-3000.
329.64	-2170.
357.11	-1650.
384.58	-1300.
412.05	-1060.
439.52	-880.
466.99	-750.
494.46	-640.
521.93	-550.
549.40	-480.
604.34	-380.
659.28	-300.
714.22	-240.
769.16	-190.
879.04	-120.
988.92	-74.
1098.80	-40.
1373.50	16.
1648.20	49.
1922.90	71.
2197.60	86.
2747.00	110.

N-BUTYL ACETATE[35]

289.50	-5900.
318.45	-3900.
347.40	-2750.
376.35	-2060.
405.30	-1620.

T K	B cm^3mol^{-1}
329.42	-1190.
354.76	-949.
380.10	-779.
405.44	-654.
430.78	-559.
456.12	-484.
481.46	-423.
506.80	-373.
557.48	-295.
608.16	-239.
658.84	-195.
709.52	-161.
810.88	-110.
912.24	-75.
1013.60	-49.
1267.00	-7.
1520.40	18.
1773.80	35.
2027.20	47.
2534.00	62.

METHYL PROPANOATE[35]

T K	B cm^3mol^{-1}
265.30	-3530.
291.83	-2420.
318.36	-1780.
344.89	-1380.
371.42	-1110.
397.95	-913.
424.48	-768.
451.01	-656.
477.54	-568.
504.07	-496.
530.60	-437.
583.66	-345.
636.72	-278.
689.78	-226.
742.84	-185.
848.96	-125.
955.08	-83.
1061.20	-52.
1326.50	-2.
1591.80	28.

T K	B cm^3mol^{-1}
434.25	-1310.
463.20	-1080.
492.15	-910.
521.10	-770.
550.05	-670.
579.00	-580.
636.90	-450.
694.80	-350.
752.70	-280.
810.60	-220.
926.40	-140.
1042.20	-86.
1158.00	-45.
1447.50	21.
1737.00	60.
2026.50	85.
2316.00	102.
2895.00	130.

ETHANOL[33][38]

313.16	-2134.
333.16	-1285.
353.15	-941.
535.16	-938.
373.15	-687.
393.16	-578.

N-PROPANOL[33]

378.20	-890.
393.20	-763.
408.20	-655.
423.20	-596.

ISO-PROPANOL[33]

333.16	-1609.
353.16	-1137.

T K	B cm^3mol^{-1}
1857.10	48.
2122.40	62.
2653.00	80.

ETHYL PROPANOATE[35]

273.00	-4300.
300.30	-2900.
327.60	-2200.
354.90	-1650.
382.20	-1320.
409.50	-1080.
436.80	-900.
464.10	-770.
491.40	-660.
518.70	-570.
546.00	-500.
600.60	-390.
655.20	-310.
709.80	-250.
764.40	-210.
873.60	-130.
982.80	-86.
1092.00	-50.
1365.00	8.
1638.00	43.
1911.00	65.
2184.00	81.
2730.00	102.

METHANOL [33][38][39]

298.15	-2075.
313.60	-1463.
323.15	-1185.
333.16	-926.
348.15	-737.
353.16	-701.
373.15	-542.
373.15	-535.
373.16	-870.
373.16	-874.
373.16	-890.
393.16	-721.
423.16	-557.
423.16	-558.
448.16	-459.
448.16	-454.
473.16	-387.
473.16	-390.

N-BUTANOL[33]

350.00	-1670.
380.00	-1220.
393.20	-1053.
408.20	-903.
423.20	-773.
439.20	-624.

2-BUTANOL[33]

378.20	-1131.
393.20	-969.
408.20	-831.
423.20	-692.

TERT-BUTANOL[33]

378.20	-935.
393.20	-810.
408.20	-660.
423.20	-540.

T K	B cm^3mol^{-1}	T K	B cm^3mol^{-1}
		ISO-BUTANOL[33]	
393.16	-433.		
398.15	-413.		
423.15	-320.		
423.15	-321.	393.20	-1039.
473.15	-219.	408.20	-904.
498.15	-181.	423.20	-789.
523.15	-156.	439.20	-631.
573.15	-113.		